Springs and Parachutes

Development and Characterization of Novel Formulations for Poorly Water-Soluble Drugs

Dissertation zur Erlangung des
naturwissenschaftlichen Doktorgrades
der Julius-Maximilians-Universität Würzburg

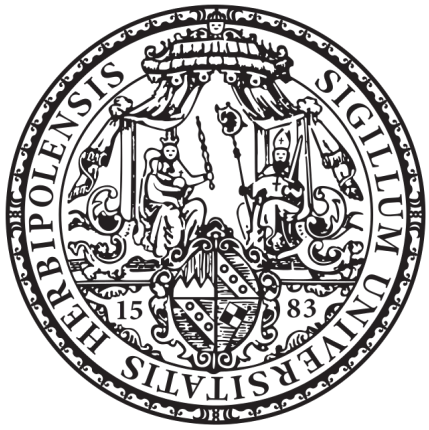

vorgelegt von

Nils Terveer

aus Kiel

Würzburg 2017

Springs and Parachutes

Development and Characterization of Novel Formulations for Poorly Water-Soluble Drugs

Dissertation zur Erlangung des
naturwissenschaftlichen Doktorgrades
der Julius-Maximilians-Universität Würzburg

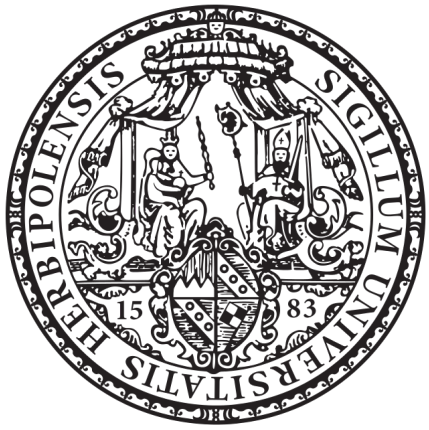

vorgelegt von

Nils Terveer

aus Kiel

Würzburg 2017

Eingereicht bei der Fakultät für Chemie

und Pharmazie am: ……..….

Gutachter der schriftlichen Arbeit:

1. Gutachter: ..…….

2. Gutachter: ……

Prüfer des öffentlichen Promotionskolloquiums:

1. Prüfer: ……

2. Prüfer: ……

3. Prüfer: ……

Datum des öffentlichen Promotionskolloquiums:

…….

Doktorurkunde ausgehändigt am:

…….

Danksagung

Die vorliegende Arbeit entstand in der Zeit von April 2013 bis Januar 2017 am Institut für Pharmazie und Lebensmittelchemie der Julius-Maximilians-Universität Würzburg unter der Leitung von

Frau Prof. Dr. Ulrike Holzgrabe.

Ich möchte mich hiermit herzlich für die freundliche Aufnahme in den Arbeitskreis, das in mich gesetzte Vertrauen, die fachkundige Unterstützung in jeder Phase der Arbeit und die Möglichkeit zum eigenverantwortlichen Erstellen meiner Dissertation bedanken.

Weiterhin bedanke ich mich bei Prof. Dr. Dr. Lorenz Meinel und dem Team der Technologie für die erfolgreiche Kooperation und die vielen kreativen Diskussionsrunden sowie ganz besonders bei Nina Hecht für die gemeinsame Arbeit an diesem Projekt.

Ich danke Dr. Curd Schollmayer für die fachkundige Unterstützung auf dem Gebiet der NMR-Spektroskopie sowie die freundschaftliche Zusammenarbeit.

Außerdem danke ich dem gesamten AK Holzgrabe für die vielen schönen Erlebnisse in Würzburg, an die ich auch nach Abschluss der Promotion immer noch gerne zurückdenke. Nicht zuletzt bedanke ich mich bei Miri, Christine, Raphael und Patrick für die tatkräftige Unterstützung bei der Praktikumsbetreuung.

Table of Contents

TABLE OF CONTENTS

1 Introduction

1 INTRODUCTION

Oral drug delivery is the most commonly used route of administration for most of the drugs in use today[1]. The high intestinal surface area and rich mucosal vasculature offers the potential for excellent drug absorption and high bioavailability[2]. The complete dissolution of the active pharmaceutical ingredient (API) in the gastrointestinal fluids is essential for absorbing it across the intestinal mucosa, for the API to reach systemic circulation, and exerts the full pharmacological effect[3]. Reaching an adequate solubility level for the time window of absorption is a major challenge in drug delivery because of the poor water solubility of most of the new small molecules currently in development and in use[4]. Looking at the portfolio of marketed drugs in comparison to developmental drugs, it becomes evident that there is a strong trend towards drugs with a very low aqueous solubility[1]. Most of the new small molecule drug candidates can be categorized as class II of the biopharmaceutical classification system. That means the drugs show excellent permeability across physiological membranes but also have a distinctively poor aqueous solubility. Thus, the drug dissolution step is the limiting factor for absorption from the small intestine and for achieving systemic circulation. To develop potent pharmaceuticals from such poorly water-soluble drugs a customized formulation strategy using supersaturation phenomena is needed.

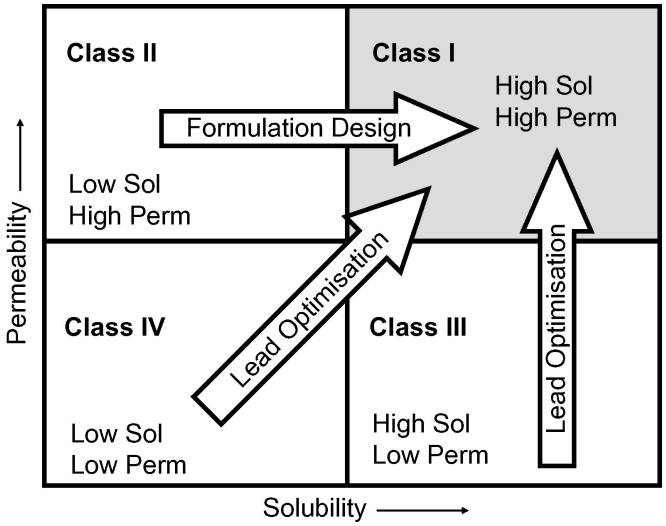

Figure 1 An illustration of the biopharmaceutical classification system representing the increase of bioavailability of a poorly water-soluble class II compound by an appropriate formulation, published by Colin W. Pouton[4]; reprinted with permission from Elsevier.

1.1 Springs & Parachutes

Pharmaceutical processes effectuating a supersaturated state above the equilibrium solubility of an API are described as 'springs and parachutes'[5].

A 'spring' can be a formulation of the API of thermodynamical higher energy providing faster dissolution and thus a higher rate and extent of absorption[5]. However, a limiting factor of this improved dissolution profile can be rapid recrystallization of a more stable and less soluble form[5]. Thus, an excipient or a process which retards the rate of recrystallization is needed. This is called the 'parachute'. For every poorly water-soluble drug an individual concept combining the benefits of 'spring and parachute' is needed to accomplish a supersaturated solution of the drug. This supersaturated state has to be maintained for the time window of absorption; for oral administration this is a process lasting about 4 h.

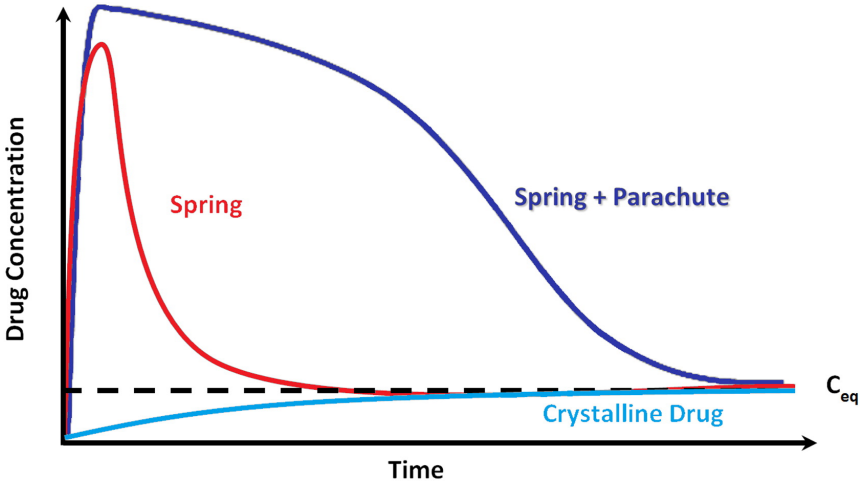

Figure 2 An illustration of the phenomena of 'spring and parachute' published by Baghel et al.[6]; reprinted with permission from Elsevier.

1.2 Formulation Strategies for Poorly Water-soluble Drugs

The pharmaceutical industry provides a variety of strategies for the formulation of poorly water-soluble drugs, such as transformation of the API into a prodrug, salt formation, particle size reduction, crystal engineering, solid dispersions, and micellar systems[7]. Some of these strategies are explained in the following section:

1.2.1 Ionic Liquid Approach

Ionic liquids are generally defined as organic salts with melting points below 100 °C and are entirely composed of ions[8]. Therefore, the ionic liquid approach is a special descendant of the salt formation strategy which is applicable for acidic or basic APIs. In comparison to crystalline organic salts ionic liquids are always amorphous materials so that no energy is needed to break up any crystal lattice resulting in a higher dissolution rate. Depending on the glass transition temperatures some ionic liquids may be liquids at room temperature. Transformation of poorly water-soluble drugs into ionic liquids is a powerful tool for increasing bioavailability: The ionic liquid approach is able to stabilize dissolved APIs in a supersaturated state for several hours following dissolution from an amorphous, solid state[9].

First applied by Walden in 1914[10], the ionic liquid concept plays an important role today for different applications: Ionic liquids are tuneable multipurpose materials for a variety of applications[11]. They are used in sensors, solar cells, as solvents and lubricants, to cite some examples[8]. In pharmaceutical applications ionic liquids are able to improve API dissolution, solubility, and bioavailability and to prevent polymorphism[9]. The ionic liquid concept makes it possible to tune the physicochemical and biopharmaceutical properties of a given drug by pairing it with various counter-ions[8]. The counter-ion can be an API itself and may offer synergies with the original drug or add some new functionality[12].

Mostly ionic liquids are prepared by a metathesis reaction[13]. Usually bulky organic moieties are selected as counter-ions because of their charge distribution and their ability to disrupt the formation of crystalline networks[12]. A bulky, long-chain counter-ion has more degrees of rotational freedom than a rigid multi-ringed structure that can become active on melting, resulting in an entropy gain and a loss of total free enthalpy[14]. Therefore, an amorphous material with a lower glass transition temperature (T_G) and a higher dissolution rate than the starting product is generated. The T_G can be below room temperature in some cases. The transformation of lidocaine HCl and the counter-ion docusate sodium into a hydrophobic room temperature ionic liquid illustrates the excellent potential of the ionic liquid approach: The solubility of lidocaine was improved, the thermal stability was increased, and a significant enhancement in the efficacy of topical analgesia in two different mouse models was observed[15].

1.2.2 Complexation with Cyclodextrins

1.2.2.1 Cyclodextrins

Cyclodextrins are cyclic oligomers of α-D-glucose formed by enzymatic hydrolysis of starch[16]. The hydrolysis is catalysed by the enzyme cyclodextrin glycosyltransferase of a certain bacteria such as *Bacillus macerans*[17]. The structure of the cyclodextrin molecule can be described as a wreath-shaped truncated cone[22]. Cyclodextrins were first isolated by Villiers in 1891[19]. In 1904, the preparation and characterization was described in detail by Schardinger[20,21]. Three different native cyclodextrins consisting of six to eight glucose units, length-wise connected by glycosidic α-1,4 bonds are available on the market called α-, β-, and γ-cyclodextrin, respectively[3,18].

As a consequence of the C-1 conformation of the glucopyranose units, all secondary hydroxyl groups (C-2 and C-3) are situated at the wider rim of the ring whereas all primary hydroxyl groups (C-6) are located at the tighter rim[22]. Because of the hydroxyl groups being located in position C-2, C-3, and C-6, the outside surface of the cyclodextrin is rather hydrophilic. The interior of the cavity is rather hydrophobic: From the wider rim inwards the cavity is lined with a row of CH-3 groups, then a row of glycosidic oxygens, and then a row of CH-5 groups[16]. The non-bonding electron pairs of the oxygen bridges are directed towards the inside of the cavity producing a high electron density there[22].

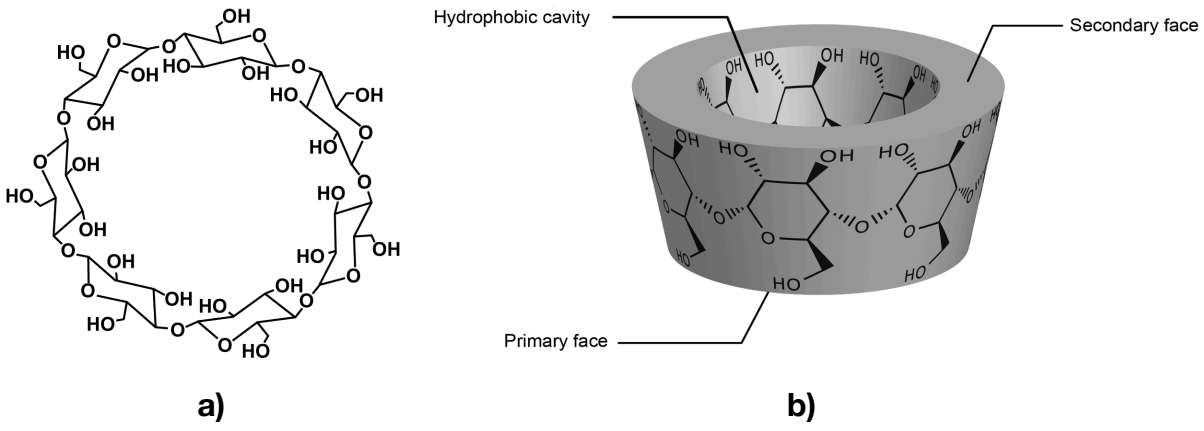

Figure 3 An illustration of **a)** the chemical structure of beta-cyclodextrin and **b)** a schematic representation of the wreath-shaped truncated cone published by Becuwe et al.[23]; Sophie Fourmentin is gratefully acknowledged for providing this illustration.

The width of the cavity, which is increasing from α- to β- and to γ-cyclodextrin, and the aqueous solubility depend on the number of glucopyranose units: In a β-cyclodextrin molecule a complete secondary belt is formed by H-bonds between the hydroxyl groups on the outside surface. Therefore, β-cyclodextrin is a rigid structure with the lowest water solubility of all cyclodextrins. In the α-cycoldextrin this hydrogen belt is incomplete because one glucopyranose unit is in a distorted position. γ-cyclodextrin is a nonplanar and more flexible structure[22]. Therefore, α– and γ-cyclodextrin have a higher water solubility than β-cyclodextrin. Chemical and enzymatic modification of substitutable hydroxyl groups was a field of intensive research during the last years. Today, more than 100 different cyclodextrin derivatives are commercially available[22]. Methylated, hydroxyalkylated, acetylated, and sulfobutylated derivatives are produced among others. They are used as solubilizers, stabilizers, separating agents in capillary electrophoresis, and as viscosity modifiers[22,24]. Some of the most important physical and chemical properties of the native cyclodextrins are shown in **Table 1**[25].

Table 1 Chemical properties of the three native cyclodextrins.

Properties	**α-CD**	**β-CD**	**γ-CD**
number of glucopyranose units	6	7	8
molecular weight (g/mol)	972	1135	1297
diameter (nm)	0.57	0.78	0.95
depth (nm)	0.78	0.78	0.78
water solubility (g/100mL)	14.5	1.85	23.2
pK_a value	12.33	12.20	12.08

The information listed in this table is partly based on the following reference: Fanali et al. (2000)[25].

1.2.2.2 Cyclodextrin Inclusion Complexes

Cyclodextrins have the remarkable property to form inclusion complexes with a variety of small molecules[18]. This interaction forms water-soluble, dynamic, and reversible inclusion complexes and makes cyclodextrins to be ideal candidates for the delivery of poorly water-soluble compounds[3]. The solubilizing capacity of a cyclodextrin depends on a number of factors including the size of the cavity, stoichiometry of the complex, complexation equilibrium constant, and the overall free energy of the system[26]. The most likely mode of interaction of a guest molecule with a cyclodextrin consists of an incorporation of the hydrophobic part of the molecule into the cyclodextrin cavity with the polar region remaining outside the cavity[27-28]. The formation of the complex is caused by van der Waals forces and hydrophobic interactions as well as hydrogen bonding between the cyclodextrin and the guest molecule[27]. Another important driving force for cyclodextrin inclusion complexes is the release of enthalpy-rich water molecules from the cyclodextrin cavity[29]. Some of the cyclodextrin-containing pharmaceutical products are listed in **Table 2**.

Table 2 Examples for pharmaceutical products containing cyclodextrins[30].

Drug	Trade name	Cyclodextrin	Formulation	Countries
Diclofenac sodium	Voltaren®	2-hydroxypropyl-γ-CD	eye-drop solution	Europe
Voriconazole	Vfend®	sulfobutylether-β-CD	i.v. solution	Europe, USA
Cephalosporine	Meiact®	β-cyclodextrin	tablet	Japan
Dexamethason	Glymesason®	β-cyclodextrin	ointment	Japan
Chloramphenicol	Clorocil®	methyl-β-CD	eye-drop solution	Europe
Cefotiam hexetil HCl	Pansporin T®	α-cyclodextrin	tablet	Japan

The information listed in this table is partly based on the following reference: Loftsson et al. (2007).

1.2.3 Microemulsion Oral Formulations

Microemulsions are defined as thermodynamically stable, isotropically, clear, liquid solutions composed of water, oil, and amphiphile[31].

First applied by Hoar and Schulman in 1943[32], the microemulsion concept has been redefined on many occasions[33]. Today microemulsions play an important role for delivering poorly water-soluble drugs thanks to their distinct potential to act as drug delivery vehicles for a wide range of drug molecules[33-34]. The main difference between a microemulsion and a classical emulsion is that emulsions, beside their cloudy appearance, are thermodynamically unstable and their phases tend to separate[33,35]. Additionally, classical emulsions require a lot of energy during preparation while microemulsions do not[33].

The formation of microemulsions is driven by the very large gain of entropy arising from both mixing of one phase into the other in the form of a large number of small droplets, and from the surfactant diffusion in the interfacial layer[33]. Taken together, the combination of a large reduction in surface tension and several favourable entropic changes results in a negative free energy[33]. Thus, the formation of a microemulsion system is spontaneous and the resulting product is thermodynamically stable[33].

Self-microemulsifying drug delivery systems (SMEDDS) are drug vehicles which are closely related to microemulsions: Usually SMEDDS are administered as homogenous, non-aqueous preconcentrates that will form a fine dispersion once they come into contact with aqueous media, such as gastrointestinal fluids[36-37]. As opposed to ready-to-use microemulsions, SMEDDS can be easily filled into hard or soft gelatine capsules thanks to a reduction of volume because of the absence of any water. Thus, they take advantage of the classical route of oral administration, and have an improved long-term stability[36].

1.2.4 Solid Dispersions

The preparation of a solid dispersion is another promising strategy for increasing bioavailability of poorly water-soluble drugs. A solid dispersion can be defined as a molecular mixture of a poorly water-soluble drug and a hydrophilic carrier[38]. The first description of a solid dispersion was published in 1964 by Sekiguchi et al.[40] who observed an increased dissolution rate and higher blood levels when presenting sulfathiazole as an eutectic mixture with urea as compared to the starting product.

An increased bioavailability up to several orders of magnitude is achieved by reduction of the particle size to its absolute minimum. The dissolution rate of the drug is determined by the dissolution rate of the carrier[39]. For the dissolution of an amorphous solid dispersion no energy is required to break up the crystal lattice as compared to the crystalline starting product. Thus, the drug is presented as a supersaturated solution[41].

Two manufacturing processes are described for the preparation of a solid dispersion: the melting method and the solvent evaporation method. For the melting method the active drug is melted within the carrier or suspended in the previously melted carrier followed by cooling and pulverization of the obtained product[38,42]. Several adaptions of the melting method were developed to avoid problems caused by degradation of the drug when exposed to high temperatures or incomplete miscibility between drug and carrier[38]: To cite only two examples, there is Meltrex™ which is a patented manufacturing process that uses a special twin screw extruder in which the temperature of the drug and the carrier are controlled separately[38,43]. On the other hand there is the hot-stage extrusion which uses carbon dioxide as a plasticizer[38,44].

To completely prevent drugs and carriers from thermal degradation, the solvent evaporation method can be used. Here drug and carrier are dissolved together in a common volatile solvent which will be evaporated afterwards[38]. Several evaporation processes are possible such as drying on a hot plate, vacuum drying, slow evaporation at room temperature, the use of a rotary evaporator, freeze drying, spray drying, the use of a stream of nitrogen, and the use of supercritical fluids. Spray drying, however, is the most commonly used method[38,45-51].

Some advantages make use of solid dispersions, a promising technique for increasing bioavailability. As solids they provide the opportunity for oral administration as tablets which is more acceptable to patients than a liquid formulation. Unlike salt formation, the solid dispersion concept is suitable for neutral drugs. In comparison to simple particle size reduction techniques (like grinding) the solid dispersion approach generates a product without poor mechanical properties such as low flowability or high adhesion[38]. A disadvantage of solid dispersions is the poor scale-up of the manufacturing process and the tendency of the amorphous product to undergo recrystallization when exposed to mechanical or storage stress[38,48,52].

1.2.5 Cocrystals

Delivering active pharmaceutical ingredients as solid dosage forms such as tablets and capsules is the most commonly applied route of administration. The ability of a safe, efficacious, and cost-effective delivery depends on stable and good water-soluble compounds[53]. The formation of pharmaceutical cocrystals is a reliable concept for improving these properties. Pharmaceutical cocrystals are defined as crystalline materials which are solids at room temperature, consisting of the API and at least one cocrystal former[53-54]. Beside major improvements in solubility, dissolution rate, bioavailability, and physical stability, pharmaceutical cocrystals enhance other essential properties such as chemical stability, compressability, flowability, and hygroscopicity[53].

Several types of interaction are involved such as hydrogen bonding, van der Waals forces, and π-stacking[54]. Water or other solvents may be included in the crystal lattice[54]. Cocrystals are multicomponent materials without any transfer of hydrogen ions to form salts[54]. Therefore, the cocrystal approach is an appropriate formulation concept for poorly water-soluble drugs which are not convenient for salt formation because of the absence of any acidic or basic functional groups. Usually, cocrystals are prepared from stoichiometric solutions of the API and the cocrystal former by evaporating or sublimating the solvent, or by growing from the melt of the two components, as well as grinding[55].

Ertugliflozin is introduced as an example for application of the cocrystal approach in drug development. Its is a glucose sodium cotransporter 2 (SGLT2) inhibitor

candidate, developed by Pfizer for the treatment of type 2 diabetes mellitus. Ertugliflozin exists as a hygroscopic amorphous solid with a low glass transition temperature and can also not be ionised near physiological pH[56]. Because this made salt formation impossible, the API was subjected to a cocrystal screening. The resulting L-pyroglutamic acid cocrystal (1:1) became the focus for further development because it improved the physical properties for manufacture and ensured an API of robust solid state[56].

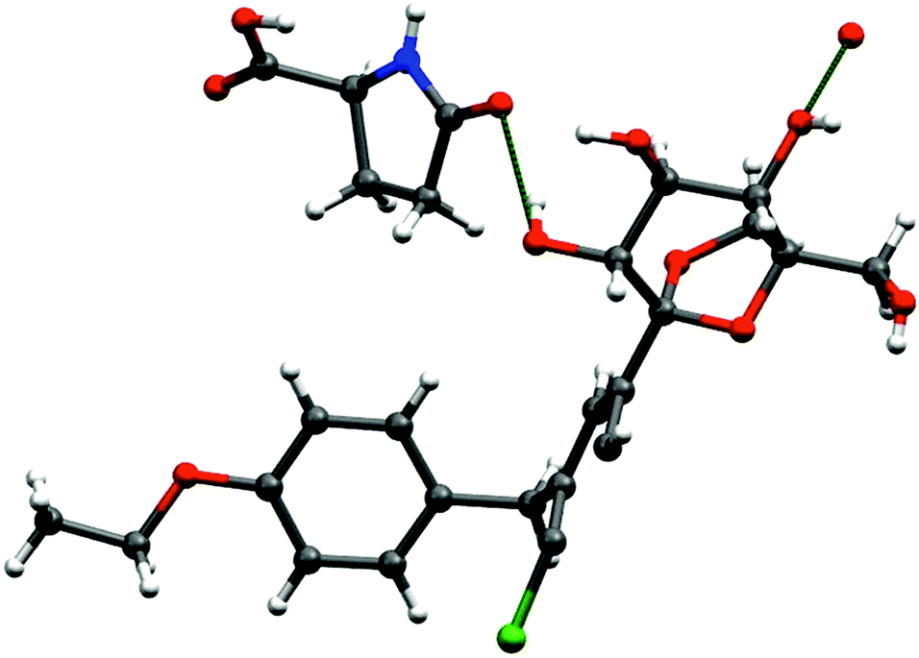

Figure 4 An illustration of the structure of the ertugliflozin L-pyroglutamic acid cocrystal published by Duggiraha et al.[57]; reprinted with permission of the Royal Society of Chemistry.

1.3 References

[1] Lipp R., The Innovator pipeline: bioavailability challenges and advanced oral drug delivery opportunities. *Am. Pharm. Rev.* **2013,** 16(3) 10–12

[2] Pouton C. W., Lipid formulations for oral administration of drugs: non-emulsifying, self-emulsifying and 'self-microemulsifying' drug delivery systems. *Eur. J. Pharm. Sci.* **2000,** 2: 93–98.

[3] Williams R. O., Watts A. B., Miller D. A., Formulating Poorly Water-soluble Drugs. *Springer,* **2012.**

[4] Pouton C. W., Formulation of poorly water-soluble drugs for oral administration: physicochemical and physiological issues and the lipid formulation classification system. *Eur. J. Pharm. Sci.* **2006,** 29(3–4): 278–287.

[5] Guzman H. R., Tawa M., Zhang Z., et al., Combined use of crystalline salt forms and precipitation inhibitors to improve oral absorption of celecoxib from solid oral formulations. *J. Pharm. Sci.* **2007,** 96(10): 2686–2702.

[6] Baghel S., Cathcart H., O'Reilly N. J., Polymeric Amorphous Solid Dispersions: A Review of Amorphization, Crystallization, Stabilization, Solid-State Characterization, and Aqueous Solubilization of Biopharmaceutical Classification System Class II Drugs. *J. Pharm. Sci.* **2016,** 105: 2527–2544

[7] Marrucho I. M., Branco L. C., Rebelo L. P., Ionic liquids in pharmaceutical applications. *An. Rev. Chem. Biomol. Eng.* **2014,** 5: 527–546.

[8] Ferraz R., Branco L. C., Prudencio C., Noronha J. P., Petrovski Z., Ionic liquids as active pharmaceutical ingredients. *Chem. Med. Chem.* **2011,** 6(6): 975–985.

[9] Balk A., Wiest J., Widmer T., Galli B., Holzgrabe U., Meinel L., Transformation of acidic poorly water-soluble drugs into ionic liquids. *Eur. J. Pharm. Biopharm.* **2015,** 94: 73–82.

[10] Walden P., Über die Molekulargröße und elektrische Leitfähigkeit einiger geschmolzener Salze. **1914,** *Bull. Acad. Sci. St. Petersburg* 8(6): 405–22

[11] Rogers R. D., Voth G. A., Ionic liquids. *Acc. Chem. Res.* **2007,** 40(11): 1077–1078

[12] Prakash A. S., The counter ion: expanding excipient functionality. *J. Ex. and Food Chem.* **2011,** 2(2): 28–40

[13] Frizzo C. P., Tier A. Z., Moreira D. N., Gindri I. M., Buriol L., Martins M. A., Pharmaceutical Salts: Solids to Liquids by Using Ionic Liquid Design. *In Tech.* **2013,** 557–579

[14] Stoimenovski J., Dean P. M., Izgorodina E. I., MacFarlane D. R., Protic pharmaceutical ionic liquids and solids: Aspects of protonics. *Faraday Discuss.* **2012,** 154: 335–352

[15] Hough W. L., Smiglak M., Rodríguez H., et al., The third evolution of ionic liquids: active pharmaceutical ingredients. *New J. Chem.* **2007,** 31(8): 1429–1436

[16] Connors K. A., The stability of cyclodextrin complexes in solution. *Chem. Rev.* **1997,** 97(5): 1325–1358

[17] Bender H., (1→ 4)-α-d-Glucopyranosyltransfer-produkte aus cyclohexaamylose. *Carbohydr. Res.* **1978,** 65(1): 85–97

[18] Saenger W., Cyclodextrin inclusion compounds in research and industry. *Angew. Chem. Int.* **1980,** 19(5): 344–362

[19] Villiers A., Sur la fermentation de la fécule par l'action du ferment butyrique. *Compt Rend. Acad Sci.* **1891,** 112: 536–538

[20] Wiener Klinische Wochenschrift. **1904,** 17: 207

[21] Schardinger F., Über thermophile Bakterien aus verschiedenen Speisen und Milch. *Zeitschr. f. Lebensm. Forsch.* **1903,** 6(19): 865–880

[22] Szejtli J., Introduction and general overview of cyclodextrin chemistry. *Chem. Rev.* **1998,** 98(5): 1743–1754

[23] Becuwe M., Landy D., Delattre F., Cazier F., Fourmentin S., Fluorescent indolizine-b-cyclodextrin derivatives for the detection of volatile organic compounds. *Sensors.* **2008,** 8(6): 3689–36705

[24] Fanali S., Controlling enantioselectivity in chiral capillary electrophoresis with inclusion–complexation. *J. Chrom. A.* **1997,** 792(1): 227–267

[25] Fanali S., Enantioselective determination by capillary electrophoresis with cyclodextrins as chiral selectors. *J. Chrom. A.* **2000,** 875(1): 89–122

[26] Challa R., Ahuja A., Ali J., Khar R. K., Cyclodextrins in drug delivery: An updated review. *Pharm. Sci. Tech.* **2005,** 6(2): 329–357

[27] Rekharsky M. V., Mayhew M. P., Goldberg R. N., et al., Thermodynamic and nuclear magnetic resonance study of the reactions of α-and β-cyclodextrin with acids, aliphatic amines, and cyclic alcohols. *J. Phys. Chem. B.* **1997,** 101(1): 87–100

[28] Szejtli J., Cyclodextrin Technology. *Springer Netherlands;* **1988,** 1–78.

[29] Loftsson T., Brewster M. E., Pharmaceutical applications of cyclodextrins. 1. Drug solubilization and stabilization. *J. Pharm. Sci.* **1996,** 85(10): 1017–1025

[30] Loftsson T., Duchêne D., Cyclodextrins and their pharmaceutical applications. *Int. J. Pharm.* **2007,** 329(1): 1–11

[31] Danielsson I., Lindman B., The definition of microemulsion. *Coll. Surf. 1981,* 3(4): 391–392

[32] Hoar T., Schulman J., Transparent water-in-oil dispersions: the oleopathic hydro-micelle. *Nature.* **1943,** 152: 102–103

[33] Lawrence M. J., Rees G. D,. Microemulsion-based media as novel drug delivery systems. *Adv. Drug. Deliv. Rev.* **2000,** 45(1): 89–121

[34] Tenjarla S., Microemulsions: an overview and pharmaceutical applications. *Crit. Rev. Ther. Drug Carrier Syst*. **1999,** 16(5) 461–521

[35] Shinoda K., Lindman B., Organized surfactant systems: microemulsions. *Langmuir.* **1987,** 3(2): 135–149

[36] Fahr A., Liu X., Drug delivery strategies for poorly water-soluble drugs. *Expert. Opin. Drug. Deliv.* **2007,** 4(4): 403–16.

[37] Strickley R. G., Solubilizing excipients in oral and injectable formulations. *Pharm. Res.* **2004,** 21(2): 201–230.

[38] Vasconcelos T., Sarmento B., Costa P., Solid dispersions as strategy to improve oral bioavailability of poor water-soluble drugs. *Drug. Discov. Today.* **2007,** 12(23): 1068–1075

[39] Leuner C., Dressman J., Improving drug solubility for oral delivery using solid dispersions. *Eur. J. Pharm. Biopharm.* **2000,** 50(1): 47–60

[40] Sekiguchi K., Obi N., Yoshio U., Studies on Absorption of Eutectic Mixture. II. Absorption of fused Conglomerates of Chloramphenicol and Urea in Rabbits. *Chem. Pharm. Bull.* **1964,** 12(2): 134–144

[41] Taylor L. S., Zografi G., Spectroscopic characterization of interactions between PVP and indomethacin in amorphous molecular dispersions. *Pharm. Res.* **1997,** 14(12): 1691–1698

[42] Owusu-Ababio G., Ebube N. K., Reams R., Habib M., Comparative dissolution studies for mefenamic acid-polyethylene glycol solid dispersion systems and tablets. *Pharm. Dev. Tech.* **1998,** 3(3): 405–412

[43] Breitenbach J., Lewis J., Two concepts, one technology: controlled-release solid dispersions using melt extrusion (Meltrex®). *Drug. Pharm. Sci.* **2008,** 183: 179

[44] Verreck G., Decorte A., Heymans K., et al., The effect of supercritical CO_2 as a reversible plasticizer and foaming agent on the hot stage extrusion of itraconazole with EC 20cps. *J. supercrit. fluids.* **2007,** 40(1): 153–162

[45] Ceballos A., Cirri M., Maestrelli F., Corti G., Mura P., Influence of formulation and process variables on in vitro release of theophylline from directly-compressed Eudragit matrix tablets. *Il. Farm.* **2005,** 60(11): 913–938

[46] Desai J., Alexander K., Riga A., Characterization of polymeric dispersions of dimenhydrinate in ethyl cellulose for controlled release. *Int. J. Pharm.* **2006,** 308(1): 115–123

[47] Karavas E., Georgarakis E., Bikiaris D., Application of PVP/HPMC miscible blends with enhanced mucoadhesive properties for adjusting drug release in predictable pulsatile chronotherapeutics. *Eur. J. Pharm. Biopharm.* **2006,** 64(1): 115–126

[48] Pokharkar V. B., Mandpe L. P., Padamwar M. N., Ambike A. A., Mahadik K. R., Paradkar A., Development, characterization and stabilization of amorphous form of a low T_g drug. *Pow. Techn.* **2006,** 167(1): 20–25

[49] Prabhu S., Ortega M., Ma C., Novel lipid-based formulations enhancing the in vitro dissolution and permeability characteristics of a poorly water-soluble model drug, piroxicam. *Int. J. Pharm.* **2005,** 301(1): 209–216

[50] Van Drooge D., Hinrichs W., Visser M., Frijlink H., Characterization of the molecular distribution of drugs in glassy solid dispersions at the nano-meter scale, using differential scanning calorimetry and gravimetric water vapour sorption techniques. *Int. J. Pharm.* **2006,** 310(1): 220–229

[51] Won D. H., Kim M. S., Lee S., Park J. S., Hwang S. J., Improved physicochemical characteristics of felodipine solid dispersion particles by supercritical anti-solvent precipitation process. *Int. J. Pharm.* **2005,** 301(1): 199–208

[52] Van den Mooter G., Weuts I., De Ridder T., Blaton N., Evaluation of Inutec SP1 as a new carrier in the formulation of solid dispersions for poorly soluble drugs. *Int. J. Pharm.* **2006,** 316(1): 1–6

[53] Lu J., Rohani S., Preparation and Characterization of Theophylline-Nicotinamide Cocrystal. *Org. Proc. Res. Dev.* **2009,** 13(6): 1269–1275

[54] Peterson M. L., Hickey M. B., Zaworotko M. J., Almarsson Ö., Expanding the scope of crystal form evaluation in pharmaceutical science. *J. Pharm. Pharm. Sci.* **2006,** 9(3): 317–326

[55] Shan N., Zaworotko M. J., The role of cocrystals in pharmaceutical science. *Drug. Discov. Today.* **2008,** 13(9-10): 440–446.

[56] Bowles P., Brenek S. J., Caron S. P., et al., Commercial route research and development for SGLT2 inhibitor candidate ertugliflozin. *Org. Proc. Res. Dev.* **2014,** 18(1): 66–81

[57] Duggirala N. K., Perry M. L., Almarsson Ö., Zaworotko M. J., Pharmaceutical cocrystals: along the path to improved medicines. *Chem. Comm.* **2016,** 52(4): 640–655

2 Aim of the Thesis

2 AIM OF THE THESIS

Today the modern hit identification strategies used for drug development coming along with high throughput screening techniques lead to a trend towards drug candidates with a high lipophilicity and therefore with a very low aqueous solubility. For these drugs, to reach acceptable solubility levels for the time window of absorption resulting in therapeutic plasma concentrations, a customized formulation development is needed. In this thesis the tyrosine-kinase inhibitor imatinib and the novel NOX inhibitor VAS3947 were selected as examples for such poorly water-soluble drug candidates. Different formulation strategies were tested and the resulting products were subjected to an extensive physicochemical characterization to evaluate the extent of supersaturation as well as the underlying reasons. Furthermore, a HPLC method was developed and validated in order to analyse the concentration of the API in solution. For the execution of further clinical drug development, a well-founded knowledge about the stability of every API is necessary. Therefore, the chemical stability of VAS3947 was examined. In particular, the following investigations were conducted:

a) Preparation and physicochemical characterization of an ionic liquid formulation for the poorly water-soluble tyrosine-kinase inhibitor imatinib addressing its solubility and dissolution behaviour.

b) Development and characterization of appropriate formulations for the poorly water-soluble NOX inhibitor VAS3947. Different techniques to increase its solubility, namely spray drying, incorporation into cyclodextrins, and preparation of a microemulsion were tested.

c) In view of preclinical investigations the compound VAS3947 was assessed for chemical stability in addition to biopharmaceutical studies by means of a microsomal assay, a plasma stability assay, a Caco-2 cell assay, and a cytotoxicity assay.

d) An appropriate HPLC method for the NOX inhibitors of the VAS-library was developed and validated.

3 Results

3 RESULTS

3.1 Ionic Liquid Concept to Improve the Solubility Profile of the Tyrosine-Kinase Inhibitor Imatinib

Nils Terveer, Curd Schollmayer, Christoph Steiger, Ulrike Holzgrabe, Lorenz Meinel

Manuscript in preparation

Abstract

Improving the solubility of new chemical entities is one of the major challenges for formulation scientists. The aim of this study was to develop a concept for transforming the tyrosine-kinase inhibitor imatinib into an ionic liquid (IL) with better physical and pharmaceutical properties. ILs of imatinib as a weak base and several acetylated amino acids as appropriate counterions were prepared. Products were characterized by NMR spectroscopy, differential scanning calorimetry (DSC), and X-ray powder diffractometry (XRPD). p*Ka* values were determined using a Sirius T3 instrument, and an accelerated stress testing was performed to evaluate the physical stability of the ILs produced. Dissolution rate and releasing profile measurements detecting the saturation concentration of the API verified dissolution rates up to 70 times higher and prolonged supersaturation times as compared to the free base. Lowering lattice forces by transforming crystalline imatinib into an amorphous IL leads to an increased dissolution rate and supersaturation time on the one hand. On the other hand an increase of hygroscopicity has been observed. In summary, the preparation of an IL from a poorly water-soluble weak base like imatinib is a reliable tool to control dissolution rate and supersaturation effects for successful oral administration.

Introduction

For patients oral drug delivery is the most favourable route of administration for pharmaceutical products[1]. The high intestinal surface area and rich mucosal vasculature offers the potential for excellent drug absorption and high bioavailability[2]. The complete dissolution of the active pharmaceutical ingredient (API) in the gastrointestinal fluids is essential for its absorption across the intestinal mucosa to reach systemic circulation and exert its pharmacological effect[1]. Reaching an adequate solubility level for the time window of absorption is a major challenge in drug delivery because of the poor water-solubility of most of the new small molecules in the pipeline[3].

The aim of this work was to develop usable formulations without changing the chemical structure of the API. Practicable approaches cover strategies like particle size reduction, hot melt extrusion, cyclodextrin inclusion complexes, polymorph selection, salt formation, and the use of self-emulsifying drug delivery systems [1,3-6]. Another simple and reliable concept to increase dissolution rate and solubility by lowering lattice forces is transforming the API into an amorphous Ionic Liquid (IL). ILs are defined as organic salts with melting points below 100 °C[7]. The IL approach has a very practical advantage because of its variability. Specific physicochemical and biological properties of ILs can be modified by changing either the anionic or the corresponding cationic components[8]. The transfer of several acidic APIs into ILs to improve the solubility profile has been described in earlier studies[9-13]. In this work, an IL approach for oral administration of the tyrosine-kinase inhibitor imatinib as a weak base was developed. Several acetylated amino acids were used as non-toxic counterions for maximum increase of dissolution rate and supersaturation time. Results were compared to the free base and the mesylate salt which is available on the market as Gleevec® by Novartis Pharma AG, Basel. Products were characterized by NMR spectroscopy, X-ray powder diffractometry, and differential scanning calorimetry. The extent of hygroscopicity was determined after storage by weighing. Dissolution rate and 24 h solubility were determined photometrically.

Materials and Methods

Materials

Imatinib mesylate salt was provided by Novartis Pharma AG (Basel, Switzerland). Several acetylated amino acids used as counterions were purchased from Sigma Aldrich (Schnelldorf, Germany). The quality of the free forms of the APIs as well as that of the counterions was assured by ^{1}H NMR spectroscopy. Potassium dihydrogen phosphate and potassium chloride were purchased from Grüssing GmbH Analytika (Filsum, Germany). Sodium dihydrogen phosphate, disodium hydrogen phosphate, sodium chloride, a standardized 0.5 M solution of potassium chloride, a standardized 0.5 M solution of hydrochloric acid, a 40% solution of sodium deuteroxide in deuteriumoxide, and methanol were also purchased from Sigma Aldrich. A standardized 0.1 M solution of sodium hydroxide was obtained from Bernd Kraft GmbH (Duisburg, Germany). Standard 5 mm NMR tubes (Boro-5-7), deutero dimethylsulfoxide (DMSO-d_6), and deutero methanol (MeOH-d_4) were purchased from Deutero GmbH (Kastellaun, Germany). All used reagents were of analytical grade. A Milli-Q system (Merck Millipore GmbH, Darmstadt, Germany) was used for the demineralization of water.

Methods

Preparation of Imatinib Free Base

2.0 g of imatinib mesylate salt were dissolved in 10.0 mL water under stirring. 3.0 mL of sodium hydroxide solution (2 mol/L) were added dropwise. Afterwards the suspension was filtered and the resulting product was washed with 200 mL of water. The free base was subsequently dissolved in 30.0 mL methanol under stirring and gentle heating. This solution was stored in a freezer at -20 °C until precipitation occurred. The resulting product was filtered again and dried at 50 °C *in vacuo* for two days.

Preparation of ILs

The general procedure of preparing ILs of APIs has been described in earlier works[9]. In brief, 200.0 mg free base of imatinib and an equimolar amount of the counterion were separately dissolved in 5.0 mL methanol. Afterwards both solutions were mixed under stirring until a clear solution was obtained. The solution was transferred into a glass vial and the solvent evaporated at 50 °C *in vacuo* for two days. An amorphous, yellow solid was obtained.

Preparation of Sodium Salts of the Counterions

20 mg of every counterion were dissolved in 700 µL MeOH-d_4. To that 50 µL of a 40% solution of sodium deuteroxide in deuteriumoxide was added.

Nuclear Magnetic Resonance Measurements

NMR measurements were performed on a Bruker Avance III spectrometer (Rheinstetten, Germany) with a 5 mm BBO broadband observer with Z-gradient. The spectrometer was operating at 400.13 MHz for ^{1}H and 40.55 MHz for ^{15}N. Data processing was done with the TopSpin® 3.2 software. The temperature was adjusted to 300 K.

Standard ^{1}H NMR spectra were recorded with a flip angle of 30°, spectral width of 20 ppm, transmitter offset of 6.15 ppm, acquisition time of 3.99 s followed by a relaxation delay of 1.00 s. 128 scans were collected in 64.000 data points resulting in a digital resolution of 0.25 Hz. Processing parameters were set to an exponential line broadening window function of 0.3 Hz, an automatic baseline correction, and manual phasing. For measurements approximately 20 mg of every sample were dissolved in 700 µL DMSO-d_6 and MeOH-d_4, respectively, and transferred into a standard 5 mm NMR tube. The solvent also served as the field frequency lock.

^{15}N HMBC NMR spectra were recorded using gradient pulses for signal selection. The delay for the evolution of heteronuclear long range couplings was optimized to 3.0 Hz. The ^{15}N spectral width was set to 400 ppm with a transmitter offset of 140 ppm. The number of scans was adjusted to 168 and 128 increments in the indirect dimension (F1) were acquired. The acquisition time was set to 1.02 s followed by a relaxation delay of 1.5 s. The experimental time was 16 h. For processing a time domain size of 4.000 was used. In both dimensions (F2 and F1)

zero filling was applied, the window function was set to a pure sine function, and a baseline correction was performed. In the indirect dimension a forward linear prediction was performed. For sample preparation approximately 20 mg substance were dissolved in 700 µL of MeOH-d_4. This solution was transferred into a 5 mm NMR tube. MeOH-d_4 also served as the field frequency lock. The ^{15}N NMR spectra were referenced to nitromethane and the ^{1}H NMR spectra were referenced to the residual proton signal of the solvent.

^{1}H-NMR imatinib (DMSO-d_6, δ [ppm], J [Hz]): 10.15 (s, H-**6**); 9.28 (d, ^{4}J = 1.8, H-**12**); 8.96 (s, H-**8**); 8.68 (dd, ^{3}J = 4.7, ^{4}J = 1.8, H-**11**); 8.51(d, ^{3}J = 5.2, H-**14**); 8.47 (td, ^{3}J = 8.0, ^{4}J = 1.8, H-**9**); 8.08 (d, ^{4}J = 1.8, H-**7**); 7.90 (m, H-**5**); 7.54 – 7.39 (m, H-**13, 17, 4, 10**); 7.20 (d, ^{3}J = 8.4, H-**16**); 3.56 (s, H-**3**); 2.40 – 2.65 (br, H-**2**); 2.23 (s, H-**15**); 2.14 (s, H-**1**)

^{15}N-NMR imatinib (HMBC, 3 Hz, MeOH-d_4, δ [ppm]): -79 (N-**pyridine**); -136 (N-**pyrimidine**); -255 (N-**amide**); -277 (N-**guanidine);** -343 (N**-piperazine)**

X-ray Powder Diffractometry

Powder diffractometric studies were performed on a Bruker Discover D8 powder diffractometer (Rheinstetten, Germany) using Cu Kα radiation at a power of 40 KV and 40 mA. For the measurements approximately 4 mg of imatinib free base, imatinib mesylate salt, and ILs, respectively, were transferred onto a silicon single crystal zero background specimen holder with a diameter of approximately 5 mm. Detection was done with a LynxEye-1D-Detector (Bruker). Measurements were performed with a step size of 0.025° and 0.250 s time per step in the range of 5–45°. Data collection and processing were performed using the software packages DIFFRAC.Suite® (V2 2.2.690, Bruker AXS, Rheinstetten, Germany) and DIFFRAC.EVA® (Version 2.1, Bruker AXS, Rheinstetten, Germany).

Differential Scanning Calorimetry

Differential scanning calorimetry was performed on a DSC 8000 instrument (Perkin Elmer, Waltham, MA, USA) using a scanning rate of 20 K/min. Sample size was 2 to 4 mg. For the free base the melting point was determined from one heating cycle. Two heating and cooling cycles were performed to determine the glass transition

temperatures of the ILs. The second heating cycle was analysed to allow residual water to evaporate during the first one.

Water Vapour Sorption

The extent of water vapour sorption was determined according to the monograph of The European Pharmacopeia 8.0[14]. About 6 mg of every powdered substance were weighed into a 1.5 mL tube. The unstoppered tubes were placed in a desiccator at 25 °C and 80% relative humidity for 24 h. Afterwards the percentage increase in mass was determined by weighing.

Photometrical Determination of Dissolution Rates

The dissolution rates were recorded on a Sirius T_3 instrument (Sirius Analytical, East Sussex, UK) as described in earlier works[15]. Tablets with a defined surface area of 0.07 cm^2 were prepared by compressing 5–10 mg substance in a special tablet disc. 0.18 tonnes of pressure were applied for 6 minutes with a manual hydraulic tablet press (Paul Weber, Stuttgart, Germany). Dissolution rates were determined photometrically in a 0.2 M acetate buffer pH 2.0 and a PBS buffer pH 6.8 at a stirring speed of 4800 rpm following the manufacturer's instructions. 300 data points were collected for each measurement. The linear part of the release profile was used for the calculation of the dissolution rate. Measurements were carried out in triplicate.

24 h Solubility Profiles

5.0 mg equivalent of free base of every dry substance were transferred into a 1.5 mL tube and 1 mL PBS buffer pH 6.8 was added. The tubes were incubated at 37 °C while being shaken at 400 rpm. After 0 min, 10 min, 30 min, 2 h, 4 h, 8 h, and 24 h tubes were centrifuged for 5 min at 13.000 rpm and 50 µL samples of solutions were taken. The concentration of the compound in supernatant was photometrically determined at 257 nm. Experiments were carried out in triplicate. For all experiments the pH was controlled after 24 h and was 6.8 ± 0.2 throughout the full duration. For quantification of the compound in supernatant an external calibration against imatinib mesylate salt was applied.

Determination of *pKa* Values of Counterions and Imatinib Mesylate

The potentiometric determination of *pKa values* was performed on a Sirius T_3 instrument (Sirius Analytical, East Sussex, UK) as described in earlier works[16]. Experiments were performed in 0.15 M KCl solution under nitrogen atmosphere at a temperature of 20 °C. All measurements were carried out in triplicate using standardized 0.5 M KOH and HCl as titrant reagents. To prepare the samples approximately 3.5 mg of every counterion and 0.2 mg imatinib free base were used.

Extrapolation of *pKa* Values of the Counterions to Methanol according to the Procedure of Yasuda and Shedlovsky[17,18]

Potentiometric titrations of all amino acid counterions and imatinib mesylate salt were performed at 20 °C using a TitroLine® 7000 titrator (SI Analytics GmbH, Mainz Germany) and standardized 0.1 M NaOH as titrant reagent. A calibrated glass electrode was used to determine the endpoints. To prepare the sample solutions approximately 75 mg of every counterion and 290 mg of imatinib mesylate salt were dissolved in four different mixtures of water and methanol. The concentration of methanol of these solutions was 30, 40, 50, and 60% (v/v). The total volume of every sample was 50.0 mL and the maximum volume of titrant was set to 20.0 mL. More than 90 pH readings were collected for every titration. According to the procedure of Yasuda[17] and Shedlovsky[18] a correlation was applied whereby a plot of p*Ka* + log (MeOH) *versus* A / ε + B produces a straight line where (MeOH) represents the molar concentration of methanol and ε denotes the dielectric constant of the mixture. The terms *A* and *B* symbolize the slope and the intercept of the plot, respectively[19]. Afterwards the p*Ka* values of all counterions and imatinib mesylate were extrapolated to the dielectric constant of pure methanol.

Stability Testing of ILs

An accelerated stability testing was performed according to the procedure of the ICH guideline Q1A[20]. About 50 mg of every IL were weighed into a 30 mL glass vial. The unstoppered vials were placed in a desiccator at 40 °C and 80% relative humidity for 6 months. At the beginning, after 3 months, and after 6 months samples were analysed by ^{1}H NMR spectroscopy, XRPD, and DSC.

Results

Preparation and Physicochemical Characteristics of Imatinib ILs

To improve the solubility profile of imatinib, ILs were prepared using the corresponding free base. Several acetylated amino acids have been selected as appropriate candidates for counterions: *N*-acteyl aspartic acid (**a**), *N*-acetyl glycine (**b**), *N*-acetyl asparagine (**c**), *N*-acetyl glutamine (**d**), *N*-acetyl alanine (**e**), and *N*-acetyl glutamic acid (**f**) (**Figure 1**). All salts produced from imatinib were slightly yellow solids.

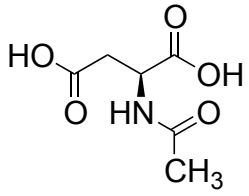

N-acetylaspartic acid **(a)**

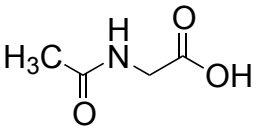

N-acetylglycine **(b)**

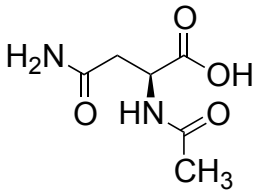

N-acetylasparagine **(c)**

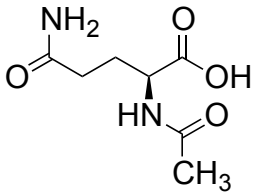

N-acetylglutamine **(d)**

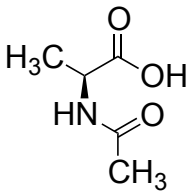

N-acetylalanine **(e)**

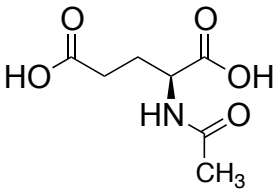

N-acetylglutamic acid **(f)**

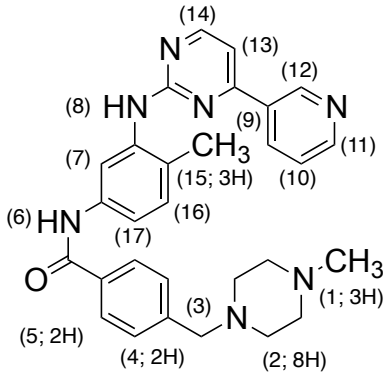

imatinib

Figure 1 Structures of imatinib and the acetylated amino acids used as counterions.

The free base, their corresponding ILs, and the mesylate salt were analysed by ^{1}H NMR spectroscopy in order to verify a 1:1 molar stoichiometry. Furthermore, ^{15}N HMBC NMR spectra were performed to confirm the protonated state of all ILs. The integration of the methyl protons of the terminal acetyl group of the counterions at approximately δ = 1.9 ppm (in MeOD-d_4) and the methyl protons of imatinib at approximately δ = 2.7 ppm (in MeOD-d_4) in the IL confirmed a 1:1 molar stoichiometry. MeOH-d_4 was selected as appropriate solvent for further experiments: To assign the signals of the nitrogens of the synthesized compounds to signals in the ^{1}H NMR spectra, ^{15}N HMBC spectra were recorded showing heteronuclear couplings between N-methyl protons and the nitrogen atom of the piperazine ring next to it. The comparison of chemical shifts of all ILs with the free base indicated a strong downfield shift of *N*-methyl protons from 2.3 to approximately 2.7 ppm in the ^{1}H NMR spectrum, and a gentle downfield shift of the piperazine nitrogen from -343 to nearly -340 ppm in the ^{15}N NMR spectrum (**Table 1**).

Table 1 Chemical shifts measured on a Bruker Avance III 400 MHz spectrometer in MeOH-d_4 of imatinib free base, mesylate salt, and the ILs produced. The corresponding counterions are: *N*-acteyl aspartic acid (**a**), *N*-acetyl glycine (**b**), *N*-acetyl asparagine (**c**), *N*-acetyl glutamine (**d**), *N*-acetyl alanine (**e**), and *N*-acetyl glutamic acid (**f**).

	^{15}N-**1**-piperazine	^{1}H-**1-**methyl protons
imatinib free base	-343.4	2.29
imatinib mesylate salt	-338.8	2.89
IL a	-340.1	2.77
IL b	-340.2	2.70
IL c	-339.9	2.71
IL d	-340.4	2.71
IL e	-340.4	2.69
IL f	-339.9	2.76

A stronger downfield shift has been observed for the mesylate salt: *N*-methyl protons shifted from 2.3 to 2.9 ppm in the ^{1}H NMR spectrum and the piperazine

nitrogen shifted from -343 to -339 ppm in the ^{15}N NMR spectrum (**Table 1**). The detected shifts were selective for the functional group where the protonation takes place. All other cross peaks in the spectrum did not shift. Similar results were observed for all amino acid counterions which were highfield shifted: Upon sodium salt formation especially the α-protons shifted particularly strong to the higher field, whereas the IL formation resulted in a less pronounced shift (**Table 2**).

Table 2 ^{1}H chemical shifts of relevant protons of the counterions, sodium salts of the counterions, and the ILs produced measured on a Bruker Avance III 400 MHz spectrometer in MeOH-d_4. The corresponding counterions are: *N*-acteyl aspartic acid (**a**), *N*-acetyl glycine (**b**), *N*-acetyl asparagine (**c**), *N*-acetyl glutamine (**d**), *N*-acetyl alanine (**e**), and *N*-acetyl glutamic acid (**f**).

	α-**H**	β-**H**	C**H**$_3$ acetyl group
N-acetyl aspartic acid	4.74	2.88 – 2.75	1.98
N-acetyl aspartic acid sodium salt	4.45	2.73 – 2.55	1.97
IL a	4.59	2.82 - 2.68	1.98
N-acetyl glycine	4.84	-	1.99
N-acetyl glycine sodium salt	4.86	-	1.98
IL b	4.85	-	1.98
N-acetyl asparagine	4.72	2.84 – 2.68	2.00
N-acetyl asparagine sodium salt	4.50	2.77 – 2.58	1.98
IL c	4.58	2.78 – 2.61	1.98
N-acetyl glutamine	4.39	2.22 – 1.88	1.99
N-acetyl glutamine sodium salt	4.21	2.22 – 1.88	2.00
IL d	4.28	2.20 – 1.88	1.98
N-acetyl alanine	4.37	-	1.97
N-acetyl alanine sodium salt	4.16	-	1.98
IL e	4.25	-	1.96
N-acetyl glutamic acid	4.43	2.24 – 1.87	1.99
N-acetyl glutamic acid sodium salt	4.17	2.17 – 1.81	1.99
IL f	4.31	2.22 – 1.89	1.98

The diffraction patterns of the free base, the mesylate salt, and the corresponding ILs were collected by powder diffractometry (**Figure 2**). Whereas the diffraction patterns of imatinib free base and mesylate salt clearly indicated crystalline materials, all ILs were completely amorphous.

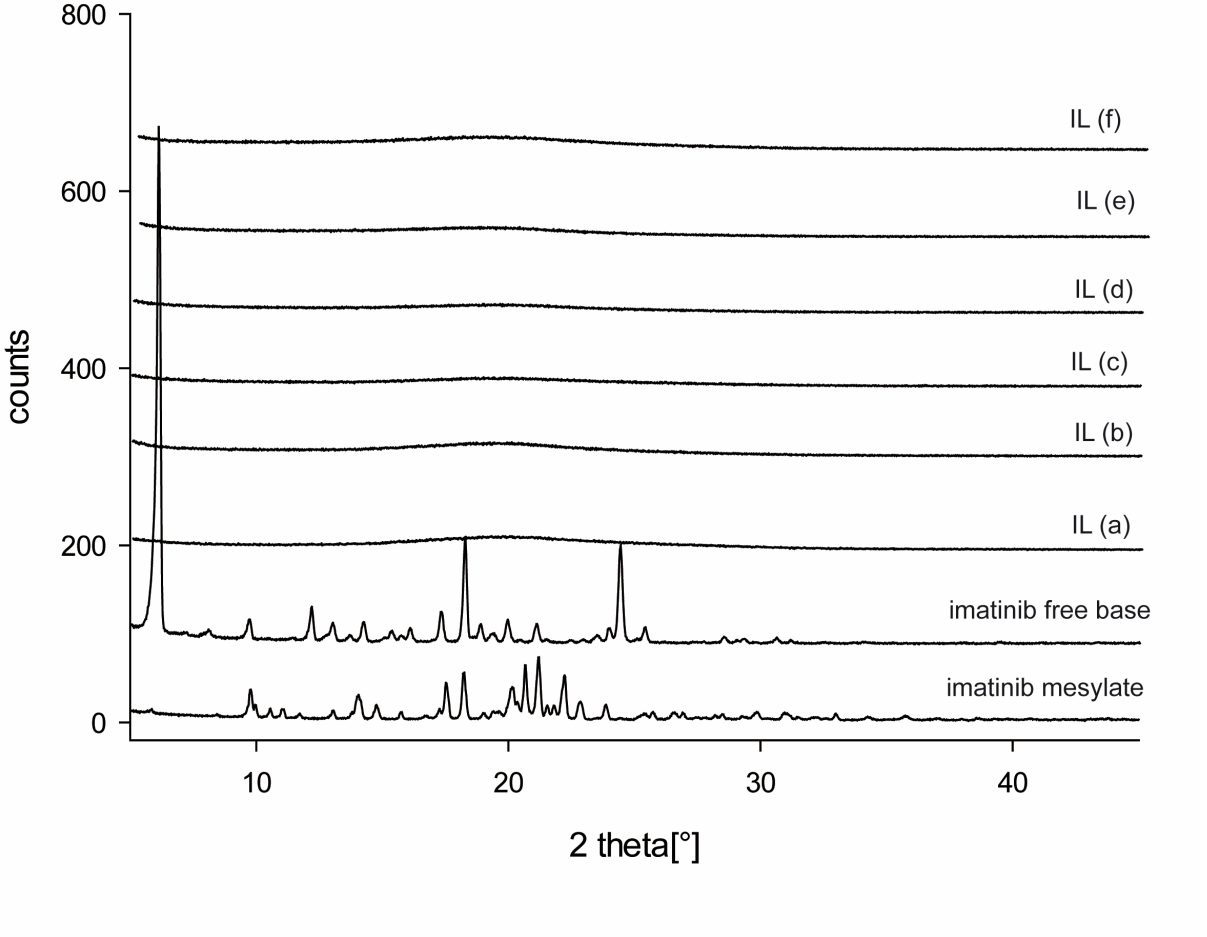

Figure 2 XRPD diffraction patterns of imatinib mesylate salt, imatinib free base, and the ILs produced. The corresponding counterions are: *N*-Acteyl aspartic acid (**a**), *N*-acetyl glycine (**b**), *N*-acetyl asparagine (**c**), *N*-acetyl glutamine (**d**), *N*-acetyl alanine (**e**), and *N*-acetyl glutamic acid (**f**).

To evaluate the stability of the ILs an accelerated stability testing according to ICH guideline Q1A[20] was performed at 40 °C and 75% relative humidity. After a time period of 6 months the XRPD diffractograms of IL (**b**), (**d**), and (**e**) indicated recrystallization of a small amount of imatinib free base. IL (**a**), (**c**), and (**f**) were still completely amorphous (**Figure 3**).

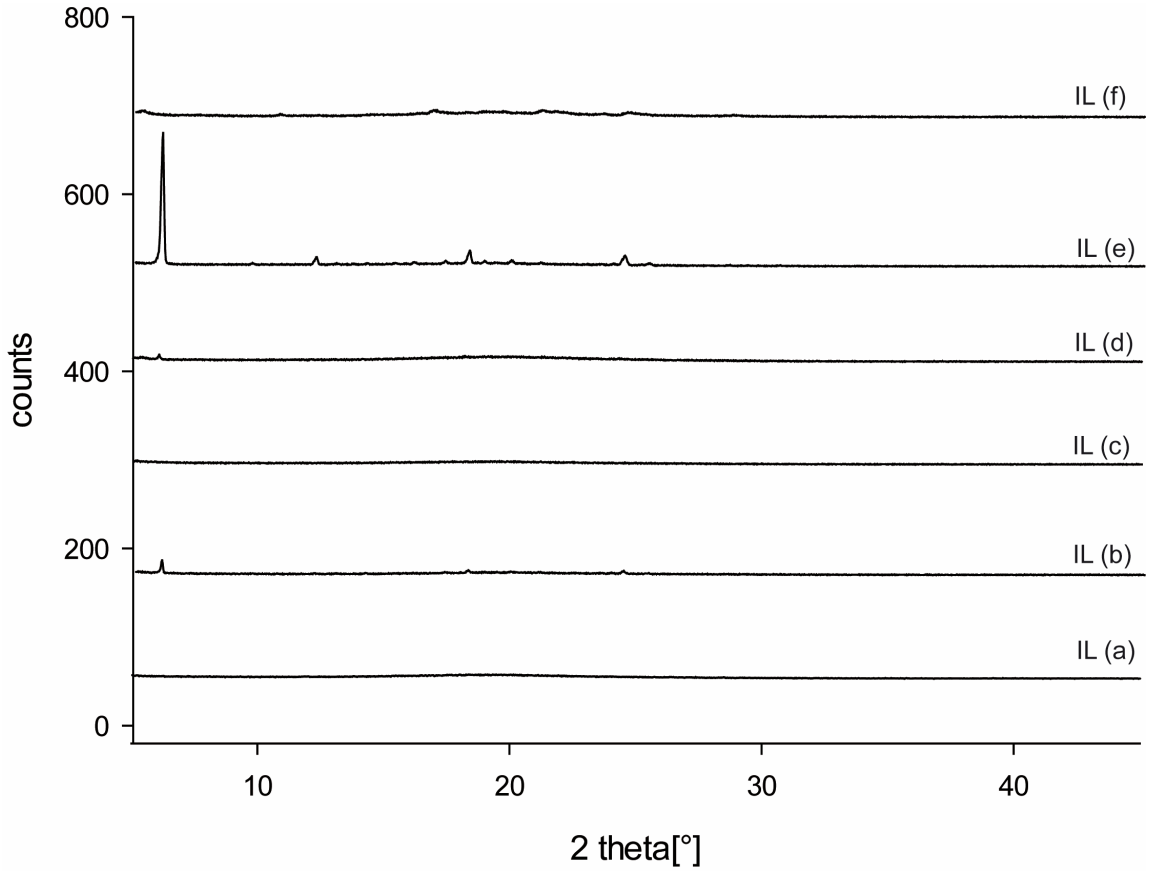

Figure 3 XRPD diffraction patterns of the ILs after 6 months of stability testing at 40 °C and 75% relative humidity. The corresponding counterions are: *N*-Acteyl aspartic acid (**a**), *N*-acetyl glycine (**b**), *N*-acetyl asparagine (**c**), *N*-acetyl glutamine (**d**), *N*-acetyl alanine (**e**), and *N*-acetyl glutamic acid (**f**).

Melting points and glass transition temperatures were determined by differential scanning calorimetry (**Table 3**). The crystalline mesylate salt had a melting point of 227 °C and the crystalline free base of imatinib had a melting point of 215 °C. Glass transition temperatures of all prepared compounds were lower than the melting points of the corresponding crystalline salts, ranging between 66 and 87 °C (**Table 3**). Hence, the compounds fulfil the definition of an IL[7]. To determine the extent of hygroscopicity a stress testing according to the procedure of The European Pharmacopeia 8.0 was performed[14]. The free base, the mesylate salt, and

all obtained ILs were exposed to a relative humidity of 80% and a temperature of 25 ± 0.5 °C. The increase in mass due to water vapour sorption was determined after 24 h by weighing. The water vapour sorption of all amorphous compounds produced was higher than that of the corresponding crystalline materials; for IL (**a-e**) water sorption ranged from 21.2 to 24.4%. IL (**f**) had the lowest amount of 19.1%. For the crystalline materials the results were totally different. The increase in mass for imatinib free base was 2.6% while the mesylate salt ranged at just 0.5% (**Table 3**).

Table 3 Melting points and glass transition temperatures as well as the increase in mass due to water sorption at 80% relative humidity and 25 °C of imatinib free base, mesylate salt, and the ILs produced. The corresponding counterions are: *N*-acteyl aspartic acid (**a**), *N*-acetyl glycine (**b**), *N*-acetyl asparagine (**c**), *N*-acetyl glutamine (**d**), *N*-acetyl alanine (**e**), and *N*-acetyl glutamic acid (**f**).

API	Water sorption (%)	RSD (%)	MP / T_g °C
imatinib free base	2.6	38.4	214.53
imatinib mesylate salt	0.5	36.0	226.68
imatinib IL a	24.1	20.0	79.31
imatinib IL b	24.4	14.4	68.40
imatinib IL c	21.2	11.4	65.58
imatinib IL d	23.2	19.4	87.96
imatinib IL e	22.7	10.6	79.29
imatinib IL f	19.1	27.5	86.71

For the counterions aqueous p*Ka* values ranging from 3.30 to 4.27 were measured on a Sirius T_3 instrument. For the API imatinib a basic p*Ka* value of 8.36 was determined (**Table 4**). For a better understanding and interpretation of the NMR experiments which were performed in MeOH-d_4, the p*Ka* values of the counterions and imatinib were extrapolated to theoretical values in pure methanol. A graphical method for extrapolation was used based on the work published by Yasuda[17] and Shedlovsky[18]. The p*Ka* values in methanol were totally different from the ones in water: Acidic p*Ka* values of the counterions ranged between 5.16 and 6.11. The basic p*Ka* value of imatinib was 6.73 (**Table 4**).

Table 4 p*Ka* values *versus* p*Ka* values extrapolated to methanol. Investigated compounds are: imatinib and all amino acid counterions. The corresponding counterions are: *N*-acteyl aspartic acid (**a**), *N*-acetyl glycine (**b**), *N*-acetyl asparagine (**c**), *N*-acetyl glutamine (**d**), *N*-acetyl alanine (**e**), and *N*-acetyl glutamic acid (**f**).

	p*Ka* values	**p*Ka* values extrapolated to methanol**
N-acetyl aspartic acid	4.27	6.11
N-acetyl glycine	3.45	5.22
N-acetyl asparagine	3.28	5.24
N-acetyl glutamine	3.30	5.16
N-acetyl alanine	3.49	5.26
N-acetyl glutamic acid	4.21	5.82
imatinib	8.36	6.73

Dissolution Rate and 24 h Solubility

The dissolution rate was determined for the free base of imatinib, the mesylate salt, and all ILs that were produced (**Figure 4**). At pH 2.0 all ILs showed significantly faster dissolution rates than the free base: IL (**a**), (**e**), and (**f**) showed a 2.5-fold and IL (**b**), (**c**), (**d**), and imatinib mesylate salt a 2-fold increase, achieving dissolution rates of about 40 µmol/min/cm^2. At pH 6.8 all ILs and the mesylate salt of imatinib had significantly faster dissolution rates than the free base, the mesylate salt 40 times and the ILs 50 to 70 times.

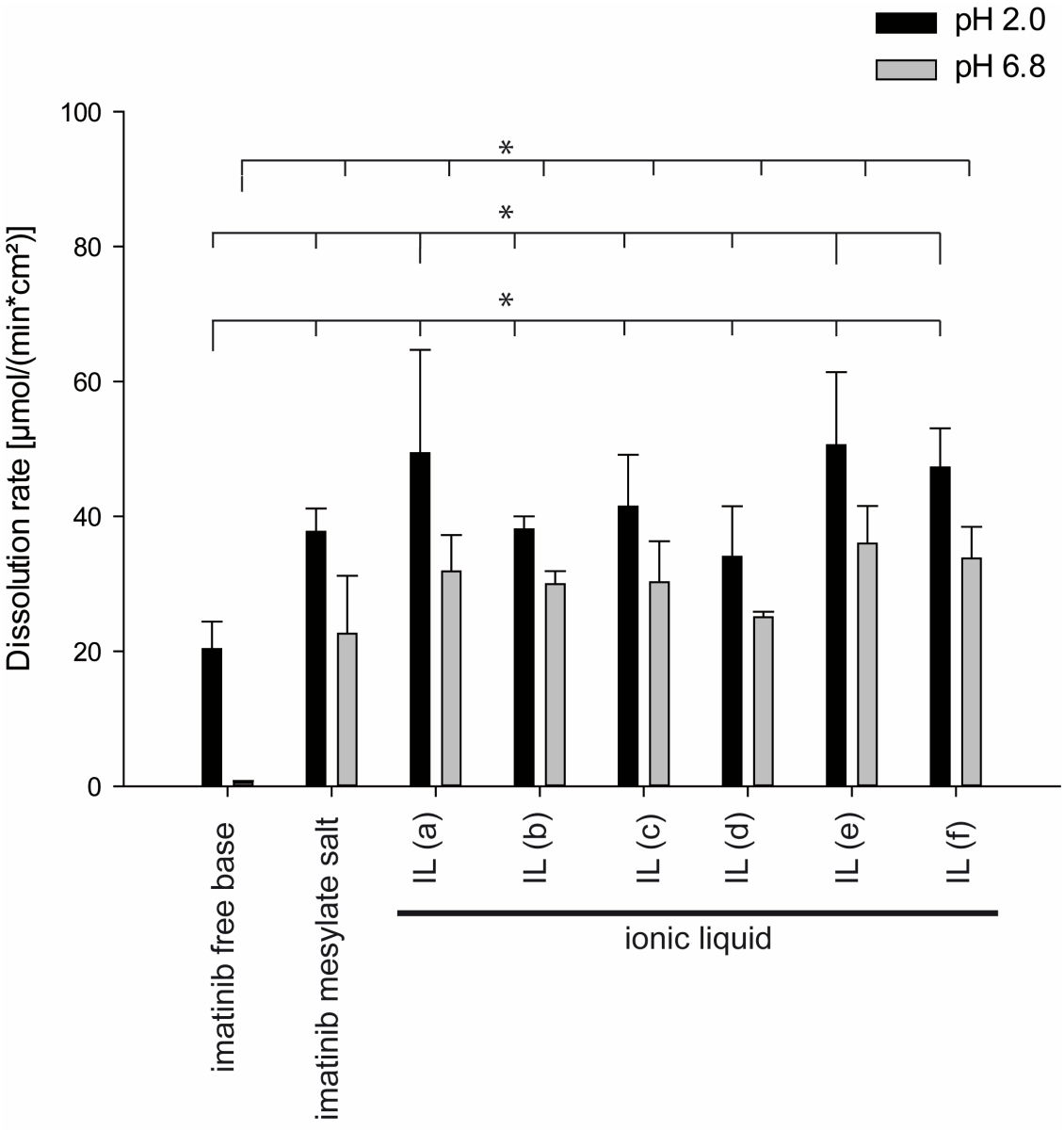

Figure 4 Dissolution rate in µmol/(min × cm^2) of imatinib free base, imatinib mesylate salt, and the ILs produced. The corresponding counterions are: *N*-acteyl aspartic acid (**a**), *N*-acetyl glycine (**b**), *N*-acetyl asparagine (**c**), *N*-acetyl glutamine (**d**), *N*-acetyl alanine (**e**), and *N*-acetyl glutamic acid (**f**).

24 h solubility profiles were recorded to compare the ILs, the free base, and the mesylate salt. Experimental conditions were set so that all compounds would reach a concentration of 10 mM when completely dissolved. The solubility of the free base in PBS buffer was quite low. The maximum concentration of 0.7 mM was reached seconds after adding the solvent. After 10 minutes recrystallization occurred, resulting in an equilibrium solubility of under 0.2 mM which was not changing within 24 h. The mesylate salt reached a plateau concentration of nearly 8 mM within seconds after adding the PBS buffer. After 8 h recrystallization occurred, reducing

the concentration level to that of the free base. All ILs reached plateau concentrations shortly after dissolution. The concentration levels ranged between 7 and 10 mM. No decrease in concentration or any recrystallization events were detected within 24 h (**Figure 5**).

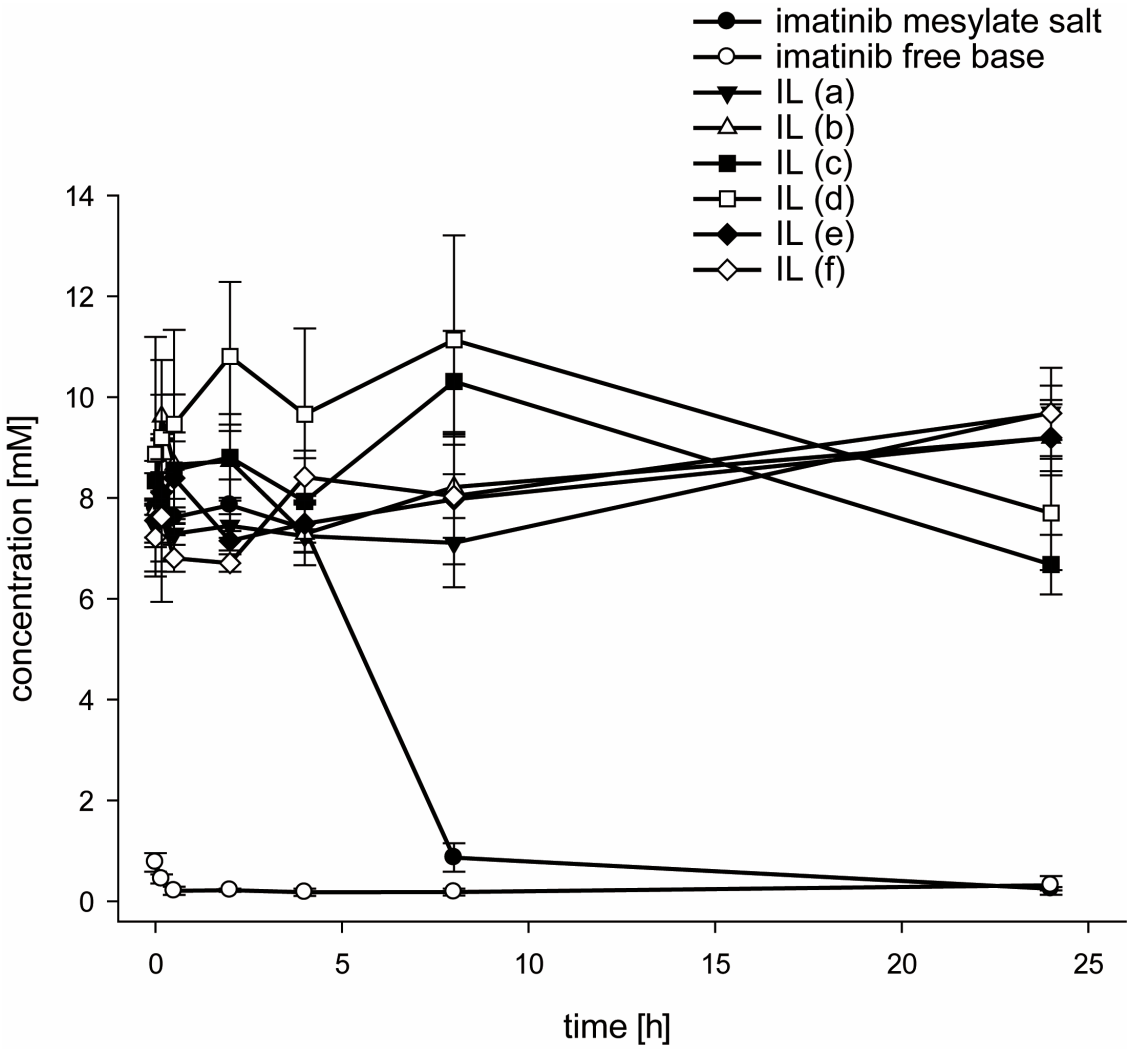

Figure 5 Concentration in mM *versus* time in h for imatinib free base, imatinib mesylate salt, and the ILs produced. The corresponding counterions are: *N*-acteyl aspartic acid (**a**), *N*-acetyl glycine (**b**), *N*-acetyl asparagine (**c**), *N*-acetyl glutamine (**d**), *N*-acetyl alanine (**e**), and *N*-acetyl glutamic acid (**f**).

Discussion

Successful oral product development needs adequate aqueous solubility and intestinal permeability[1]. Even if a drug candidate has reasonable membrane permeability, the absorption of the drug is often limited by its low solubility [5]. An adequate formulation development is very important for many new chemical entities being categorized as class II of the biopharmaceutical classification system (BCS)[21]. The aim of this study was to develop an IL concept for BSC class II compound imatinib as a weak base to optimize the rate and the extent of dissolution in gastrointestinal fluids for improvement of bioavailability. This kind of salt formation is a convenient way of improving dissolution kinetics. No additives or surfactants are necessary to get the API in solution. The right combination of API and counterion resulting in an ionized amorphous compound is responsible for improved solubility profile. Minimum difference of three *log* units between the p*Ka* value of the API and that of the counterion is required to form a stable salt[22]. Imatinib has four basic functional groups. As described in the literature the p*Ka* values are: 8.0, 3.7, 2.6, and 1.5[23]. The nitrogen in the piperazine ring next to the methyl group is the strongest base in the molecule with a p*Ka* of 8.36 according to experimental determination on Sirius T_3 instrument (**Table 4**). Thus, the nitrogen is protonated. Therefore, several acetylated amino acids with p*Ka* values ranging from 3.3 to 4.27 were selected as counterions (**Table 4**). The counterions used in this study are completely uncritical because of their character as amino acids. In contrast, alkyl sulfonates like the mesylate anion used as counterions in many marketed products like Gleevec® were criticised for the last years because of their genotoxic risks[24]. Six different ILs were successfully prepared for imatinib (**Figure 1**).

Comparison of the chemical shifts of the piperazine methyl group in the free base and the mesylate salt indicates a strong downfield shift for the mesylate salt whereas more gentle downfield shifts were found for the ILs. NMR studies of the counterions and their corresponding sodium salts, performed separately, confirm these hypothesis. Whereas a strong downfield shift is observed for every protonated counterion as compared to the corresponding sodium salt, also in this case the IL formation resulted in a less pronounced shift (**Table 2**).

It is well known that the chemical shifts of all atoms are related to the amount of charge present at the atom[25]. They can be used to determine both the p*Ka* values

and the locus of protonation[26]. Evaluation of pH depending NMR shifts results in titration curves which can be used to calculate the p*Ka* values of substances[26]. Thus, NMR spectroscopy is a powerful tool to monitor the proton transfer from a Brønsted acid to a Brønsted base in a protic IL and to determine the degree of proton transfer and thus whether the substance is ionized or hydrogen bonded complexes are present[12,27,28]. Downfield shifts of both the ^{1}H and the ^{15}N spectra of imatinib indicate weaker electron density through H-bonding. Upfield shifts of the ^{1}H NMR spectra of the counterions indicate stronger electron density because of loss of the proton. Thus, the ionic nature of all compounds produced is successfully proved by NMR studies (**Table 1**). It has to be considered that NMR studies only indicate the ILs existing in equilibrium with excess acid or amine. Due to the fast proton exchange between excess of acid or amine, only an average of protons is observed on the NMR time scale[29]. Nevertheless, the results indicate the formation of ionized compounds, but the protonation may not be at 100% like in the mesylate salt because of less pronounced chemical shifts. The reason for this phenomenon is due to the weaker tendency of imatinib as well as amino acid counterions to dissociate in methanol in comparison to water. Methanol was used as appropriate solvent for NMR studies. Imatinib is a weaker base and the counterions are weaker acids in methanol than in water. p*Ka* values of imatinib and the counterions were extrapolated to theoretical values in pure methanol using the procedure published by Yasuda and Shedlovsky[16-19,30,31]. The basic p*Ka* value of imatinib in methanol was 6.73 compared to an aqueous value of 8.36. Acidic p*Ka* values of the counterions ranged between 5.16 and 6.11 in methanol in comparison to aqueous values from 3.28 to 4.27 (**Table 4**). Thus, the minimum difference of three *log* units between the p*Ka* value of the API and that of the counterion to form a stable salt is not given when methanol is used as solvent. In contrast, methanesulfonic acid is a much stronger acid in such a way as to protonate imatinib completely even though methanol is used as solvent.

Whereas the free base and the mesylate salt of imatinib were crystalline materials, the diffraction patterns of all compounds produced were showing amorphous structures (**Figure 2**). An accelerated stability testing at 40 °C and 75% relative humidity indicated good physical stability of all ILs. After a time period of 6 months

at these conditions, there was no indication for recrystallization in IL (**a**), (**c**), and (**f**). IL (**b**), (**d**), and (**e**) indicated recrystallization of imatinib free base in a very small extent (**Figure 3**). Glass transition temperatures of the ILs produced were a lot lower than the melting points of the crystalline salts (**Table 3**). Nevertheless, having glass transition temperatures at more than 65 °C all ILs were solids at room temperature which is an important factor for handling and administration. A more diffuse charge distribution because of the used asymmetric and bulky counterions lowers the melting points as compared to the crystalline salts[32].

For analysis of the dissolution rates two different media were used: To imitate physiological conditions of the stomach, measurements were performed in an acetate puffer pH 2.0. A PBS buffer pH 6.8 was applied as an appropriate dissolution medium to mimic conditions in the small intestine. At both conditions all ILs prepared had significant faster dissolution rates than the corresponding free base (**Figure 4**). Additionally, at pH 2.0 IL (**a**, **e**, **f**) had significant faster dissolution rates than imatinib mesylate salt (**Figure 4**). This observation is interesting because of the complete protonation of the carboxylate anions of the counterions at this pH value. No relevant concentration of counterion is present in these conditions, but imatinib performs as an IL.

The results indicate that lowering lattice forces by forming amorphous ILs, is a reliable tool to improve their solubility profile. 24 h solubility profiles in PBS buffer of the ILs, the mesylate salt, and the free base indicate a higher solubility and a prolonged supersaturation time for every IL produced as compared to the corresponding crystalline materials. Whereas the equilibrium solubility of the free base ranged at just 0.2 mM, the mesylate salt had initially a 40-fold higher solubility which can be interpreted as a supersaturation phenomenon. However, this supersaturated state was unstable and recrystallization occurred after 8 h resulting in the solubility level of the free base (**Figure 5**). In contrast, all ILs showed a distinctive supersaturation phenomenon which was more stable. Concentration values ranging between 7 and 10 mM were reached seconds after adding the solvent. No decrease in concentration or any recrystallization event was observed within 24 h. Data indicate also that the rate and extent of dissolution and especially the time of supersaturation is not only an effect of the protonated state of the API. A special tailor made counterion is necessary for every individual API to get the

dissolution kinetics up to the favoured level to reach acceptable plasma concentrations. According to the criteria of the European Pharmacopeia 8.0 imatinib free base can be categorized as ‘hygroscopic’ whereas imatinib mwsylate salt can be categorized as ‘slightly hygroscopic’[14]. All ILs are ‘very hygroscopic’ whereas the mesylate salt shows no indication of water vapour sorption. The process of water vapour sorption is reversible and no degradation was observed according to NMR measurements. Therefore, special demands on packaging material and handling are necessary.

Conclusion

ILs were successfully prepared for imatinib resulting in lower melting points as compared to the corresponding crystalline materials. All compounds produced were slightly yellow solids at room temperature. Dissolution rates and solubility as well as supersaturation time were significantly increased. The increased property of water vapour sorption is an disadvantage in handling which shouldn’t be neglected. The IL concept was first time applied to the API imatinib as a weak base and is demonstrating its excellent suitability for formulating poorly water-soluble drugs.

Acknowledgments

The Bayerische Forschungsstiftung (BFS) is gratefully acknowledged for financial support. We thank Novartis Pharma AG for providing imatinib mesylate salt. We thank Nora Scharfenberger for the support in experimental work and for plenty of fruitful discussions.

References

[1] Williams R. O., Watts A. B., Miller D. A., Formulating Poorly Water-soluble Drugs. *Springer*. **2012.**

[2] Hillery A. M., Lloyd A. W., Swarbrick J., Drug delivery and targeting: for pharmacists and pharmaceutical scientists: *CRC Press*, **2002.**

[3] Fahr A., Liu X., Drug delivery strategies for poorly water-soluble drugs. *Expert. Opin. Drug Deliv.* **2007,** 4(4): 403–416.

[4] Pouton C. W., Lipid formulations for oral administration of drugs: non-emulsifying, self-emulsifying and 'self-microemulsifying' drug delivery systems. *Eur. J. Pharm. Sci.* **2000,** 11 (2): 93–98.

[5] Pouton C. W., Formulation of poorly water-soluble drugs for oral administration: physicochemical and physiological issues and the lipid formulation classification system. *Eur. J. Pharm. Sci.* **2006**, 29(3–4): 278–287.

[6] Serajuddin A. T., Salt formation to improve drug solubility. *Adv. Drug Deliv. Rev.* **2007,** 59(7): 603–616.

[7] Ferraz R., Branco L. C., Prudencio C., Noronha J. P., Petrovski Z., Ionic liquids as active pharmaceutical ingredients. *Chem. Med. Chem.* **2011,** 6(6): 975–985.

[8] Shamshina J.L., Barber P.S., Rogers R. D., Ionic liquids in drug delivery. *Expert. Opin. Drug Deliv.* **2013,** (10): 1367–1381.

[9] Bica K., Rijksen C., Nieuwenhuyzen M., Rogers R. D., In search of pure liquid salt forms of aspirin: ionic liquid approaches with acetylsalicylic acid and salicylic acid. *Phys. Chem. Chem. Phys.* **2010,** 12(8): 2011–2017.

[10] Hough W. L., Rogers R. D., Ionic Liquids Then and Now: From Solvents to Materials to Active Pharmaceutical Ingredients. *Bul. Chem. Soc. Jap.* **2007,** 80(12): 2262–2269.

[11] Tang S., Liu S., Guo Y., Liu X., Jiang S., Recent advances of ionic liquids and polymeric ionic liquids in capillary electrophoresis and capillary electrochromatography. *J. Chromatogr A.* **2014,** 1357: 147–157.

[12] Balk A., Holzgrabe U., Meinel L., 'Pro et contra' ionic liquid drugs - Challenges and opportunities for pharmaceutical translation. *Eur. J. Pharm. Biopharm.* **2015,** 94: 291–304.

[13] Balk A., Wiest J., Widmer T., Galli B., Holzgrabe U., Meinel L., Transformation of acidic poorly water-soluble drugs into ionic liquids. *Eur. J. Pharm. Biopharm.* **2015,** 94: 73–82.

[14] European Directorate for the Quality of Medicines. Characters Section in Monographs. Hygroscopicity. *European Pharmacopeia 8.0.* **2014,**: 695.

[15] Gravestock T., Box K., Comer J., Frake E., Judge S., Ruiz R., The “GI dissolution” method: a low volume, in vitro apparatus for assessing the dissolution/precipitation behaviour of an active pharmaceutical ingredient under biorelevant conditions. *Anal. Methods.* **2011,** (3): 560.

[16] Schönherr D., Wollatz U., Haznar-Garbacz D., Hanke U., Box K., Taylor R., et al., Characterisation of selected active agents regarding pK a values, solubility concentrations and pH profiles by SiriusT3. *Eur. J. Pharm. Biopharm.* **2015,** 92:1 55–70.

[17] Yasuda M., Dissociation constants of some carboxylic acids in mixed aqueous solvents. *Bul. Chem. Soc. of Jap.* **1959,** 32(5): 429–432.

[18] Shedlovsky T., The behaviour of carboxylic acids in mixed solvents. *Electr. Pergamon Press, NY.* **1962,**: 146–151.

[19] Avdeef A., Box K., Comer J., Gilges M., Hadley M., Hibbert C., et al., PH-metric logP 11. pK a determination of water-insoluble drugs in organic solvent–water mixtures. *J. Pharm. Biomed. Anal.* **1999,** 20(4): 631–641.

[20] Food and Drug Administration, Guidance for industry Q1A (R2) stability testing of new drug substances and products. *Food and Drug Administration Rockville, MD*. **2003.**

[21] Yu L. X., Amidon G. L., Polli J. E., Zhao H., Mehta M. U., Conner D. P., et al., Biopharmaceutics classification system: the scientific basis for biowaiver extensions. *Pharm. Res.* **2002,** 19(7): 921–925.

[22] Bastin R. J., Bowker M. J., Slater B. J., Salt selection and optimisation procedures for pharmaceutical new chemical entities. *Org. Proc. Res. Dev.* **2000,** 4(5): 427–435.

[23] Budavari S., O'Neil M., Smith A., Heckelman P., Obenchain J. R., Gallipeau J., et al., The Merck Index, An Encyclopedia of Chemicals, Drugs, and Biologicals, *Merck & Co. Inc;* **2001.**

[24] Kim S., Salt Formation of Pharmaceutical Compounds and Associated Genotoxic Risks. Pharmaceutical Industry Practices on Genotoxic Impurities. *Lee, Heewo*n. **2014,** 385–426.

[25] Callaghan P. T., Principles of nuclear magnetic resonance microscopy: *Oxf. Univ. Press Dem.* **1993.**

[26] Holzgrabe U., Wawer I., Diehl B., NMR spectroscopy in drug development and analysis. *John Wiley & Sons;* **2008.**

[27] Moreira D. N., Fresno N., Pérez-Fernández R., Frizzo C. P., Goya P., Marco C., et al., Brønsted acid–base pairs of drugs as dual ionic liquids: NMR ionicity studies. *Tetrahedron.* **2015,** 71(4): 676–685.

[28] Noack K., Schulz P. S., Paape N., Kiefer J., Wasserscheid P., Leipertz A., The role of the C2 position in interionic interactions of imidazolium based ionic liquids: a vibrational and NMR spectroscopic study. *Phys. Chem. Chem. Phys.* **2010,** 12(42): 14153–14161.

[29] Nuthakki B., Greaves T. L., Krodkiewska I., Weerawardena A., Burgar M. I., Mulder R. J., et al., Protic ionic liquids and ionicity. *Aus. J. Chem.* **2007,** 60(1): 21–28.

[30] Avdeef A., Comer J. E., Thomson S. J., pH-Metric log P. 3. Glass electrode calibration in methanol-water, applied to pKa determination of water-insoluble substances. *Anal. Chem.* **1993,** 65(1): 42–49.

[31] Takács-Novák K., Box K. J., Avdeef A., Potentiometric pK a determination of water-insoluble compounds: validation study in methanol/water mixtures. *Int. J. Pharm.* **1997,** 151(2): 235–248.

[32] Stoimenovski J., MacFarlane D. R., Bica K., Rogers R. D., Crystalline vs. ionic liquid salt forms of active pharmaceutical ingredients: a position paper. *Pharm. Res.* **2010,** (4): 521–526.

3.2 Overcoming Solubility Challenges of Triazolopyrimidine NOX-Inhibitors

Nina Hecht, Nils Terveer, Ulrike Holzgrabe, Lorenz Meinel

Manuscript in preparation

Abstract

Triazolopyrimidine derivatives have been found to be efficient and selective NADPH oxidase inhibitors *in vitro*. Presently, there are numerous publications examining these promising compounds intended for the treatment of cardiovascular diseases, however none of these studies have gone beyond cell culture tests. Yet the poor aqueous solubility of triazolopyrimidines has proven to be a severe drawback in the drug development process hindering *in vivo* application. In this work, a characterization of the solubility of the three triazolopyrimidine derivatives VAS2870, VAS3947, and VAS4024 was performed. Based on these results, VAS3947 was selected for further formulation development. Three commonly used formulation approaches were investigated to create a supersaturated solution and thus to improve the bioavailability of the API, namely spray drying, microemulsification, and incorporation into cyclodextrins. The poor aqueous solubility of VAS3947 was improved with all approaches. Finally, a microemulsion intended for oral administration and a cyclodextrin formulation of VAS3947 suitable for intravenous application were prepared in order to conduct *in vivo* studies. In conclusion, this work demonstrates the great utility of supersaturation formulation strategies for the solubility improvement of drugs in order to enable the *in vivo* application and to promote further clinical development.

Introduction

Reactive oxygen species (ROS) play an important role e.g. in cell signalling processes[1], however, harmful effects caused by oxidative stress clearly predominate the advantages and are among the main causes of death in industrialized countries. There is a clear evidence that ROS contribute to the development of cardiovascular diseases such as hypertension, atherosclerosis, as well as neurodegenerative disorders, and the progression of carcinogenesis[2]. Due to the aging population in developed countries it is to be expected that the mortality caused by oxidative stress will further increase. This illustrates the urgent need of effective therapeutic options for the treatment of high ROS levels which are generating when the ratio between ROS and antioxidants becomes pathologically unbalanced[3]. NADPH oxidases have been identified as the main source of endothelial ROS formation[4]. Consequently, efforts were focused on therapeutically targeting these NADPH oxidases by inhibitors known as VAS2870, VAS3947, and VAS4024 (**Figure 1**). There are great expectations that these compounds are able to clearly reduce the high incidence of deaths resulting from endothelial dysfunctions such as myocardial and ischemic strokes.

Scores of publications confirm the *in vitro* efficacy of the VAS compounds[5-7]. VAS2870 was found to inhibit oxidized low-density lipoprotein (oxLDL)-mediated ROS formation in human endothelial cells[5]. VAS3947 was found to completely inhibit the NADPH-dependent ROS production in CaCo-2 cell homogenates (IC_{50} 12 µM), in HL-60 human cells (IC_{50} 2 µM), and in the vascular cell line A7r5 from rats (IC_{50} 13 µM), which is far below the IC_{50} of other known NADPH oxidase inhibitors[6]. Furthermore, the NADPH inhibition by VAS2870 and VAS3947 was confirmed in different cell free systems, cells, and tissues[7]. In spite of these highly promising effects, the therapeutic application in humans is compromised by their low aqueous solubility. The aim of this research work was to overcome the compounds' limitations through formulation strategies without modifying their chemical structure.

Following a physicochemical characterization (determination of melting points, log *P*, kinetic and thermodynamic solubility), three different formulation strategies were deployed: spray drying, preparation of a microemulsion, and complexation with cyclodextrins. The incorporation of the API into the cyclodextrin cavity was

confirmed by ^{1}H NMR and ROESY studies. Finally, one microemulsion for oral administration and one cyclodextrin formulation for i.v. application were presented.

Materials and Methods

Materials

VAS2870, VAS3947, and VAS4024 were kindly supplied by Vasopharm GmbH (Würzburg, Germany). Solvents, reagents, excipients, and materials were purchased from Sigma Aldrich (Schnelldorf, Germany), unless noted otherwise. Deionized water was taken from an in-house supply with a Milli-Q® system (Merck Millipore GmbH, Darmstadt, Germany), or purchased from Fisher Scientific (Schwerte, Germany).

96-well plates with flat bottom were from Greiner (Frickenhausen, Germany).

Suppliers of polymers and excipients used for the spray dried formulations and microemulsions are listed in **Table 5** and **6.** Cyclodextrins were purchased from Sigma Aldrich and Wacker Chemie AG (München, Germany). Capryol®, PGMC, and Labrafac® Lipophile WL 1349 were from Gattefossé (Bad Krozingen, Germany). Biorelevant medium (FaSSIF) was obtained from biorelevant (London, UK).

HPLC columns were purchased from Phenomenex (Aschaffenburg, Germany). 5 mm NMR tubes (S-5-900-7) and related coaxial inserts (WGS 5-BL) were purchased from Norell Inc. (Marion, NC). Deuterium oxide, deutero dimethylsulfoxide, and deutero chloroform were from Deutero GmbH (Kastellaun, Germany).

Petroleum ether, ethyl acetate, and syringe filters (0.22 µm) were from VWR International GmbH (Darmstadt, Germany). All compounds were at least of analytical or pharmaceutical grade and were used without further purification.

Methods

Physicochemical Characterization of the Starting Products

a) Differential Scanning Calorimetry

A DSC 8000 instrument from Perkin Elmer (Waltham, MA) was used for differential scanning calorimetry (DSC) studies. The sample (2–5 mg) was weighed into an aluminium pan and sealed including a small hole for pressure equilibration. Melting points were determined from the first heating cycle. The process parameters were as follows: the heating rate was 20 K/min, the nitrogen gas flow was 20 mL/min, the temperature range was -50 °C to 200 °C. Subsequently, samples were cooled to -50 °C at a cooling rate of 50 K/min and then again heated up to 200 °C at a rate of 20 K/min for the determination of glass transition temperatures and degradation events.

b) Log *P* Assessment

The log *P* value was experimentally determined on an Agilent 1100 chromatographic system (Agilent Technologies GmbH) equipped with an online degasser (G1322A), a binary pump (G1312A), an autosampler (G1313A), a thermostated column department, and a diode array UV/VIS detector (G1315B). The ChemStation® software package was used for data handling (Agilent Technologies GmbH).

HPLC-UV analysis was performed according to the method as described previously[7]. A Phenomenex Synergi Max RP (150 × 4.6 mm, 4 µm particle size) analytical column was used. Isocratic elution was performed with a 10 mM phosphate buffer pH 7.0 (30% v/v) and methanol adjusted with 0.02% *N,N*-dimethylhexylamine (70% v/v). The column compartment was maintained at 30 °C, the flow rate was 1.0 mL/min, and 40 µL volume of every sample were injected. The stop time was 20 min.

For sample preparation all substances were dissolved in methanol at a concentration of 40 µg/mL. Afterwards, each solution was transferred into a separate HPLC vial. Thiourea was used for determination of dead time. 2-phenylethanol, benzene, N,N-dimethylaniline, toluene, chlorobenzene, ethylbenzene, biphenyl, and anthracene were used as reference substances with known log *P* values.

c) Solubility Assessment of Starting Products

For the kinetic solubility assessment nephelometrical studies were conducted using a NEPHELOstar system from BMG Labtech GmbH (Ortenberg, Germany). A 5 mM stock solution of VAS2870 and VAS4024 and a 15 mM stock solution of VAS3947 were prepared in DMSO. Thereafter, dilution series in PBS buffer (pH 7.4, 5% DMSO) were performed. The following concentrations were created: VAS2870 and VAS4024: 25, 50, 75, 100, 125, 150, 175, 200, 225, 250 µM, VAS3947: 75, 150, 225, 300, 375, 450, 525, 600, 675, 750 µM. The temperature was set to 37 °C, the laser intensity was set to 80% and the laser beam focus was 2.20 mm. The mean solubility of the compounds was determined immediately after preparation (T0) and after 60 minutes (T60).

The investigation of the thermodynamic solubility was performed using a heatable shaker from Eppendorf AG (Hamburg, Germany) and an HPLC-UV system from Jasco (Groß-Umstadt, Germany) equipped with an online degasser (DG-2080-53), a gradient pump (PU-1580), an autosampler (AS-2051Plus), an UV/VIS detector (UV-2075Plus), and a column compartment from Phenomenex (Thermasphere TS-130). The Galaxie® chromatography software package was used for data handling (Version 1.9.3.2., Varian, Inc., CA).

Approximately 3 mg of VAS3947 were weighed into an Eppendorf vial, PBS buffer (pH = 7.4) was added, and samples were sonicated in a Sonorex ultrasonic bath (Bandelin electronic GmbH, Berlin, Germany) for 5 seconds and incubated in a heated shaker at 37 °C and 800 rpm.

70 µL samples of the suspension were taken after 2, 10, 30, 60, 120, and 240 minutes. The samples were immediately centrifuged for 2 minutes at 13.000 rpm using a Mikro 22R centrifuge from Andreas Hettich GmbH (Tuttlingen, Germany).

The supernatant was collected, diluted with acetonitrile (1/1), shaken, and analysed by HPLC. The chromatographic conditions are illustrated in **Table 1**. The sample concentration was calculated from a regression line ranging from 0.1 to 250 µg/mL.

Table 1 Chromatographic conditions for the assessment of the solubility of pure VAS compounds.

Analytical column	Phenomenex Synergi Polar RP (80 Å, 40 × 4.6 mm, 4 µm)
Mobile phase A	water and acetonitrile at a ratio of 90/10% and 0.05% TFA
Mobile phase B	water and acetonitrile at a ratio of 10/90 and 0.05% TFA
Gradient profile	from 0 min to 1.5 min from 80% to 60% mobile phase A from 1.5 min to 4.0 min 60 mobile phase A
Flow rate:	2.0 mL/min
Injection volume	15 µL
Detection wavelength	λ = 277 nm
Column temperature	room temperature

Execution of Three Different Formulation Approaches

a) Spray Dried Formulations in Comparison to Physical Mixtures

The first approach to be investigated for solubility improvement of VAS397 was the spray drying concept. The solubilities of VAS3947 presented in different spray dried formulations were compared to those derived from physical mixtures of the respective excipients. Physical mixtures of VAS3947 and seven different excipients (Eudragit® L100, Eudragit® L100-55, Eudragit® RL PO, HPMC, Kollidon® 30, Kollidon® VA 64, and Soluplus®) were prepared by mixing in a mortar and subsequent pestling for 1 minute resulting in a mass ratio of 1 amount of VAS3947 + 10 amounts of the excipient.

Spray dried nanoparticles were prepared from VAS3947 and the excipients listed above in a 1+10 mass ratio using a Nano Spray Dryer B-90 from Büchi Labortechnik GmbH (Essen, Germany).

Samples were prepared from VAS3947 and excipients which were dissolved in either methanol or 2-propanol **(Table 1)** to result in 0.2% VAS3947 and 2% excipient in solution. This solution was spray dried with the spray head in the vertical position, 7 µm mesh size and a spray rate of 100%. The formulations were stored in amber glass vials in an exsiccator with silica gel at room temperature.

Characterization by X-Ray Powder Diffractometry (XRPD)

Powder diffractometric studies were performed on a Bruker Discover D8 powder diffractometer (Rheinstetten, Germany). Cu K-alpha radiation at a power of 40 kV and 40 mA, a focusing Goebel Mirror, and a fixed divergence slit were used. Approximately 4 mg of each of the samples were transferred onto a silicon single crystal zero background specimen holder. The step size was set to 0.025° and 0.25 s time per step in the range of 5–45°. Samples were analysed in reflection geometry and detection was done with a LynxEye® 1D-detector (Bruker AXS) using the full detector range of 192 channels. 2.5° axial soller slits were mounted in the primary and secondary beam path. Data collection and processing were done using the software packages DIFFRAC.Suite® (V2 2.2.690, Bruker AXS 2009-2011) and DIFFRAC.EVA® (Version 3.0, Bruker AXS 2010-2013).

Dissolution of Spray Dried Formulations and Physical Mixtures

The dissolution rates of VAS3947 from spray dried formulations and physical mixtures were determined using the dissolution conditions as described for the investigation of thermodynamic solubility (see p. 55).

Approximately 3 mg of the spray dried formulations and the respective physical mixtures were dosed into PBS buffer. The solubility was determined in triplicate using the HPLC instrument and method as described for the determination of thermodynamic solubility (see p. 55 to 56).

Supersaturation ratios were calculated based on the solubility of pure VAS3947 after 120 minutes (standardized to 1) in relation to the concentration resulting from the respective spray dried formulation or physical mixture at the same time-point.

Determination of pH, Particle Size, Zeta Potential, and Crystallinity

pH value, particle size, and zeta potential were assessed after 120 minutes. The pH value was measured with an InLab® Semi-Micro-L pH electrode from Mettler-Toledo (Greifensee, Switzerland). Particle size and zeta potential were determined using a Delsa™ Nano HC system (Beckman Coulter GmbH, Krefeld, Germany).

Prior to the determination of the particle size, a filtration step was performed using Acrodisc 25 mm syringe filters with a 5 µm Versapor membrane. Afterwards, samples were diluted with PBS buffer (1:5), transferred into disposable cuvettes (1 cm path length), and the particle size was determined (scattering angle: 165 °, accumulations: 50, repetitions: 3, temperature: 37 °C).

Outliers from 50 accumulations were excluded when the standard deviation was > 30 µm. Results were reported as mean ± SD from three repetitions.

Samples were further characterized regarding zeta potential after 1:4 dilution with PBS buffer (15° scattering angle, 8 accumulations, 3 repetitions, temperature of 25 °C). After termination of the dissolution experiment, precipitates of the spray dried formulations were evaporated to dryness and analysed by XRPD.

b) Microemulsion Concept

Pre-Formulation Study with Different Excipients

The second concept for improving the solubility of VAS3947 to be investigated was the microemulsion approach. At first, a pre-formulation study was conducted to identify appropriate excipients:

For this purpose binary mixtures of VAS3947 (approx. 2.5 mg) and 32 different lipid excipients (approx. 250 mg) were weighed into 1.5 mL vials, respectively. PBS buffer served as negative control. After vortex-mixing for 3 minutes, the samples were centrifuged for 2 minutes at 10.000 rpm and 37 °C. 40–50 mg of the particle-free supernatant were collected, diluted with 1900 µL acetonitrile, sonicated for 10 minutes, and again centrifuged for 10 minutes at 10.000 rpm and 37 °C.

The concentration of VAS3947 (T0) in the clear supernatant was analysed by HPLC using the instrument and method as described for the determination of the thermodynamic solubility (see p. 55 to 56). Afterwards, the binary mixtures were placed on a shaker for 24 h at 250 rpm, again sonicated for 3 minutes and prepared as described above for the HPLC analysis (see p. 55 to 56).

Preparation and Characterization of the Final Microemulsions

For the preparation of microemulsions, excipients (**Table 6**) were weighed into a 2 ml vial and shaken for 30 seconds. Subsequently, VAS3947 was added and shaken for 3 minutes, followed by 10 minutes of sonication at 50 °C.

The microemulsions were visually controlled for the absence of any crystals and precipitates. To measure the particle size, the microemulsions were diluted with water (1:10) and analysed by dynamic light scattering using the instrument and method as described for the determination of particle size after dissolution of spray dried formulations (see p. 58).

To determine the maximum drug load that could be dissolved in each of the four microemulsions, VAS3947 was added to the respective blank microemulsion and shaken until a precipitate was observed. Subsequently, the microemulsions were centrifuged for 10 minutes at 14.000 rpm and 37 °C.

The concentration of VAS3947 in the supernatant was analysed by means of HPLC-UV analysis. This was done by diluting 25 mg of the clear supernatant with 500 µL acetonitrile, shaking the solution for 2 minutes, and followed by centrifugation for 10 minutes at 10.000 rpm and 5 °C. The samples were further diluted with acetonitrile (1:40) and analysed using the HPLC instrument and method as described for the determination of thermodynamic solubility (see p. 55 to 56).

The dissolution of VAS3947 from the microemulsions was performed as described by other groups before[8]: 200 mg of the respective microemulsion were weighed into 10 mL Falcon tubes and diluted with 3.6 mL digestion medium (FaSSiF). After 10 minutes of incubation in a heated shaker at 37 °C and 750 rpm, 0.4 mL of a freshly prepared pancreatin solution (0.2 g/mL in digestion buffer) were added to the samples.

Aliquots (0.2 mL) were taken at 2, 5, 10, 15, 20, 30, 45, 60, 90, and 120 minutes, respectively, and immediately treated with 3 µL of a 1M solution of 4-bromophenylboronic acid in methanol to stop further pancreatin mediated lipolysis of the formulation.

All samples were centrifuged for 30 minutes at 14.000 rpm and 37 °C. The supernatant was diluted with acetonitrile (1:10), shaken, and centrifuged for 20 minutes at 14.000 rpm and 37 °C. HPLC analysis was performed using the instrument and method as described for the determination of thermodynamic

solubility (see p. 55 to 56). Throughout the dissolution study, pH was monitored (pH Meter 744 from Metrohm, Herisau, Switzerland) and maintained at 6.5 ± 0.1 by adding 0.4 M sodium hydroxide if required. Supersaturation ratios were calculated based on the solubility of VAS3947 after 120 minutes in relation to the concentration of VAS3947 as released from microemulsions.

c) Complexation with Cyclodextrins

Screening for Appropriate Cyclodextrins

The third concept for improving the solubility of VAS3947 to be investigated was the complexation with cyclodextrins. At first, a screening was performed to identify appropriate cyclodextrin candidates and their amount of increasing the aqueous solubility of VAS3947: 10 different cyclodextrins were dissolved in PBS buffer (pH = 7.4) and diluted as outlined (**Table 2**) depending on the maximum solubility in the dilution medium.

Table 2 List of tested cyclodextrins and respective concentrations.

Cyclodextrin	Concentration (% w/w)
α-cyclodextrin	0.625, 1.25, 2.5, 5, 10
β-cyclodextrin	0.0625, 0.125, 0.25, 0.5, 10
γ-cyclodextrin	1.25, 2.5, 5, 10, 20
sulfated-β-cyclodextrin	2.5, 5, 10, 20, 40
methyl-β-cyclodextrin	2.5, 5, 10, 20, 40
heptakis-2.6-di-O-methyl-β-cyclodextrin	2.5, 5, 10, 20, 40
hydroxy-propyl-α-cyclodextrin	2.5, 5, 10, 20, 40
hydroxy-propyl-β-cyclodextrin	1.88, 3.75, 7.5, 15, 30
hydroxy-propyl-γ-cyclodextrin	2.5, 5, 10, 20, 40
carboxy-methyl-β-cyclodextrin	2.5, 5, 10, 20, 40

Approximately 5 mg of VAS3947 were each weighed into ten Eppendorf vials, and 0.5 mL of the corresponding cyclodextrin solution were added to each. Additionally, a negative control containing a saturated solution of VAS3947 in PBS buffer pH = 7.4 was prepared in the same way. All samples were incubated in a shaker for 20 h at 37 °C and 800 rpm, the vials were centrifuged for 5 minutes at 13.000 rpm, and the supernatant was collected from each.

The dissolved amount of VAS3947 was quantified by means of HPLC analysis. The same system as described for the log *P* assessment was used (see p. 54). The chromatographic conditions are illustrated in **Table 3**. The samples were diluted in a mixture of acetonitrile/PBS buffer: 15/85 (v/v) and the concentration was calculated using a regression line over the range of 1 µg/mL–250 µg/mL.

Table 3 Chromatographic conditions for the quantification of VAS3947 in cyclodextrin formulations.

Analytical column	Phenomenex Synergi Max RP (50 × 4.6 mm, 4 µm)
Mobile phase A	water and acetonitrile at a ratio of 90/10% and 0.05% TFA
Mobile phase B	water and acetonitrile at a ratio of 10/90 and 0.05% TFA
Gradient profile	from 0 min to 8 min at 100% to 20% mobile phase A from 8 min to 9 min at 20% mobile phase A from 9 min to 10 min at 20% to 100% mobile phase A
Flow rate	1.5 mL/min
Injection volume	10 µL
Detection wavelength	λ = 254 nm and λ = 280 nm
Column temperature	23 °C
Post time	5 min

The validation of this HPLC method is explained in an own chapter. (See appendix page 91).

^{1}H NMR Investigation of "Complexation Induced Chemical Shifts" (CICS)

^{1}H NMR measurements of VAS3947 and heptakis-2.6-di-O-methyl-β-cyclodextrin (DMCD) were performed on a Bruker Avance III spectrometer operating at 400.13 MHz for ^{1}H, equipped with a 5 mm BBO broadband observer with Z-gradient. Spectra were recorded with a flip angle of 30°, spectral width of 20 ppm, transmitter offset of 6.15 ppm, acquisition time of 3.99 s followed by a relaxation delay of 1.00 s. 128 scans were collected in 64.000 data points resulting in a digital resolution of 0.125 Hz. The processing parameters were set to an exponential line broadening window function of 0.3 Hz, an automatic baseline correction and manual phasing. The solvent served as the field frequency lock. The temperature was adjusted to 300 K.

For buffer preparation, 8.0 g NaCl, 0.2 g KCl, 1.42 g Na_2HPO_4, and 0.78 g KH_2PO_4 were dissolved in 800 mL of purified water. pH was adjusted to 4.5 by adding concentrated phosphoric acid and the volume was filled up with purified water to 1000 mL. The solution was sonicated for 15 minutes. Afterwards, 20.0 mL of this buffer were lyophilized and re-dissolved in 20.0 mL D_2O. This lyophilisation procedure was replicated twice.

Seven samples with different concentrations of VAS3947 and DMCD were prepared in the buffer (**Table 4**). The final concentration of VAS3947 was 5 mM, the ratio of VAS3947:cyclodextrin varied.

Table 4 Composition of the seven samples investigated by ^{1}H-NMR spectroscopy for "CICS"

Sample Number	1	2	3	4	5	6	7
Final Concentration of VAS3947	5 mM						
Ratio of VAS3947:cyclodextrin	1:5	1:3.33	1:1.5	1:1	2.5:1	3.33:1	5:1

Spectra were referenced to TSP (δ = 0.0 ppm) which was introduced in a coaxial insert (WGS 5-BL, Norell Inc., Morganton, NC) as external reference in the deuterated buffer. ^{1}H spectra with a digital resolution of 0.125 Hz were analysed for CICS, and Δδ values were determined according to the following equation:

Δδ value = δ (free VAS3947) – δ (complexes of VAS3947 and CD)

ROESY Measurements

Transverse ROESY NMR measurements were performed on a Bruker Avance III HD spectrometer operating at 600.13 MHz for ^{1}H, equipped with a 5 mm DCH cryoprobe with Z gradient. Data processing was done with TopSpin® 3.2 software. Spectra were recorded using the spin lock pulse with a mixing time of 150 ms. Spectral width was set to 10 ppm with a transmitter offset of 4.7 ppm. The number of scans was adjusted to 24, and 410 increments in the indirect dimension (F1) were acquired. The acquisition time was set to 0.64 s, followed by a relaxation delay of 3.00 s. The experimental time was about 10 h. For processing a spectrum size in F1 of 2.000 was used. In both dimensions (F2 and F1) zero filling was applied, the window function was set to a pure cosine squared function, and a baseline correction was performed. In indirect dimension forward linear prediction was performed. The temperature was adjusted to 300 K.

For sample preparation the same deuterated buffer was used as described for the CICS measurements (p. 59). 7.8 mg of VAS3947 and 33.3 mg of DMCD were weighed into a 2 ml vial and were dissolved in 1.0 mL of the deuterated buffer. 500 µL of this solution were transferred into a NMR tube. Spectra were referenced to TSP (δ = 0.0 ppm), which was introduced in a coaxial insert as external reference in the deuterated buffer.

Cyclodextrin Formulation for i.v. Application

A saturated solution of VAS3947 was prepared by dissolving an excess of VAS3947 in 2 mL of an aqueous solution containing 40% (w/w) of hydroxypropyl-β-cyclodextrin (pH = 4.5). To prepare the final formulation, this solution was diluted with 0.9% NaCl solution 1:1. For solubility and stability assessment, samples were incubated in a heated shaker for 24 h at 400 rpm and 22 °C. After 0, 10, 30, 120 minutes, and 24 h an aliquot was taken and centrifuged for 5 minutes at 13.000 rpm. The supernatant was analysed for content by HPLC as described previously for the cyclodextrin dissolution study (see p. 60 to 61).

Statistics

Statistical analysis was performed using Minitab® 17.2.1 (Minitab Inc., Coventry, UK). Comparisons between groups for the assessment of statistically significant differences (**Figures 2H, 3C, 4B, 4C, 6**) were performed using ANOVA and the Tukey *post hoc* test with 95% CI and $p < 0.05$. Results were reported as mean ± standard deviation and measurements were carried out in triplicate unless noted otherwise.

Results

Physicochemical Characterization of VAS Compounds

The structures of VAS2870, VAS3947, and VAS4024 are shown in **Figure 1A**. Their melting points were determined by DSC to be 165 °C, 115 °C, and 178 °C, respectively (**Figure 1B-D**). Whereas VAS2870 and VAS3947 did not recrystallize, VAS4024 had a melting point of 160 °C in the second heating run.

The log *P* was experimentally determined to be 3.6, 1.8, and 1.7 for VAS2870, VAS3947, and VAS4024, respectively.

The kinetic solubility from freshly prepared solutions (T0) was 56 µg/mL for VAS2870, 91 µg/mL for VAS3947, and 51 µg/mL for VAS4024 (data not shown). The solubility was again assessed by means of nephelometry after 60 minutes and was 58 µg/mL, 88 µg/mL, and 61 µg/mL for VAS2870, VAS3947, and VAS4024, respectively (data not shown). Based on its favourable solubility properties, VAS3947 was selected for further formulation developmental work. The thermodynamic solubility of the crystalline VAS3947 was determined at approximately 5 µg/mL after 10 minutes and approximately 12 µg/mL after 24 h (**Figure 2 A-G**).

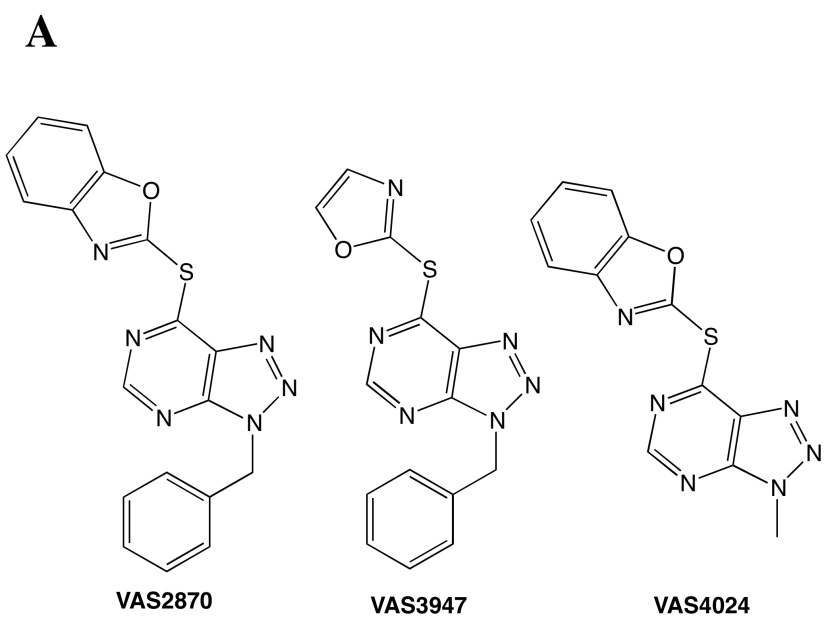

Figure 1 A) Chemical structures of VAS2870, VAS3947, and VAS4024.

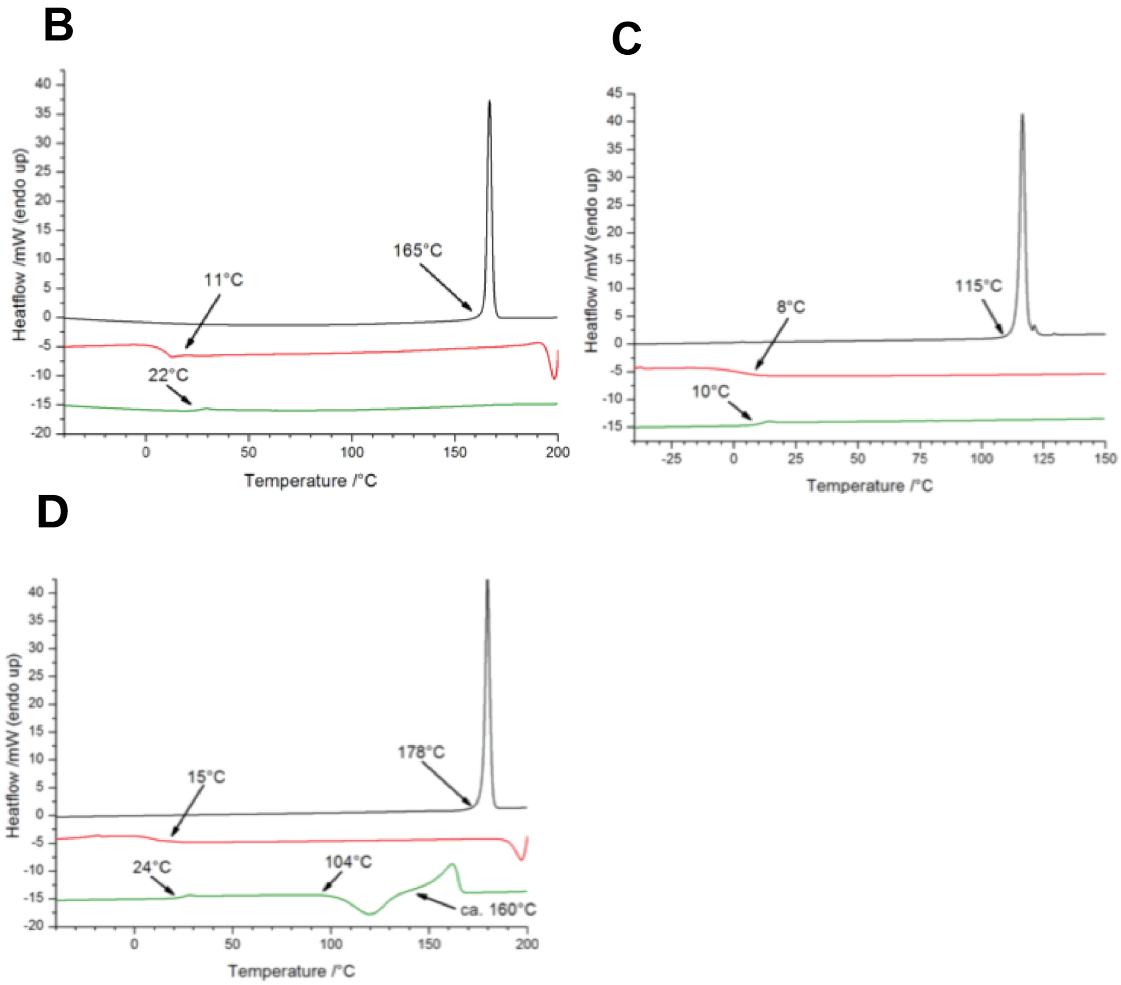

Figure 1 B-D) Determination of melting points and glass transitions temperatures of **B**) VAS2870, **C**) VAS3947 and **D**) VAS4024 by differential scanning calorimetry (DSC). The black curve represents the first heating run, the red curve the subsequent cooling run and the green curve the second heating run.

Characterization of the Spray Dried Formulations

VAS3947 was spray dried with seven different excipients (**Table 5**). All spray dried formulations were found to be amorphous as determined by XRPD (data not shown). In contrast, VAS3947 starting product as well as the physical mixtures of VAS3947 and the excipients had crystalline reflexes (data not shown). The amorphous character of VAS3947 in the spray dried formulations was additionally confirmed by means of a DSC analysis. In contrast to the starting product and to the compound's physical mixtures, no melting points were determined.

Table 5 Characterization of the spray dried formulations of VAS3947 and different excipients after dissolution (120 minutes).

Preparation of Spray Dried Formulations			**Characterization of Spray Dried Formulations after Dissolution**		
Excipient	Supplier (excipient)	Solvent	pH	Particle Size [nm]	Zeta Potential [mV]
1. Eudragit® L100	Evonik	Methanol	5.95	191.0	- 36.2
2. Eudragit® L100-55	Evonik	Methanol	5.82	185.5	- 34.9
3. Eudragit® RL PO	Evonik	Methanol	7.41	n.d.	+ 29.6
4. HPMC	Sigma Aldrich	Methanol	7.34	182.0	- 4.8
5. Kollidon® 30	BASF	2-Propanol	7.32	151.3	- 4.6
6. Kollidon® VA 64	BASF	2-Propanol	7.37	202.7	- 2.0
7. Soluplus®	BASF	2-Propanol	7.27	146.5	± 0.0

n.d. = not determined (determination of particle size was not possible)

Dissolution of VAS3947 from Spray Dried Formulations

The dissolution of VAS3947 from the spray dried formulations with various excipients (**Table 5**) was measured over time in comparison to physical mixtures and the pure substance (**Figure 2A-2G**). Throughout all tested conditions, the physical mixtures slightly enhanced the concentration of VAS3947 as compared to the starting product.

In contrast, spray drying had a profound effect for some formulations. An increased dissolution rate could be observed (in ascending order): Eudragit® RL PO, Kollidon® VA 64, HPMC, Eudragit® L100-55, and Soluplus®.

Eudragit® L100 and Kollidon® 30 did not preserve the metastable supersaturated state throughout the study period of 240 minutes.

In comparison to the starting product, the supersaturation ratio observed after 120 minutes was the highest for Eudragit® L100 (9-fold) and Soluplus® (8-fold) (**Figure 2H**). HPMC (5-fold), Eudragit® L100-55 (5-fold), Kollidon® VA 64 (4-fold), Eudragit® RL PO (3-fold), and Kollidon® 30 (3-fold) resulted in lower supersaturation ratios, respectively. However, all spray dried formulations significantly increased the concentration of VAS3947 after 120 minutes in comparison to the starting product (**Figure 2H**).

After 120 minutes, the sample pH ranged from 7.3 to 7.4 with the exception of the samples containing the anionic polymers Eudragit® L100-55 and Eudragit® L100 which reached 5.8 to 6.0 (**Table 5**). The particle sizes were in the low nanomolar range for all samples as determined by dynamic light scattering (**Table 5**). Solutions containing anionic polymers exhibited negative zeta potentials (Eudragit® L100, Eudragit® L100-55), solutions with neutral polymers (HPMC, Kollidon® 30, Kollidon® VA 64, Soluplus®) resulted in zeta potentials around zero and the cationic polymer Eudragit® RL PO showed a positive zeta potential (**Table 5**), implying that zeta potential results are in accordance with pH.

After evaporation of the solvent, recrystallization was observed for the precipitates of the spray dried formulations containing Eudragit® L100-55, Eudragit® RL PO, HPMC, Kollidon® 30, and Kollidon® VA64 but not for Eudragit® L100 and Soluplus® (data not shown). In summary, the formulations containing Soluplus® and Eudragit® L100 lead to the highest maximum solubility of VAS3947.

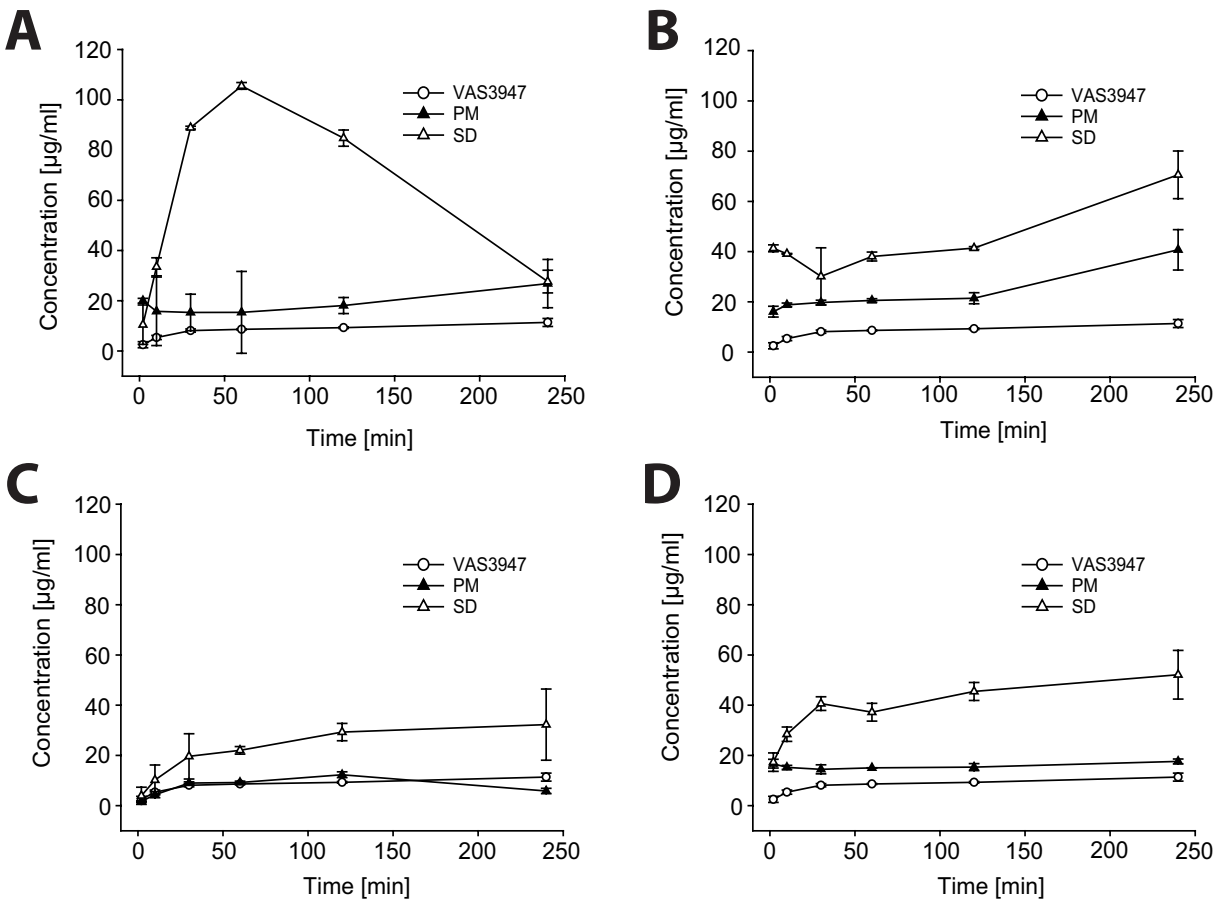

Figure 2 Dissolution profiles of VAS3947 starting product (**Fig. 2A-2G**, white circles) as well as from physical mixtures (PM, black triangles) and spray dried formulations (SD, white triangles) with different excipients (**Table 1**) in PBS buffer. The excipients were in detail: **A**) Eudragit® L100, **B**) Eudragit® L100-55, **C**) Eudragit® RL PO, **D**) HPMC.

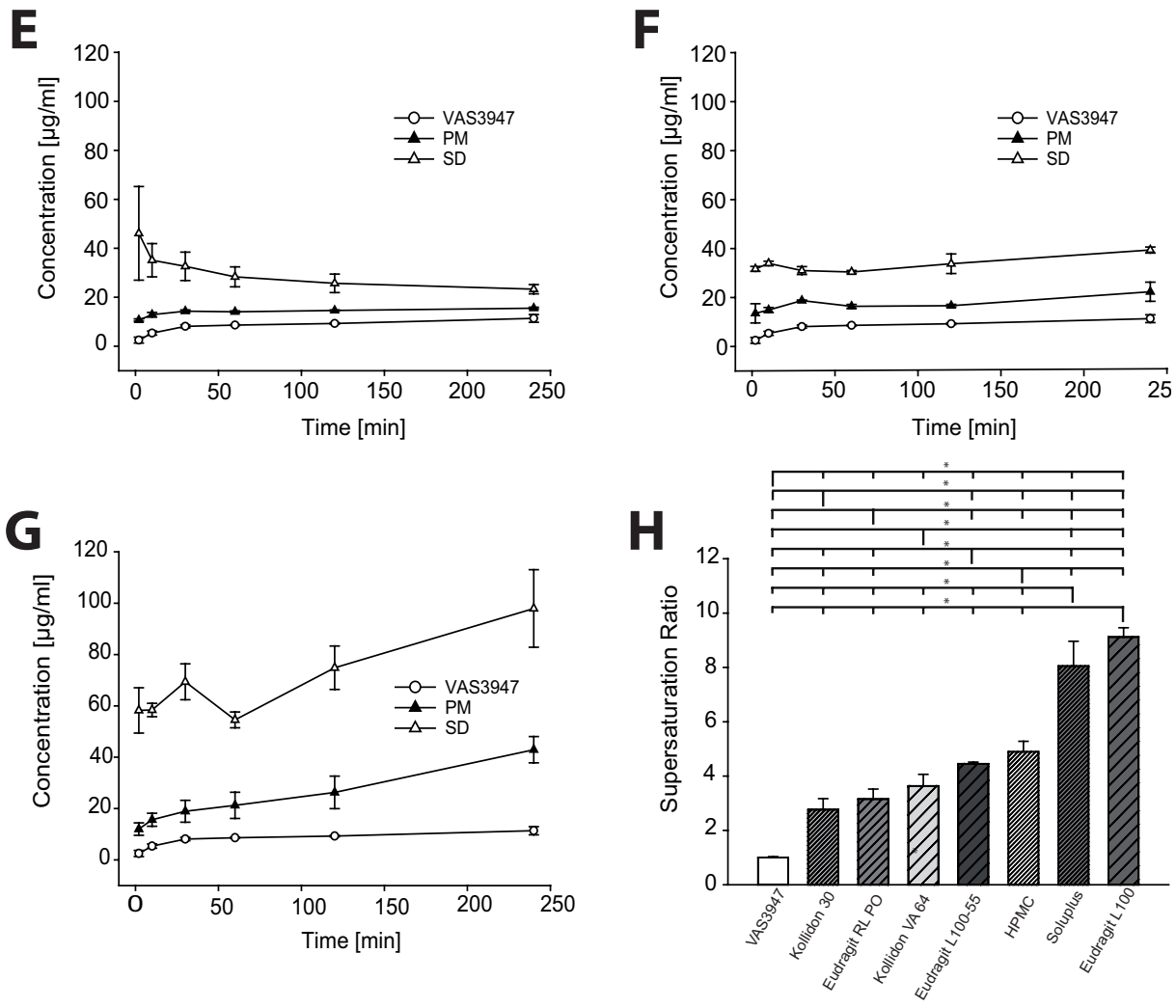

Figure 2 Dissolution profiles of VAS3947 starting product (data set is shown seven-fold in **Figure 2A-2G**, white circles) as well as from physical mixtures (PM, black triangles) and spray dried formulations (SD, white triangles) with seven different excipients (**Table 1**) in PBS buffer. The excipients were **E**) Kollidon® 30, **F**) Kollidon® VA 64, **G**) Soluplus®

H) Solubility of VAS3947 starting product (standardized to 1) and respective supersaturation ratios of the spray dried formulations with seven different excipients after 120 minutes.

Excipient Screening and Characterization of Microemulsions

The preformulation screening of 32 liquid and semisolid excipients and surfactants (**Figure 3A**) in binary combinations with VAS3947 revealed high solubilizing power for Benzylalcohol, Capmul® MCM C8, Capryol® PGMC, Labrafac® Lipophile® WL 1349, Labrafac® PG, Lauroglycol, Linalool, Miglyol® 812, PEG 300, PEG 400, and Triacetin after 24 h. Derived from these results, four final microemulsions were prepared containing 1% VAS3947 (**Table 6**). All of them fulfilled the expectations, which were (i) absence of phase separation for at least 4 h, (ii) absence of precipitation upon 1:10 dilution with water, and (iii) absence of recrystallization events in the formulation over a time period of 4 weeks[12]. Dynamic light scattering experiments were performed upon dilution of these microemulsions with water (1:10), the measured particle sizes can be found in **(Table 6)**.

Table 6 Composition and characterization of the microemulsions.

Preparation of Microemulsions			**Characterization of Microemulsion**
Composition	Content of excipient [%]	Supplier of excipient	Particle Size [nm]
1. Type II			
Cremophor® RH	44.5	BASF	70.7
Miglyol® 812	35.5	Caesar & Loretz	
Lauroglycol	9.0	Gattefossé	
Ethanol (pure)	11.0	Fisher Scientific	
2. Type IIIa			
Cremophor® RH	42.0	BASF	42.8
Labrafac® PG	25.0	Gattefossé	
PEG 400	17.0	Caesar & Loretz	
Ethanol (pure)	9.4	Fisher Scientific	

3.	**Type IIIa**			
	Cremophor® RH	42.0	BASF	
	Capmul® MCM C8	25.0	ABITEC	192.6
	PEG 400	17.0	Caesar & Loretz	
	Ethanol (pure)	9.5	Fisher Scientific	
4.	**Type IIIa**			
	Cremophor® RH	40.0	BASF	
	Capmul® MCM C8	24.0	ABITEC	167.7
	Propylenglycol	16.0	Caesar & Loretz	
	Ethanol (pure)	8.9	Fisher Scientific	

Dissolution of VAS3947 from Microemulsions

The maximum drug load of VAS3947 was incorporated into the respective formulations and resulted in 35 mg/g for microemulsion 1, 43 mg/g for microemulsion 2, 40 mg/g for microemulsion 3, and 29 mg/g for microemulsion 4.

The dissolution profiles of VAS3947 starting product and from microemulsions were explored in FaSSIF (**Figure 3B**). The concentration of VAS3947 starting product in FaSSIF was found to be 7 µg/mL after 10 minutes. The highest solubility improvement was observed for microemulsion 1. 1152 µg/mL VAS3947 were determined 2 minutes after dissolution. This supersaturated state was stable for more than 1 hour.

For microemulsion 2 the solubility was found to be 834 µg/mL 2 minutes after dissolution, but decreased rapidly within 20 minutes to result in an equilibrium solubility around 300 µg/mL.

For microemulsion 3 and 4, a minor distinct supersaturation occurred with 211 µg/mL and 175 µg/mL 2 minutes after dissolution. However, no stabilization of the metastable state was observed and both microemulsions resulted in an equilibrium solubility of around 120 µg/mL.

The supersaturation ratio observed after 120 minutes was the highest for microemulsion 2 (18-fold), followed by microemulsion 1 (10-fold), microemulsion 3 (8-fold), and microemulsion 4 (7-fold) (**Figure 3C**).

In summary, all microemulsions significantly improved the solubility of VAS3947 in FaSSiF and exceeded the concentrations observed for the spray dried formulations.

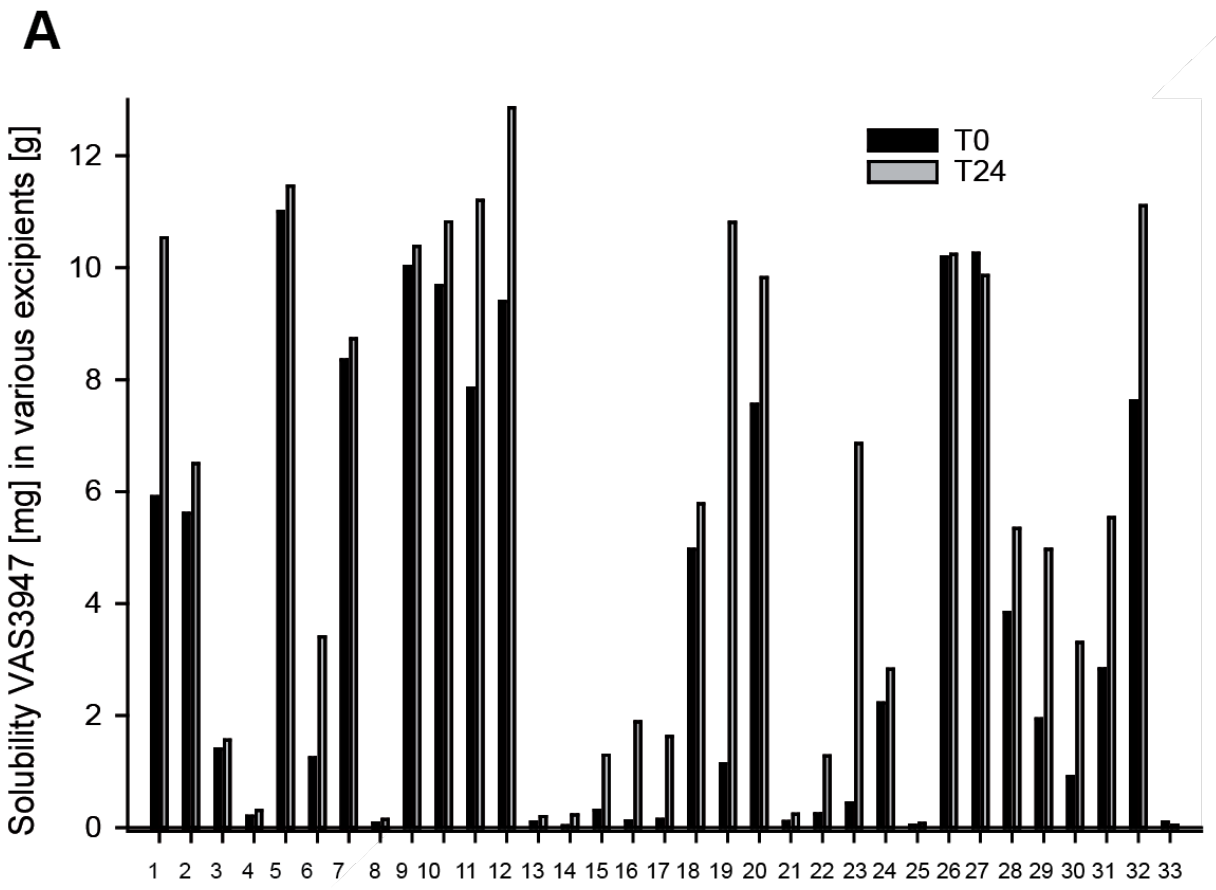

Figure 3 A) Solubility of VAS3947 in various liquid excipients immediately after preparation (T0) and after 24 h of shaking (T24). Formulation success was defined as solubility of VAS3947 > 10 mg/g excipient. Excipients were in detail: 1 Miglyol® 812, 2 Isopropylpalmitate, 3 Squalene, 4 Squalane, 5 Linalool, 6 Sesam Oil, 7 Transcutol® HP, 8 Plurol® Oleique, 9 Capryol® PGMC, 10 Labrafac® PG, 11 Labrafac® Lipophile WL 1349, 12 Lauroglycol, 13 Castor Oil Refined, 14 Castor Oil Virgin, 15 Peceol, 16 Tween® 20, 17 Tween® 40, 18 Tween® 80, 19 PEG 400, 20 PEG 300, 21 Cremophor® RH 40, 22 Etocas® 35, 23 Triton X, 24 Ethylenglycol, 25 Glycerol, 26 Benzylalcohol, 27 Triacetin, 28 Propylenglycol, 29 Wheat Germ Oil, 30 Peanut Oil, 31 Corn Oil, 32 Capmul® MCM C8, 33 PBS Buffer (negative control).

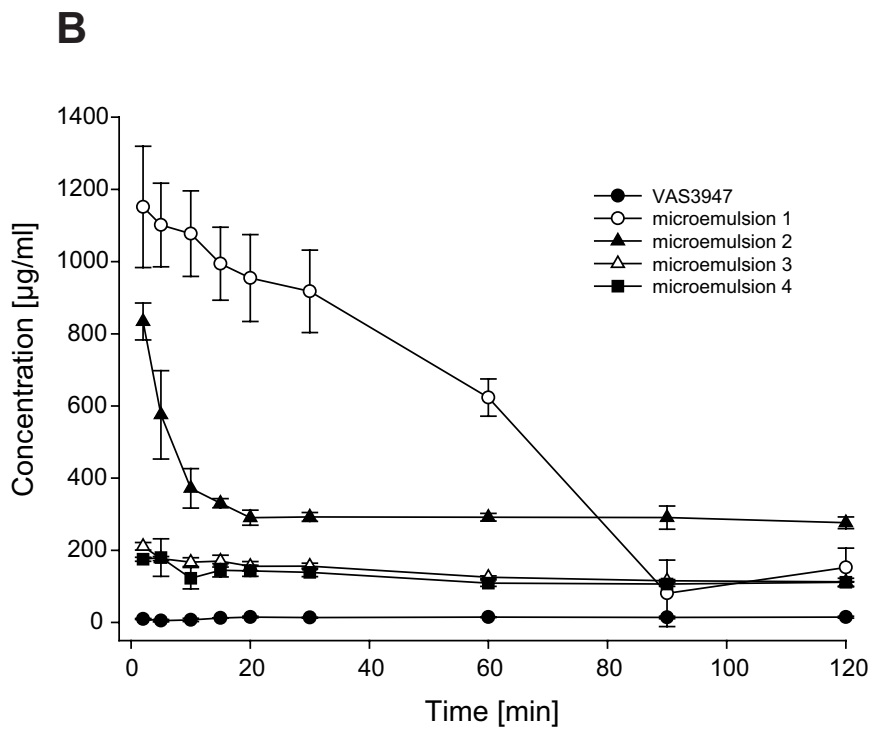

Figure 3 B) Dissolution profiles of VAS3947 starting product and from four microemulsions with different compositions (**Table 6**) in FaSSiF.

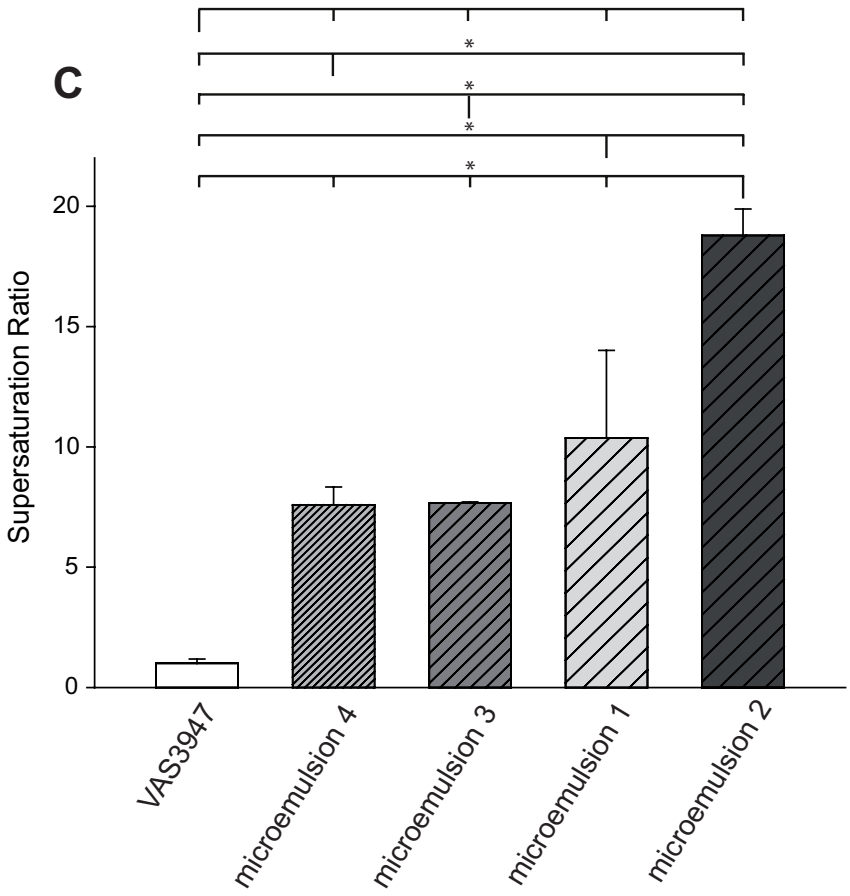

Figure 3 C) Solubility of pure VAS3947 (standardized to 1) and respective supersaturation ratios of VAS3947 from four microemulsions with different compositions after 120 minutes.

Screening for Appropriate Cyclodextrins

Ten cyclodextrins were tested for their ability to improve the solubility of VAS3947, and studied at different concentrations up to the maximum solubility of the respective cyclodextrin in PBS buffer (**Table 1**). In general, a linear increase of the VAS3947 solubility was detected with increasing concentrations of the respective cyclodextrin (**Figure 4A**). The modified α-, β-, and γ-cyclodextrin derivatives showed a higher solubility in PBS buffer than the unmodified cyclodextrins (see max. values in **Table 7**), and improved the solubility of VAS3947 to a higher extent (**Figure 4A**). In contrast, the unmodified α-, β- and γ-cyclodextrins were excluded from further formulation studies as of lack of high solubility in PBS buffer and hence only minor solubility improvement of VAS3947 (data not shown). Additionally, sulfated β-cyclodextrin was excluded because of not increasing the aqueous solubility of VAS3947 (data not shown). The six cyclodextrins that were best at improving the solubility of VAS3947 with increasing concentrations of CD were, in increasing order of solubility improvement, (1) hydroxy-propyl-α-CD, (2) hydroxy-propyl-γ-CD, (3) carboxy-methyl-β-CD, (4) hydroxy-propyl-β-CD, (5) heptakis-2.6-di-O-methyl-β-CD, (6) methyl-β-CD (**Figure 4B**). To compare the cyclodextrin fomulations under equal conditions, **Figure 4C** shows the solubility of VAS3947 when formulated with 10% [w/w] of the respective cyclodextrin in PBS buffer. The solubility of VAS3947 after 20 h varied dramatically depending on the cyclodextrin derivatives, with sulfated β-cyclodextrin even delivering a worse solubility (12 µg/mL) than raw VAS3947 (18 µg/mL). Detailed data are shown in **Table 7**.

Table 7 Solubility of VAS3947 when formulated with 10% [w/w] of the respective cyclodextrin in PBS buffer.

Cyclodextrin	Solubility of VAS3947 (µg/mL)
heptakis-2.6-di-O-methyl-β-CD	3072
methyl-β-CD	1614
hydroxy-propyl-γ-CD	51
hydroxy-propyl-α-CD	51
α-CD	33
γ-CD	26
sulfated β-CD	12

It could be seen that the lipophilic derivatives of β-cyclodextrin led to a higher increase of VAS3947 solubility than the derivatives of α- and γ-cyclodextrin. This was attributed to the more appropriate size of the cyclodextrin cavity.

In summary, the lipophilic derivatives, namely DMCD and methyl-β-cyclodextrin, showed the highest solubility improvement of VAS3947.

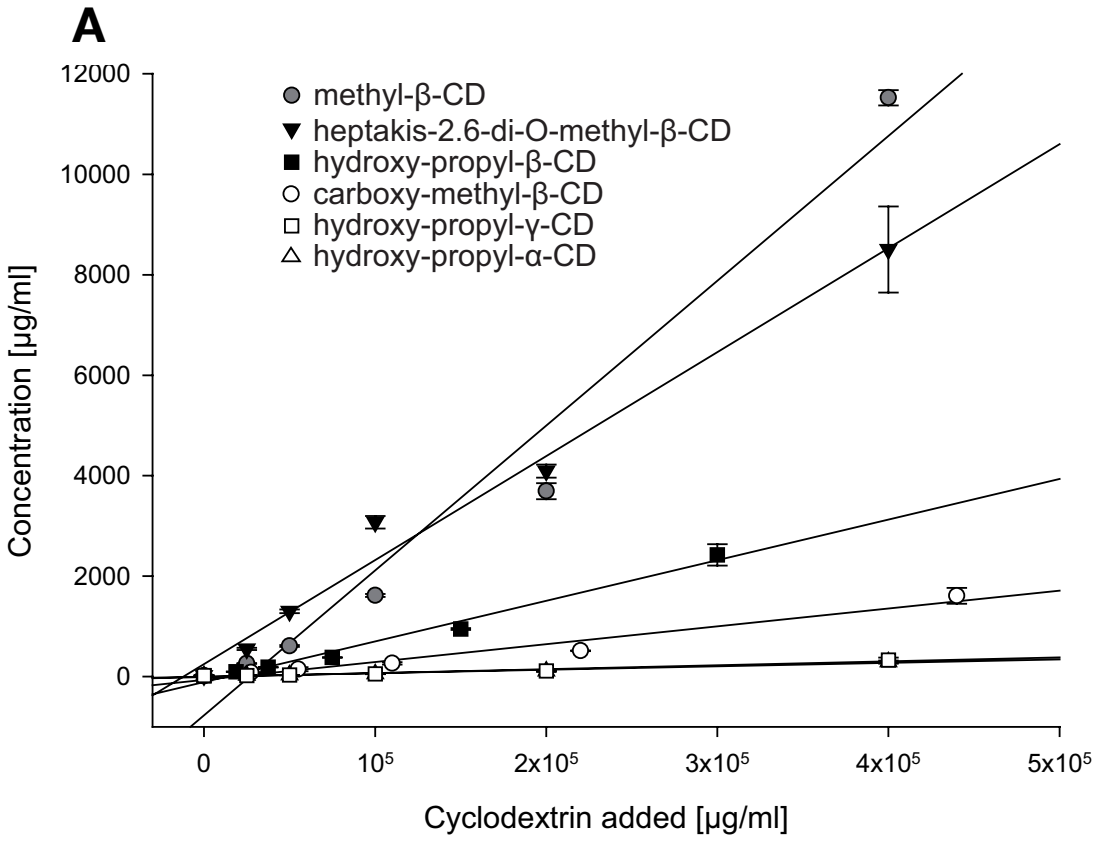

Figure 4 A) Phase solubility plot of VAS3947 and different cyclodextrins: Solubility improvement of VAS3947 when formulated with different cyclodextrins.

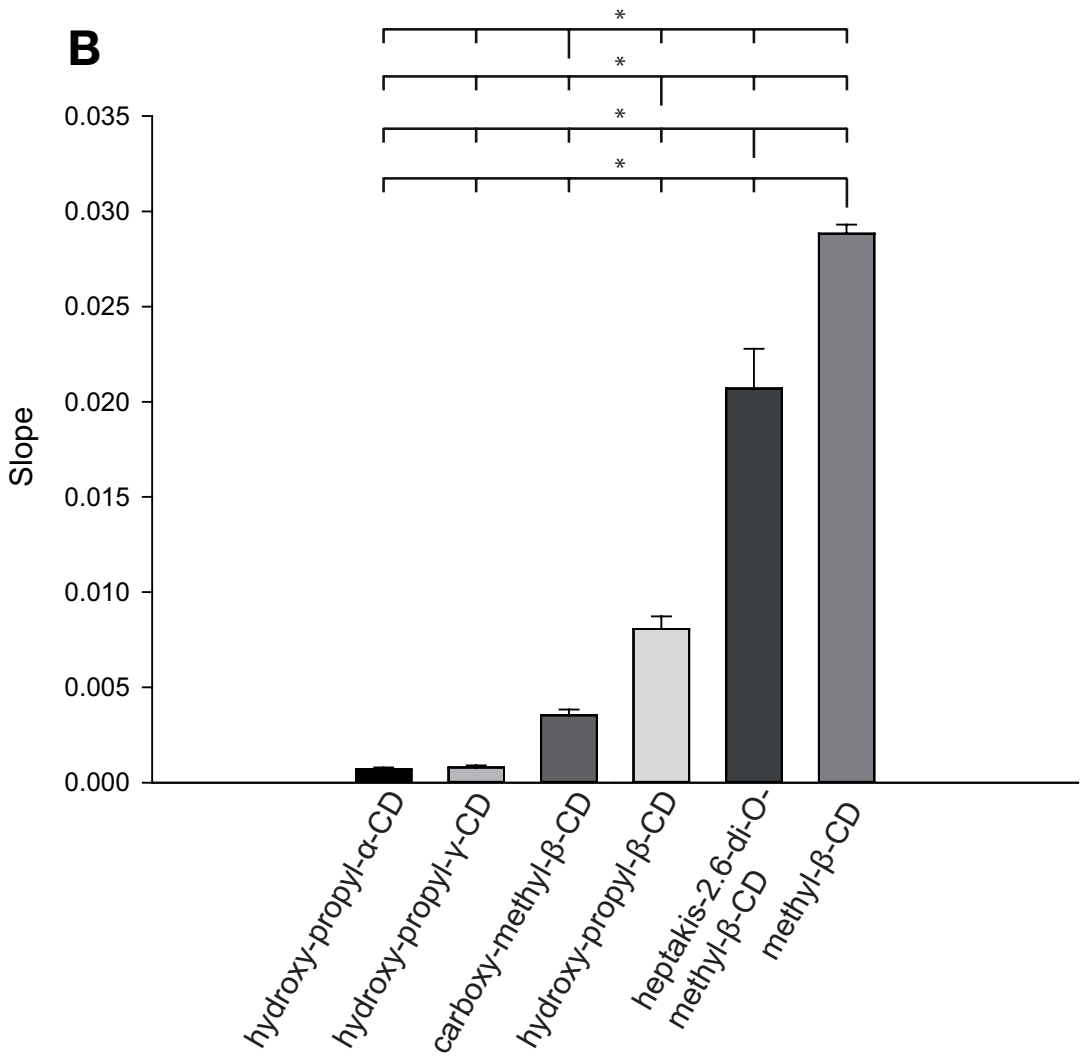

Figure 4 B) Solubility improvement of VAS3947 when formulated with different cyclodextrins, calculated as slope over increasing cyclodextrin concentrations.

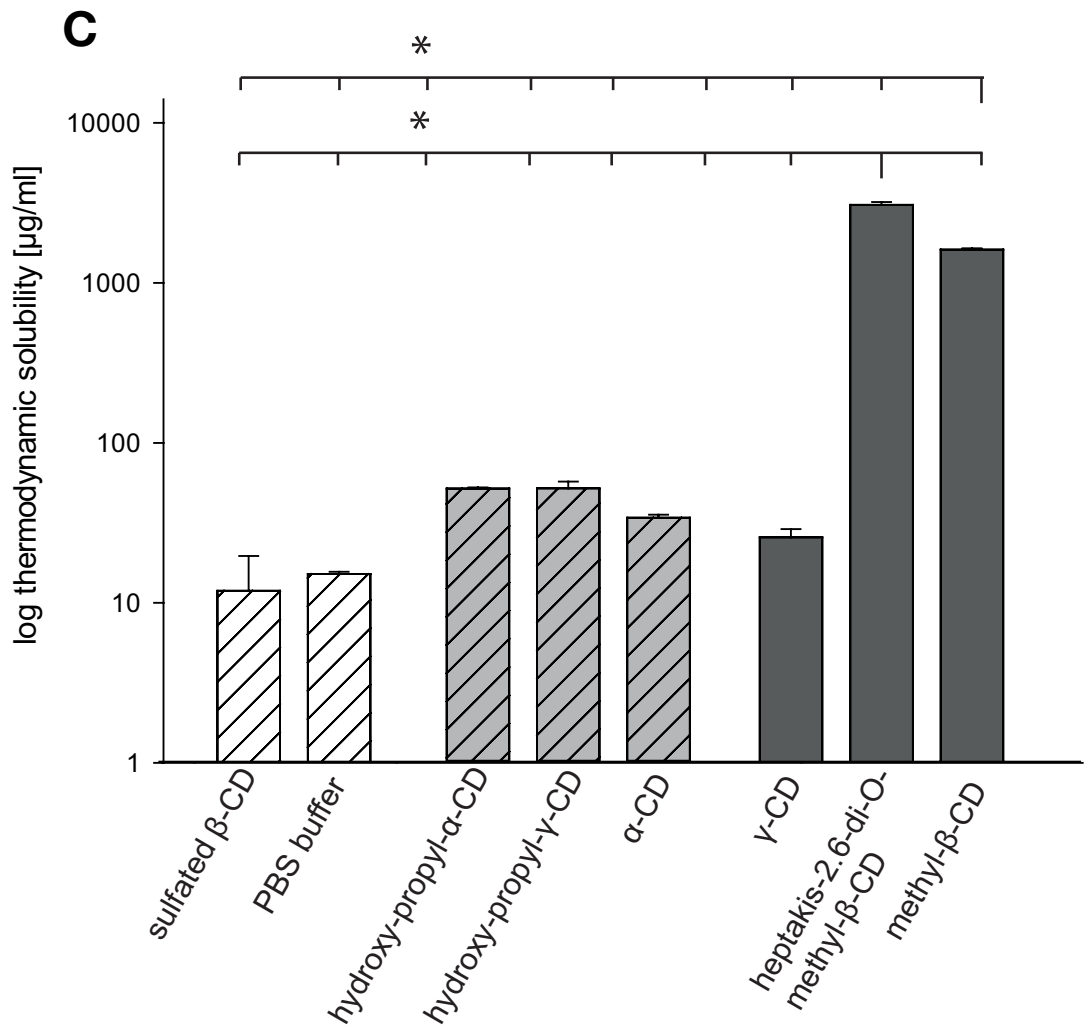

Figure 4 C) Thermodynamic solubility of VAS3947 formulated with a 10% [w/w] solution of different cyclodextrins in PBS buffer.

Nuclear Magnetic Resonance Measurements

^{1}H and ROESY NMR measurements were performed to detail the interaction of VAS3947 with the relatively hydrophobic DMCD. A distinct shift of all proton signals of VAS3947 in comparison to the pure compound indicated the incorporation of the compound's aromatic rings into the lipophilic cavity of the cyclodextrin (**Figure 5A**). These observations were corroborated by the results found for the cyclodextrin protons, with H-5' and H-6' having the strongest shifts (0.05 to 0.09 ppm) and H-1', H-2', and H-3' showing smaller shifts (0.01 to 0.04 ppm, **Figure 5B**). The ROESY spectra confirmed the strong interactions of API protons with cyclodextrin protons with the exception of H-1' (**Figure 5C**).

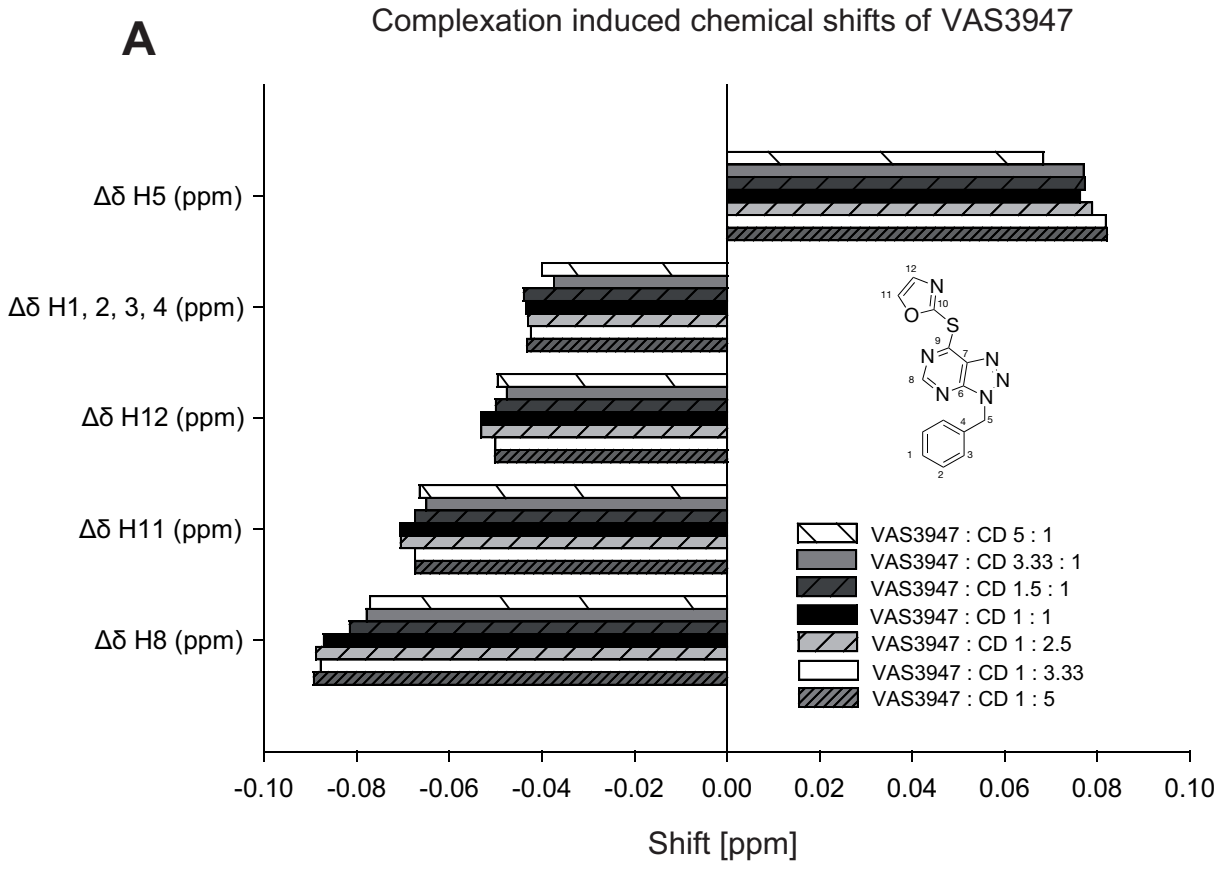

Figure 5 A) ^{1}H NMR investigation of complexation induced chemical shifts of VAS3947 formulated with DMCD with reference to the VAS3947 starting material.

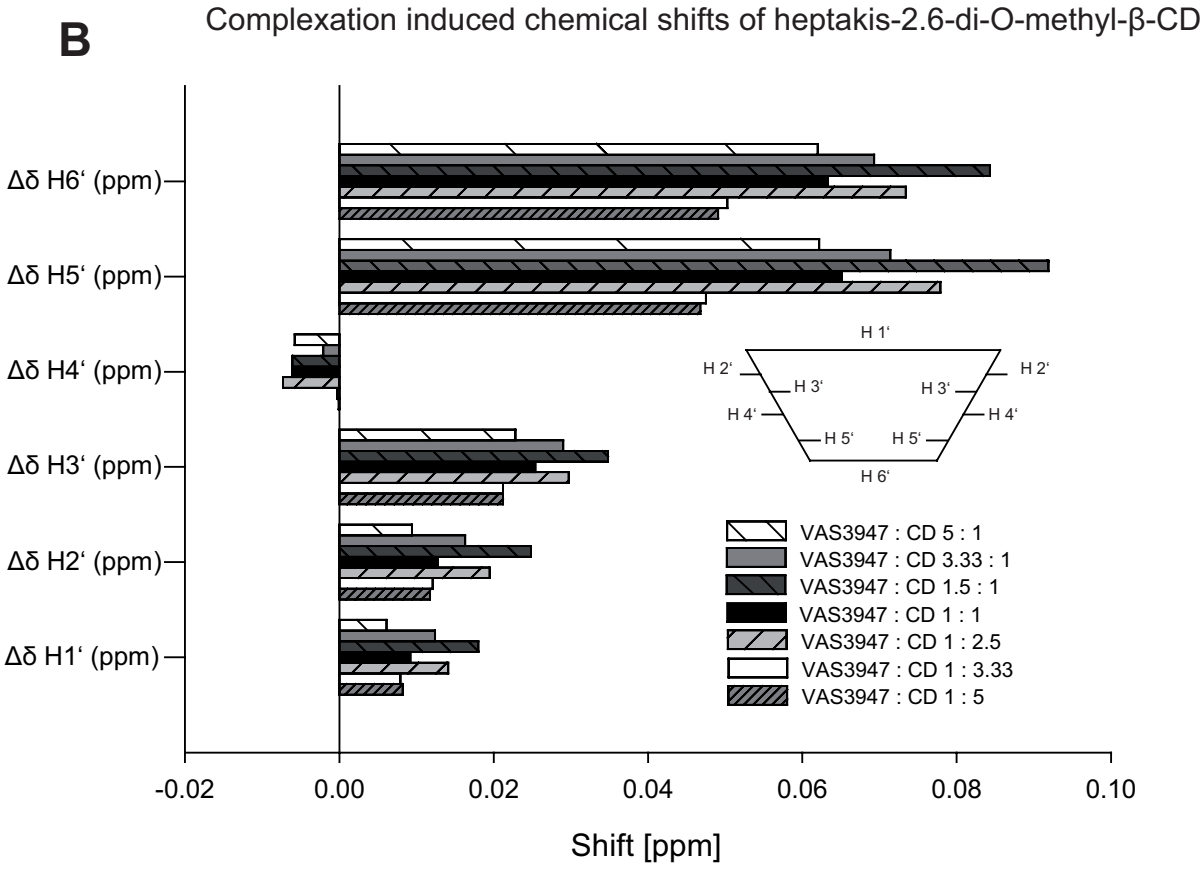

Figure 5 B) ^{1}H NMR investigation of complexation induced chemical shifts of DMBC formulated with VAS3947 with reference to DMCD.

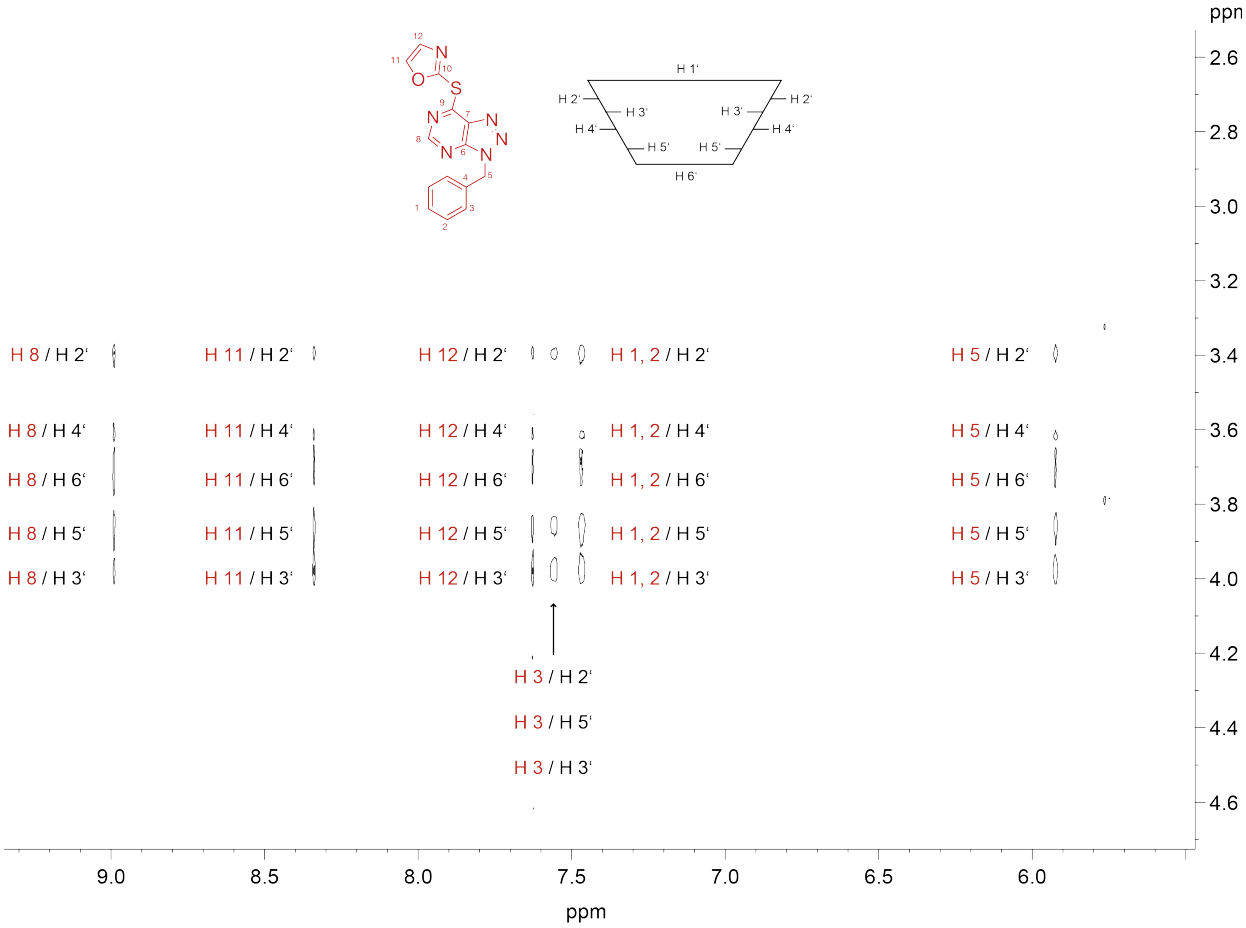

Figure 5 C) ROESY spectrum showing the interactions of protons from VAS3947 (red) with protons from DMCD (black).

VAS3947 – Cyclodextrin Formulation for i.v. Application

One of the goals of this work was to provide suitable i.v. formulations based on VAS3947–cyclodextrin complexes. Hydroxy-propyl-β-cyclodextrin (40% w/w) is an accepted excipient for parenteral use[19]. As we could show above, it also yielded very good results, so we can justify focusing on this CD. The VAS3947–cyclodextrin complex was stable for at least 24 h at a concentration of approximately 1000 µg/ml (**Figure 6**). After 24 h 85% of VAS3947 were still in solution. The diluted formulation with 0.9% saline had a higher stability with more than 90% being in solution after 24 h (data not shown).

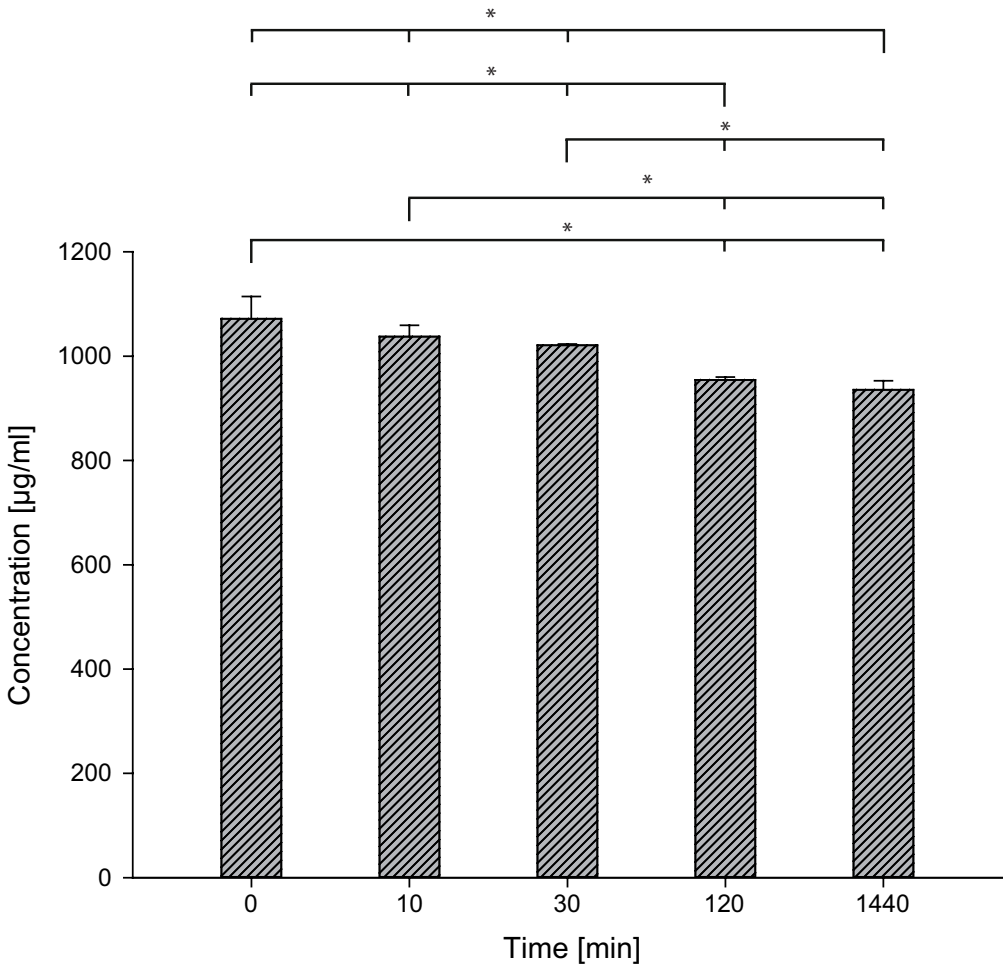

Figure 6 Solubility assessment of an intravenous formulation of VAS3947 formulated with hydroxypropyl-β-cyclodextrin (40% w/w) in PBS buffer.

Discussion

The formation of reactive oxygen species (ROS) accounts for pathomechanisms in human vascular endothelium causing diseases like atherosclerosis, myocardial strokes, and lipometabolic disorders. All of them show an increased incidence in developed countries[2]. Novel NOX-inhibitors like VAS2870, VAS3947, and VAS4024 (**Figure 1A**) have been described as promising candidates for the reduction of ROS in different cell assays[5-7]. However, like many other efficient drug candidates, this substance class is limited by its poor aqueous solubility, leading to low bioavailability upon administration. This means that the investigation of *in vivo* studies being important for further drug development is significantly impeded. Generally, higher melting points and higher log *P* values indicate less favourable solubility properties, and thus higher obstacles for *in vivo* application[9]. The NOX-inhibitor VAS3947 was selected as model compound for further formulation

approaches aiming to overcome the drawback of poor solubility and bioavailability for this promising substance class. To comply with the portfolio of feasible *in vivo* studies, formulations for two different routes of administration were developed. One is intended for the oral route of administration and the other one is determined for intravenous application. Three different formulation techniques were applied to reach this target:

In a first approach solid dispersions were prepared by spray drying **(Table 5)**. Here, the API was dispersed in an inert carrier at solid state[10]. Different carriers were used to maximize the phenomenon of 'spring and parachute'[11].

The amorphous conversion of VAS3947 in the spray dried formulations, confirmed by XRPD (**Figure S2A-G**), caused a significant solubility improvement as compared to the respective physical mixtures (**Figure 2A-G**) and to the starting product (**Figure 2H**). However, the overall effects were only moderate. The solubility still averaged in the low micromolar range and supersaturation ratios ranged between 3 and 9 (**Figure 2H**). The solubility improvement that could be achieved is not adequate for reaching plasma concentrations that are sufficient for therapeutic effects. Additionally, the spray dried formulations containing Eudragit® L100 and Soluplus® were unstable after dissolution and precipitated in their amorphous form (data not shown).

To achieve a better 'spring and parachute' effect, a microemulsion approach was tried which previously proved to be efficient for the development of oral formulations of poorly water-soluble drugs[12]. Different excipients providing high solubilizing capacity for VAS3947 in a pre-formulation screening were identified (**Figure 3A**).

Based on the outcome, on patent EP 1715848 A1[13] as well as on the classification system proposed by Pouton et al.[14], type II and type IIIa lipid systems were prepared as suitable carriers for VAS3947 **(Table 6)**. The vehicles were thermodynamically stable for four weeks and provided high solubilizing capacities for the API.

A trend towards higher solubilizing capacity was observed with decreasing polarity of the formulation, which could be expected, considering the hydrophobic structure of VAS3947. Upon contact with water the microemulsions formed fine dispersions with particle sizes in the low nanomolar range, favouring dissolution, re-dissolution, and equilibrium solubility due to their high wettability and huge surface area[15].

A remarkable initial 'spring' followed by a subsequent decrease of the solubility was achieved for microemulsion 1 and 2, whereas 3 and 4 constantly maintained lower amounts of VAS3947 in solution (**Figure 3B**). The equilibrium solubility of all microemulsions substantially exceeded the concentration of the pure API. Supersaturation ratios ranged between 8 and 19 (**Figure 3C**). This formulation approach exceeded the supersaturation ratios determined for the spray drying approach.

Finally, as a third solubility improvement approach, several cyclodextrin formulations were prepared **(Table 7)**. Cyclodextrins are cyclic oligosaccharides with a hydrophilic outer surface and a lipophilic central cavity. This structure facilitates the inclusion of small molecules like VAS3947 into their lipophilic cavity[16]. A screening study was performed to identify suitable cyclodextrins and concentrations for the formulation of VAS3947 (**Figure 4A-C**). Whereas the natural cyclodextrins showed only modest solubility improvements , the lipophilic methylated derivatives of β-cyclodextrin dramatically increased the concentration of VAS3947 in the aqueous medium. Adding 10% (w/w) of DMCD led to an increase of VAS3947 solubility to 3072 µg/ml (which corresponds to a supersaturation ratio of 170). Adding 10% (w/w) of methyl-β-cyclodextrin increased the solubility of VAS3947 to 1614 µg/ml, or a supersaturation ratio of 90.

The achieved solubility values for VAS3947 also indicate that β-cyclodextrin is more suitable than α- and γ-cyclodextrin, likely due to the more adequate size of its cavity.

NMR studies revealed strong interactions between VAS3947 and the model cyclodextrin DMCD: "Complexation Induced Chemical Shifts" (CICS) in the ^{1}H NMR spectrum gave insight into the interaction of VAS3947 and DMCD (which achieved the highest solubility increases) (**Figure 5A-B**). The distinct shift of H-5', located inside the cyclodextrin cavity, indicated the penetration of VAS3947 into the cyclodextrin. The similar shift of H-6' confirmed an incorporation of VAS3947 entering from the tighter rim of the cyclodextrin. However, the expected stoichiometry of a 1/1 molar ratio VAS3947/CD was not confirmed. Rather, it was found that H-2' and H-1', located at the outside surface of the cyclodextrin, were part of the interaction. This indicates that a full incorporation of VAS3947 into the cyclodextrin is not possible.

The strongest CICS were observed at a molar ratio VAS3947/CD : 1.5/1, indicating a stoichiometry of 1.5/1. The results derived from the ROESY analysis confirmed the close contact between API and CD with the exception of H-1' which was found to have a distance to the VAS3947 molecule exceeding 5 Å (**Figure 5C**).

Based on the outcomes of the cyclodextrin screening, a formulation for the intravenous *in vivo* application was developed. Although the lipophilic cyclodextrin derivatives, such as DMCD and methyl-β-cyclodextrin produced the highest concentration levels of VAS3947, they were excluded from the intravenous administration route due to safety reasons[17]. These derivatives have been shown to be toxic after parenteral administration[17].

Finally, a formulation containing hydroxy-propyl-β-cyclodextrin and VAS3947 was prepared. This cyclodextrin was chosen because it is an accepted excipient for parenteral use and yielded good solubility results[19]. The same formulation as described for the marketed antifungal product Sporanox® was applied due to its favourable solubilizing properties for the poorly water-soluble drug itraconazole[18].

The formulation stabilized VAS3947 at a concentration around 1000 µg/mL (**Figure 6**). To sum up, the evaluation of dissolution profiles from three commonly used formulation approaches shows an increased aqueous solubility of VAS3947 in comparison to the equilibrium solubility of the starting product. In comparison to the spray dried formulation and the microemulsion approach the cyclodextrins have the strongest potential for solubility improvement of compound VAS3947.

By developing the cyclodextrin formulation intended for intravenous application and the microemulsion formulation intended for oral administration, this study enables *in vivo* studies at a dose high enough to achieve the efficient concentrations published by Wind et al[5]. Overcoming the solubility challenges of this promising substance class, further drug development can be spurred to achieve effective treatment of cardiovascular diseases.

Conclusion

Many efficient drug candidates exhibit poor aqueous solubility, leading to low bioavailability upon administration. This is why strategies to overcome this hindrance are important for the development of many new drug formulations.

Three approaches to increase low water solubility ('spring') and to maintain this supersaturated state ('parachute') were exercised for the poorly water-soluble compound VAS3947, which was not suitable for *in vivo* experiments up to now.

Using spray drying, microemulsification, and the incorporation into cyclodextrins the thermodynamic solubility of VAS3947 was successfully enhanced for a certain time period, long enough to enable the absorption *in vivo*. An oral and an i.v. formulation were developed and can provide the investigation of further clinical development for the promising NOX-inhibitor VAS3947.

Acknowledgements

This study was funded by the Bayerische Forschungsstiftung (BFS) within the project 'Springs and Parachutes - New Formulations for Poorly Water Soluble Drugs'. We thank Vasopharm GmbH for the financial support as well as for the input of scientific knowledge. We gratefully acknowledge ACC GmbH (Analytical Clinical Concepts GmbH, Leidersbach) for the financial and the instrumental support. We thank Niclas Förtig and Jonas Löffler for the support in experimental work and for plenty of fruitful discussions. We thank Jens-Christoph Rybak for support in DSC and XRPD experiments.

References

[1] Holzerová E., Prokischa H., Mitochondria: Much ado about nothing? How dangerous is reactive oxygen species production? *Int. J. Biochem. Cell Biol.* **2015,** 63: 16–20

[2] Cifuentes-Pagano E., Meijles D. N., Pagano P. J., The quest for selective NOX inhibitors and therapeutics: challenges, triumphs and pitfalls. *Antiox. Red. Sign.* **2014,** 20(17): 2741–2754

[3] Schramm, A., et al., Targeting NADPH oxidases in vascular pharmacology. *Vascul. Pharmacol.* **2012.** 56(5-6): 216–231

[4] Griendling K. K., Sorescu D., Ushio-Fukai M., NAD(P)H Oxidase: Role in Cardiovascular Biology and Disease. *Circ. Res.* **2000,** 86(5): 494–501

[5] Stielow C., Catar R. A., Muller G., Wingler K., Scheurer P., Schmidt H. H., et al., Novel NOX inhibitor of oxLDL-induced reactive oxygen species formation in human endothelial cells. *Biochem. Biophys. Res Commun.* **2006,** 344(1): 200–205

[6] Wind S., Beuerlein K., Eucker T., Muller H., Scheurer P., Armitage M. E., et al., Comparative pharmacology of chemically distinct NADPH oxidase inhibitors. *Br. J. Pharmacol.* **2010**, 161(4): 885–898

[7] Altenhofer S., Kleikers P. W., Radermacher K. A., Scheurer P., Rob Hermans J. J., Schiffers P., et al., The NOX toolbox: Validating the role of NADPH oxidases in physiology and disease. Cell. Mol. Life. Sci. **2012,** 69(14): 2327–2743

[8] Alptüzün V., Prinz M., Hoerr V., Scheiber J., Radacki K., Fallarero A., et al., Interaction of (benzylidene-hydrazono)-1,4-dihydropyridines with β-amyloid, acetylcholine, and butyrylcholine esterases. *Bioorg. Med. Chem.* **2010,** 18(5): 2049–2059

[9] Williams H. D., Sassene P., Kleberg K., Calderone M., Igonin A., Jule E., et al., Toward the establishment of standardized in vitro tests for lipid-based formulations, part 4: proposing a new lipid formulation performance classification system. *J. Pharm. Sci.* **2014,** 103(8): 2441–2455

[10] Ran Y., Yalkowsky S. H., Prediction of Drug Solubility by the General Solubility Equation (GSE). *J. Chem. Inf. Com. Sci.* **2001,** (41):354–357

[11] Chiou W. L., Riegelman S., Pharmaceutical Applications of Solid Dispersion Systems. *J. Pharm. Sci.* **1971,** 60(9): 1281–1302

[12] Guzman H. R., Tawa M., Zhang Z., Ratanabanangkoon P., Shaw P., Gardner C. R., et al., Combined use of crystalline salt forms and precipitation inhibitors to improve oral absorption of celecoxib from solid oral formulations. *J. Pharm. Sci.* **2007,** 96(10): 2686–2702

[13] Danielsson I., Lindman B., The definition of microemulsion. *Coll. Surf.* **1981,** 3: 391–392

[14] Lückel B., Bueb W., Ottinger I., Reinhart T., Ries A., Microemulsion formulations comprising particular substance p antagonists. *Patent EP 1715848 A1.* **2005**

[15] Pouton C. W., Lipid formulations for oral administration of drugs: non-emulsifying, self-emulsifying and 'self-microemulsifying' drug delivery systems. Eur. J. Pharm. Sci. **2000,** 11(2): 93–98.

[16] Williams H. D., Trevaskis N. L., Charman S. A., Shanker R. M., Charman W. N., Pouton C. W., et al., Strategies to Address Low Drug Solubility in Discovery and Development. *Pharm. Rev.* **2013,** 65(1): 315–499

[17] Loftsson T., Jarho P., Masson M., Järvinen T., Cyclodextrins in drug delivery. Exp. Opin. Drug Del. **2005,** 2(2): 335–351

[18] Brewster M. E., Loftsson T., Cyclodextrins as pharmaceutical solubilizers. *Adv. Drug Del. Rev.* **2007,** 59(7): 645–666

[19] Strickley R., Solubilizing excipients in oral and injectable formulations. *Pharm. Res.* **2004,** 21(2): 201–230

3.3 Appendix to Chapter 3.2 – Overcoming Solubility Challenges of Triazolopyrimidine NOX-Inhibitors

In the course of the formulation development for the VAS compounds several investigations were carried out which are not part of the manuscript. These investigations were in detail: the development and validation of an HPLC method for the quantitative determination of VAS3947 and the preparation of the triazolopyrimidine compound VAS3947. These experiments are explained in the following section:

Materials and Methods

Materials

VAS3947 was provided by Vasopharm GmbH (Würzburg, Germany). Trifluoroacetic acid, formic acid, methanol (CHROMASOLV® gradient grade), and acetonitrile (CHROMASOLV® gradient grade) were procured from Sigma-Aldrich Chemie GmbH (Schnelldorf, Germany). 2 mL Verex vials for HPLC analysis were purchased from Phenomenex Ltd. (Aschaffenburg, Germany), *N,N*-dimethylhexylamine from Alfa Aesar GmbH & Co. KG (Karlsruhe, Germany), petroleum ether and ethyl acetate as well as syringe filters (0.22 µm) from VWR International GmbH (Darmstadt, Germany), and POLYGRAM® SIL G/UV_{254} polyester sheets for thin layer chromatography from Macherey-Nagel GmbH & Co. KG (Düren, Germany). Dichloromethane, ethanol, triethylamine, sodium sulphate, glycolaldehyde dimer, potassium thiocyanate, and sodium hydrogen carbonate were purchased from Sigma-Aldrich Chemie GmbH as well as aniline, benzene, toluene, ethylbenzene, biphenyl, anthracene, and thiourea. 3-Benzyl-7-chloro-triazolopyrimidine was purchased from Asta Tech, Inc. (Bristol PA). Hydrochloric acid was purchased from Bernd Kraft GmbH (Duisburg, Germany). All reagents were of analytical grade.

Instruments

All HPLC measurements were performed on an Agilent 1100 chromatographic system (Agilent Technologies GmbH, Waldbronn, Germany) equipped with an online degasser (G1322A), an autosampler (G1313A), a binary pump (G1312A), a thermostated column department, and a diode array UV/VIS detector (G1315B). The ChemStation® software package was used for data handling (Agilent Technologies GmbH, Waldbronn, Germany). Unless stated otherwise, an aliquot of 10.0 µL of the sample solutions was injected into the chromatographic system. The mobile phases for liquid chromatography as well as all samples and standard solutions were passed through membrane filters (0.45 µm) prior to injection into the chromatographic system.

Other equipment included a 744 pH meter from Metrohm AG (Herisau, Switzerland), a Sonorex ultrasonic bath from Bandelin electronic GmbH (Berlin, Germany), an analytical balance from Sartorius AG (Göttingen, Germany), and an heatable shaker from Eppendorf AG (Hamburg, Germany). A Milli-Q system (Merck Millipore GmbH, Darmstadt, Germany) was used for the demineralization of water.

Methods

Chromatographic Conditions for the Quantitative Determination of VAS3947

The chromatographic conditions were as follows: As a stationary phase a Phenomenex Synergi Max RP (50 × 4.6 mm; 4 µm particle size) analytical column was used. The run time was 10 minutes followed by a post time of 5 minutes. A binary gradient was applied with a mixture of water and acetonitrile (90/10% v/v) adjusted with 0.05% trifluoroacetic acid as mobile phase A and a mixture of water and acetonitrile (10/90% v/v) adjusted with 0.05% trifluoroacetic acid as mobile phase B. The gradient profile is shown in **Table 1**. The UV detection was performed at 254 and 280 nm. The column compartment was maintained at 23 °C, the flow rate was 1.5 mL, and 10 µL of every sample were injected.

Table 1 Gradient profile: Mobile Phase A: water and acetonitrile (90 / 10%) adjusted with 0.05% trifluoroacetic acid. Mobile phase B: water and acetonitrile (10 / 90%) adjusted with 0.05% trifluoroacetic acid. Flow rate: 1.5 mL /min.

time (min)	% A	% B
0 - 8	100 - 20	0 - 80
8 - 9	20	80
9 - 10	20 - 100	80 - 0

Method Validation

The optimized method was validated in accordance with the guideline of the International Council on Harmonisation (ICH) Q2 (R1)[1] in terms of specificity, linearity, range, accuracy, repeatability, limit of quantification (LOQ), and limit of detection (LOD).

Preparation of the Mobile Phase

2250 mL of purified water were mixed with 250 mL acetonitrile and 1.25 mL trifluoroacetic acid. This solution was sonicated for 15 minutes and then used as mobile phase A. 100 mL of purified water were mixed with 900 mL acetonitrile and 0.5 mL trifluoroacetic acid. This solution was sonicated for 15 minutes and then used as mobile phase B.

Linearity of the Calibration Line

15 mg of VAS3947 were dissolved in 10 mL acetonitrile. Six calibration solutions were prepared by diluting appropriate aliquots of this stock solution with mobile phase A to obtain concentration levels of 25, 50, 75, 100, 125, and 150 µg/mL.

Specificity

The method specificity was confirmed by injecting a solution containing VAS3947 and the related substances VAS2870 and VAS4024 at a concentration of 100 µg/mL. Peak identification was achieved by single injection of each API into the HPLC system. Mobile phase A was used as solvent.

Recovery

In order to evaluate the method accuracy and range, contents of three different solutions at concentration levels of 80, 100, and 120% of nominal content were determined. 12.0 mg of VAS3947 were dissolved in 10.0 mL acetonitrile. Nine different solutions were prepared by diluting appropriate aliquots of this stock solution with mobile phase A to obtain three different concentration levels in the range of 80, 100, and 120 µg/mL.

Precision

To confirm the repeatability, three replicate injections of three solutions covering 80 to 120% of the specified range were analysed. The relative standard deviation (RSD) values of the peak areas were determined. 12 mg of VAS3947 were dissolved in 10.0 mL acetonitrile. Nine different solutions were prepared by diluting appropriate aliquots of this stock solution with mobile phase A to obtain three different concentration levels in the range of 80, 100, and 120 µg/mL.

Limit of Quantification (LOQ) and Limit of Detection (LOD)

The limit of quantification (LOQ), based on a signal-to-noise ratio (S/N) of 10:1, was evaluated employing a solution of VAS3947 in a concentration resulting in an S/N-ratio between 25 and 50 and extrapolation to 10. The limit of detection (LOD), based on a signal-to-noise ratio (S/N) of 3:1, was evaluated employing a solution of VAS3947 in a concentration resulting in an S/N-ratio between 25 and 50 and extrapolation to 3. Mobile phase A was used as solvent.

Preparation of VAS3947

The preparation of VAS3947 was performed according to the procedure patented by Tegtmeier et al.[2]:

1. Preparation of 2-Mercaptooxalzole:

oxazole-2-thiol (**1a**)

6.2 g of concentrated hydrochloric acid were added drop wise under stirring to a suspension of 5.8 g (60 mmol) of potassium thiocyanate in 150 mL acetonitrile. After stirring the suspension at room temperature for 1 h, the deposited crystals were removed by filtration. 2.4 g (20 mmol) of glycolaldehyde dimer were added to the obtained solution of thiocyanic acid in acetonitrile and the solution was refluxed for 4 h. After cooling, the solvent was evaporated and the residue was purified by column chromatography. The product was obtained as a beige solid.

empirical formula:	C_3H_3NOS
molecular mass:	100,99 g/mol
melting point:	143.5 °C
reaction control:	DC, ^{1}H-NMR, ^{13}C-NMR
yield:	(3.2g, 98%)

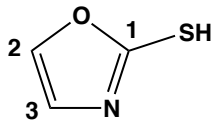

1a

^{1}H-NMR (DMSO-d_6, δ [ppm], J [Hz]): 13.07 (s, S**H)**; 7.74 (d, ^{3}J = 2.3, H-**2);** 7.36 (d, ^{3}J = 2.3, H-**3**)

^{13}C-NMR (DMSO-d_6, δ [ppm]): 150.6 (C-**1**); 138.1 (C-**2)**; 127.0 (C-**3**)

2. Preparation of VAS3947:

2-((3-benzyl-3H-[1,2,3]triazolo[4,5-d]pyrimidin-7-yl)thio)oxazole (**1b**)

A solution of 0.2 g (1 eq.) 3-benzyl-7-chloro-triazolopyrimidine (Asta Tech, Inc. Bristol PA.), 1 eq. 2-mercaptooxazole, and 1 eq. triethylamine in 5 mL acetonitrile was stirred at room temperature for 5 h. The mixture was diluted with dichloromethane, washed with a saturated solution of sodium hydrogen carbonate and brine, dried over sodium sulphate, and evaporated. Purification by column chromatography gave the title compound.

empirical formula:	$C_{14}H_{10}N_6OS$
molecular mass:	310,06 g/mol
melting point:	118.0 °C
reaction control:	DC, ^{1}H-NMR, ^{13}C-NMR
yield:	74%

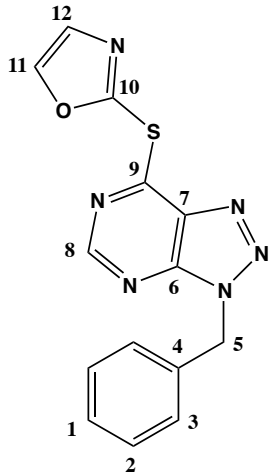

1b

^{1}H-NMR (CDCl3, δ [ppm], J [Hz]): 8.78 (s, H-**8**); 7.96 (d, ^{3}J = 0.9, H-**11**); 7.44 – 7.38 (m, 3H, H-**12**, H-**3**); 7.35 – 7.28 (m, 3H, H-**1**, H-**2**,); 5.80 (s, 2H, H-**5**)

^{13}C-NMR (CDCl3, δ [ppm]): 162.9 (C-**9**); 155.3 (C-**8**); 150.4 (C-**10**); 148.3 (C-**6**); 144.1 (C-**11**); 134.2 (C-**4**); 133.5 (C-**7**); 130.8 (C-**12**); 129.2 (C-**2**); 129.0 (C-**1**); 128.7 (C-**3**); 51.2 (C-**5**)

Results

Development and Validation of an HPLC Method for the Quantitative Determination of VAS3947

In order to analyse the solubility profile of VAS3947 over 24 h and to investigate if other new formulations improve the solubility, an adequate HPLC method is necessary. Thus, a simple and reliable HPLC method was developed using a standard C12 reversed phase column as stationary phase and a mixture composed of water and acetonitrile adjusted with 0.05% trifluoroacetic acid as mobile phase. Combining a flow rate of 1.5 mL / min with a binary gradient (**Table 1**) the run time was set to 15 minutes. The method was validated according to ICH guideline Q2 (R1)[15] in terms of specificity, linearity, range, accuracy, repeatability, limit of quantification, and limit of detection.

Linearity of the Calibration Line

The method proved to be linear within the concentration ranges of 25–150 µg/mL. The correlation coefficient of VAS3947 was $R^2 = 0.999$ (**Figure 1**).

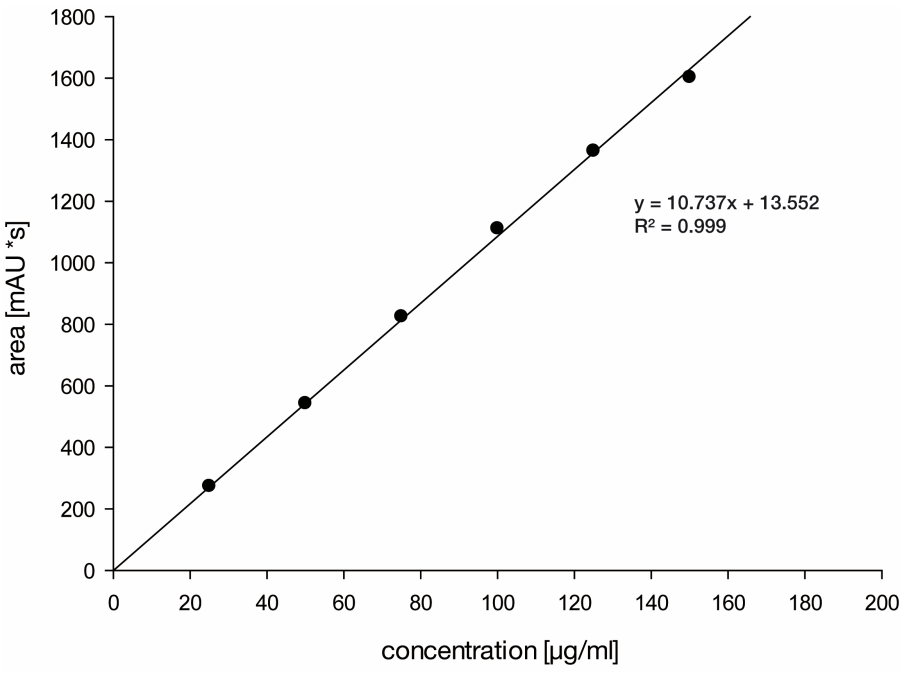

Figure 1 Validation results for the optimized HPLC method for investigated API VAS3947: The contributed term is linearity. Linear regression of known contents of 6 different solutions against corresponding peak areas obtained the method linearity. The correlation coefficient was $R^2 = 0.999$.

Specificity

No signals in the blank injections interfered with the signal due to VAS3947. The related compounds VAS2870 and VAS4024 were resolved from the API. A complete baseline separation of was achieved (**Figure 2**). Thus, the method was found to be specific.

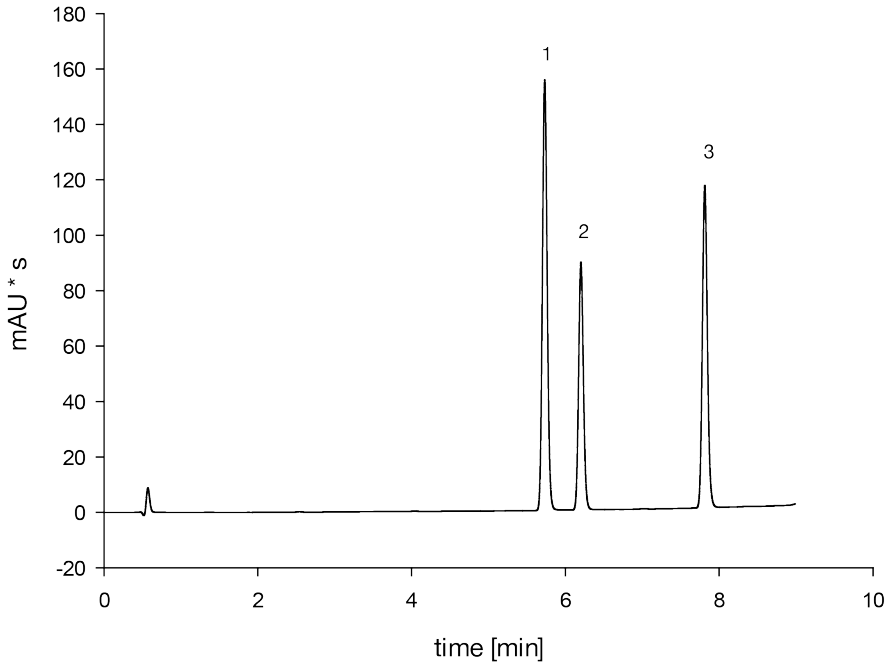

Figure 2 Validation results for the optimized HPLC method for the investigated API VAS3947: The contributed term is specificity. Separation of VAS3947 and the related substances VAS4024 and VAS2870 is shown. Peak assignment: 1 – VAS3947, 2 – VAS4024, 3 – VAS2870.

Accuracy and Precision

Recovery rates ranging at values from 99.93 to 101.21% and relative standard deviation values from 0.06 to 0.18% were within the acceptable limits which were released by the 'International Conference On Harmonization' (ICH). The limits range from 97.0 to 103.0% and RSD values of 0 to 2% at all three concentration levels[3] (**Table 2**).

The investigation of intra-day precision provided RSD values ranging from 0.05 to 0.17%. These values are within the acceptable limits of the ICH guideline which tolerates 0 to 2% at all three concentration levels[3] (**Table 2**). Thus, the method was found to be accurate and precise.

Limit of Quantification (LOQ) and Limit of Detection (LOD)

LOQ, based on a signal-to-noise ratio (S/N) of 10:1, obtained an acceptable value of 0.13 µg/mL. LOD, based on a signal-to-noise ratio (S/N) of 3:1, obtained an acceptable value of 0.04 µg/mL. The detailed results are shown in **Table 2**. The results indicate that an validated HPLC method is provided offering quantification of VAS3947 during further formulation development.

Table 2 Validation results for the optimized HPLC method A for the investigated API VAS3947: The contributed terms are: Range, accuracy, repeatability, limit of quantification, and limit of detection. The chromatographic conditions are described in section 'materials and methods'.

Precision (repeatability)				
nominal content	(µg/mL)	**120**	**100**	**80**
area	(mAU*s)	1319.96	1087.11	872.34
area	(mAU*s)	1317.25	1086.34	872.31
area	(mAU*s)	1315.42	1085.94	873.84
RSD	(%)	0.17	0.05	0.10
Accuracy and Range				
nominal content	(µg/mL)	**120**	**100**	**80**
content found	(µg/mL)	121.67	99.99	79.98
content found	(µg/mL)	121.42	99.92	79.98
content found	(µg/mL)	121.25	99.88	80.12
mean value	(µg/mL)	121.45	99.93	80.03
RSD	(%)	0.18	0.06	0.10
recovery rate	(%)	**101.21**	**99.93**	**100.04**
LOD				
content found	(µg/mL)	0.04		
LOQ				
content found	(µg/mL)	0.13		

References

[1] International Council on Harmonisation, ICH Harmonised Tripartite Guideline,Validation of Analytical Procedures: Text and Methodology, **2005,** http://www.ich.org/fileadmin/Public_Web_Site/ICH_Products/Guidelines/Quality/Q2_R1/Step4/Q2_R1__Guideline.pdf. (access date: 23.06.2016)

[2] Tegtmeier W., Schinzel R., Wingler K., Scheurer P., Schmidt H., Compounds containing a N-heteroaryl moiety linked to fused ring moieties for the inhibition of NAD(P)H oxidases and platelet activation, *patent EP1598354*. **2005.**

[3] Geetha G., Raju, K., Kumar V., M., Raja M., Analytical Method Validation: An Updated Review, *Int. J. Adv. Pharm. Bio. Chem.* 1 **2012,** 65–71.

3.4 Triazolopyrimidines as NOX-Inhibitors: Limited Drug Stability of VAS3947 Hindering Investigation of ROS Formation by NADPH Oxidases and Preventing Further Clinical Development

Nils Terveer, Nina Hecht, Marcus Gutmann, Marco Saedtler, Lorenz Meinel, and Ulrike Holzgrabe

Manuscript in preparation

Abstract

Many studies have described the triazolopyrimidine derivatives as efficient and selective NADPH oxidase inhibitors *in vitro*, which makes them promising compounds for the control of ROS action, a known cause of cardiovascular diseases. In view of preclinical investigations the triazolopyrimidine compound VAS3947 was assessed for chemical stability in addition to biopharmaceutical studies. These investigations comprised a microsomal assay, a plasma stability assay, a Caco-2 cell assay, and a cytotoxicity assay. VAS3947 was found to be remarkably chemical instable in buffer, when exposed to light, and when exposed to metabolic enzymes and human plasma. The isoxazolyl moiety linked with a thioether to the triazolopyrimidine is prone to hydrolysis which results in a cleavage and further reactions. Hence, VAS3947 and the related compounds are neither appropriate as a tool for ROS studies nor suitable for clinical studies.

Introduction

Endothelial dysfunctions causing diseases such as hypercholesterolemia, atherosclerosis, hypertension, diabetes, and heart failure are one of the main causes of death for humans[1]. It has been well known for some decades that reactive oxygen species (ROS) are involved in the formation of cardiovascular diseases[2] and that an accelerated inactivation of nitrogen monoxide by ROS causes the endothelial dysfunction[3]. Since NADPH oxidases are one of the predominant sources of ROS in the vascular cell[4-6], selective inhibition of the production of ROS is one of the strategies for effective therapy of cardiovascular diseases[2].

Triazolopyrimidine compounds such as VAS2870 and VAS3947 (**Figure 1**)[6,7] are such specific inhibitors of the NADPH oxidases[8]. During the last years more than 50 papers have described the VAS compounds as effective NADPH oxidase inhibitors and hence suitable for the treatment of cardiovascular diseases.

Additionally, the VAS compounds have been shown to have biological effects in preliminary cell culture studies:

VAS2870 was found to inhibit oxidized low-density lipoprotein (oxLDL)-mediated ROS formation in human endothelial cells[9]. Furthermore, VAS2870 was found to suppress PDGF-mediated ROS liberation in vascular smooth muscle cells[6] and to blunt pro-vasculogenetic effects of PDGF-BB in mouse embryonic stem cells[10]. VAS2870 was able to inhibit wound margin H_2O_2 production and leucocyte recruitment in zebrafish larvae[11].

VAS3947, a novel derivative of VAS2870 with a higher solubility, was introduced as an apparently specific inhibitor of the NADPH oxidase which did not interfere with commonly used ROS assays[8]. Using VAS3947, the pharmacological evidence of NADPH oxidases being indeed a relevant source of ROS formation was provided in the animal model of “Spontaneously Hypertensive Rats” (SHR)[8].

In view to planned preclinical studies the aim of this paper was to study the inherent stability of VAS3947 because all compounds from the VAS library consist of a hemiaminal moiety which is typically prone to hydrolysis. Thus, the compounds are likely to be not suitable for pharmacological studies.

VAS3947 was assessed for its stability against exposure to light, and the degradation products were identified. Additionally, a biopharmaceutical characterization of VAS3947 was performed, including microsomal stability, plasma stability, permeability assays, and cytotoxicity investigations in human liver and human embryonic kidney cells.

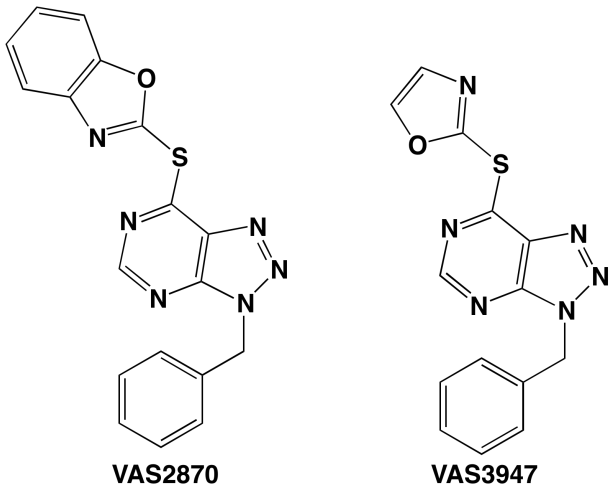

Figure 1 The chemical structures of VAS2870 and VAS3947.

Materials and Methods

Materials

VAS2870 and VAS3947 were supplied by Vasopharm GmbH (Würzburg, Germany). Deionized water was taken from an in-house supply with a Milli-Q® system (Merck Millipore GmbH, Darmstadt, Germany), or purchased from Thermo Fisher Scientific GmbH (Schwerte, Germany). Male mice microsomes (CD-1, 10 mg per vial) were purchased from Sigma Aldrich GmbH (Schnelldorf, Germany) and NADPH+H^+ from AppliChem (Darmstadt, Germany). K2 EDTA and heparin plasma were obtained from Sera Laboratories International Ltd. (Haywards Heath, UK). 12-well plates and filter inserts were purchased from Greiner Bio-One GmbH (Frickenhausen, Germany). Penicillin G and streptomycin solutions were purchased from Biochrom AG (Berlin, Germany), and fetal bovine serum (FBS) from Thermo Fisher Scientific GmbH. Hank's balanced salt solution (HBSS), Dulbecco´s modified eagle medium (DMEM), Minimum Essential Medium (MEM), and Non-essential Amino Acids solution 100x (NEAA) were purchased from Sigma Aldrich GmbH. Caco-2 cells, Hep-G2 cells, and

HEK-293 cells were purchased from DSMZ GmbH (Braunschweig, Germany). CELLSTAR® tissue culture dishes (100 mm) and 96-well plates were purchased from Greiner Bio-One GmbH (Frickenhausen, Germany), and WST-1 Solution from Roche Diagnostics Deutschland GmbH (Mannheim, Germany). 5 mm NMR tubes (S-5-900-7) were purchased from Norell Inc., (Marion, NC), deutero dimethylsulfoxide, and deutero chloroform from Deutero GmbH (Kastellaun, Germany). 2 mL Verex vials for HPLC analysis were purchased from Phenomenex Ltd. Deutschland (Aschaffenburg, Germany), petroleum ether and ethyl acetate as well as syringe filters (0.22 µm) from VWR International GmbH (Darmstadt, Germany), and POLYGRAM® SIL G/UV254 polyester sheets for thin layer chromatography from Macherey-Nagel GmbH & Co. KG (Düren, Germany). Acetonitrile and methanol (CHROMASOLV® gradient grade), trifluoroacetic acid, and formic acid were purchased from Sigma Aldrich GmbH. All compounds were at least of analytical or pharmaceutical grade and were used without further purification.

Instruments

All HPLC measurements were performed on an Agilent 1100 chromatographic system (Agilent Technologies GmbH, Waldbronn, Germany) equipped with an online degasser (G1322A), an autosampler (G1313A), a binary pump (G1312A), a thermostated column department, and a diode array UV/VIS detector (G1315B). Additionally, a fluorescence detector LS50B from Perkin Elmer (Waltham, MA) and an Agilent LC/MSD G2445D ESI ion trap (Agilent Technologies GmbH) with a syringe pump KDS100 (KD Scientific, Holliston MA) coupled to the electro spray ionization (ESI) interface were used. The ChemStation® software package was used for data handling (Agilent Technologies GmbH).

^{1}H and ^{13}C NMR spectra were measured using a Bruker Avance III spectrometer (Bruker Rheinstetten, Germany) operating at 400.13 MHz for ^{1}H and 100.13 MHz for ^{13}C, equipped with a 5 mm BBO broadband observer with Z-gradient. Data processing was done with the TopSpin® 3.2 software.

A Suntester CPS+ instrument from Atlas Material Testing Technology GmbH (Linsengericht-Altenhaßlau, Germany) was used for photostability testing.

Column chromatography was performed on a Puri Flash 430 instrument from Interchim S. A. (Montlucon, France) equipped with a 4 g silica column, UV detector,

and automatic sampling of fractions. For cytotoxicity assays a SPECTRAmax® 250 automated microtiter plate reader from Molecular Devices LLC. (Sunnyvale, CA) was used operating at 450 nm and at 650 nm. Other equipment included an InLab® Semi-Micro-L pH electrode from Mettler-Toledo Inc. (Greifensee, Switzerland), a Sonorex ultrasonic bath from Bandelin electronic GmbH (Berlin, Germany), an analytical balance from Sartorius AG (Göttingen, Germany), a Mikro 22R centrifuge from Andreas Hettich GmbH (Tuttlingen, Germany), and an heatable shaker from Eppendorf AG (Hamburg, Germany) operating at 37 °C and 800 rpm.

For Caco-2 cell assays a Neubauer improved hemocytometer from LO-Laboroptik Ltd. (Lancing, UK), 12-well plates from Corning Life Science Inc. (Amsterdam, The Netherlands), and a chopstick EVOM2 STX3 electrode connected to a EVOM2 epithelial voltammeter (World Precision Instruments, Sarasota, FL) was used.

Methods

Stability Testing

A photostability testing of VAS3947 was performed according to Singh et al.[12] and the guideline of the International Council on Harmonization Q1B[13]: The test substance was dissolved in a mixture of acetonitrile and water (60/40% v/v) at a concentration of 1 mg/mL. This solution was transferred into two 5 mL glass vials and exposed to light, providing an overall illumination of 1.2 million lux h and 6 million lux h, respectively, using near ultraviolet energy of 250 watt h/m^2 produced by the Suntester CPS+ instrument. Another set of two samples, wrapped in aluminium foil, was used as dark control to evaluate the thermally induced change in comparison to the total observed change of drug content. Concentrations of drug in all solutions were determined by HPLC. The chromatographic conditions are illustrated in **Table 1**. The samples were diluted in a mixture of acetonitrile/water 60/40 (v/v) and the concentration was calculated using a regression line over the range of 1 µg/mL–250 µg/mL. All experiments were carried out in triplicate.

Chromatographic Conditions for Stability Testing

The chromatographic conditions were as follows: As a stationary phase a Phenomenex Synergi Max RP (50 × 4.6 mm; 4 µm particle size) analytical column was used. The run time was 10 minutes followed by a post time of 5 minutes. A binary gradient was applied with a mixture of water and acetonitrile (90/10% v/v) adjusted with 0.05% trifluoroacetic acid as mobile phase A and a mixture of water and acetonitrile (10/90% v/v) adjusted with 0.05% trifluoroacetic acid as mobile phase B. The gradient profile was as follows: from 0 min to 8 min from 100% to 20% mobile phase A, from 8 min to 9 min at 20% mobile phase A, and from 9 min to 10 min from 20% to 100% mobile phase A. UV detection was performed at 254 and 280 nm. The column compartment was maintained at 23 °C, the flow rate was 1.5 mL, and 10 µL of every sample were injected.

Production and Isolation of Degradation Products

For the determination of degradation products 30 mg of VAS3947 were dissolved in 10 mL methanol. This solution was transferred into a 30 mL glass vial and exposed to light, providing an overall illumination of 6 million lux h using near ultraviolet energy of 250 watt h/m^2 using Suntester CPS+ instrument to reach complete degradation of the API. The reaction was controlled by thin layer chromatography using petroleum ether and ethyl acetate (2:1 v/v) as the eluent and POLYGRAM® SIL G/UV254 polyester sheets as the stationary phase. Afterwards, the solvent was evaporated and the degradation products were separated by flash chromatography. Petroleum ether and ethyl acetate were used as eluents (2:1 v/v). A 4 g silica column was used as stationary phase.

After the solvents were evaporated, the structure of every purified degradation product was elucidated by NMR spectroscopy and mass spectrometry.

Chromatographic Conditions for Mass Analysis

The chromatographic conditions were as follows: As a stationary phase an Agilent Zorbax SB-CN (50 × 4.6 mm; 3.5 µm particle size) analytical column was used. The run time was 20 minutes followed by a post time of 5 minutes. A binary gradient was applied water adjusted with 0.1% formic acid as mobile phase A and acetonitrile adjusted with 0.1% formic acid as mobile phase B.

The gradient profile was as follows: from 0 min to 5 min 5% mobile phase B, from 5 min to 10 min from 5% to 90% mobile phase B, from 10 min to 15 min 90% mobile phase B, and from 15 min to 20 min from 90% to 5% mobile phase B.
UV detection was performed at 254 and 280 nm. The column compartment was maintained at 23 °C, the flow rate was 0.4 mL, and 10 µL of every sample were injected.
The parameters for the ESI ion trap were as follows: The flow rate was 0.4 mL/min, the nebulizer pressure was 15 psi, the dry gas flow 5 L/min, the dry temperature 325 °C, the capillary voltage 3500 V, and helium was used as collision gas.

Microsomal Assay

VAS3947 was subjected to an *in vitro* microsomal stability assay in order to simulate Phase-I metabolism. Liver enzymes were prepared from male mice microsomes and gently thawed on ice prior to use. A 10 mM stock solution of VAS3947 was prepared in dimethylsulfoxide. 5 µL of the stock solution were dissolved in a mixture of 445 µL of a 100 mM potassium phosphate buffer (pH 7.4), 50 µL of liver enzyme preparation (concentration: 10 mg/mL), and 0.5 mg NADPH/H^+ (final volume: 500 µL). This resulted in final concentrations of 100 µM VAS3947, 1 mg/mL protein, and 1.2 mM NADPH/H^+. The solutions were incubated at 37 °C in a water bath and aliquots (50 µL) were taken at 0 min, 15 min, 30 min, 60 min, 90 min, 120 min, 150 min, 180 min, 210 min, 240 min, and 270 min. The samples were immediately 1:1 diluted with acetonitrile to stop the enzymatic activity, vortex mixed for 30 seconds and centrifuged for 2 minutes at 10.000 rpm at a temperature of 4 °C. The clear supernatant was analysed by HPLC using the same method as described for the stability testing (see p. 106). Two groups of control samples consisting of 5 µL VAS3947 stock solution and 495 µL potassium phosphate buffer and 5 µL VAS3947 stock solution, 495 µL potassium phosphate buffer, and 0.5 mg NADPH/H^+ were investigated under the same conditions.

Plasma Stability Assessment

The *in vitro* assessment of plasma stability of VAS3947 was performed in human K2-EDTA plasma and heparin plasma. 100 µL of a 100 µg/mL stock solution of VAS3947 in acetonitrile were added to 1000 µL pre-warmed plasma. The final

concentration of VAS3947 was 9.09 µg/mL. Equivalent control samples were prepared using water instead of plasma. All samples were incubated in a water bath at 37 °C and aliquots (110 µL) were taken after 0, 15, 30, and 60 minutes. After sampling, the aliquots were immediately diluted with 300 µL of acetonitrile and centrifuged for 10 minutes at 10.000 rpm at a temperature of 4 °C. The clear supernatant was analysed by HPLC using the same method as described for the stability testing (see p. 106). Additionally, the experiment was repeated with plasma which was spiked with 0.5% sodium fluoride and again with heat inactivated plasma[14].

Caco-2 Cell Assay

Caco-2 cell assays were performed as described by Hubatsch et al.[15]. In brief, Caco-2 cells were cultured in Dulbecco's modified Eagle's medium high glucose (DMEM) containing 10% heat inactivated fetal bovine serum, 100 U/mL penicillin G and 100 µg/µL streptomycin at 37 °C and 5% CO_2 as described before[15].

2.6×10^5 cells / cm^2 were seeded on polycarbonate filter inserts (diameter 12 mm; 0.4 µm membrane pore size) on 12-well plates. Cells typically had at least 3 passages. The monolayer integrity was monitored by measuring the transepithelial electrical resistance (TER). TER measurements were performed for each cell-seeded filter using a chopstick electrode EVOM2 STX3 electrode connected to a EVOM2 epithelial voltammeter. Specifications for cell-seeded filters required TER values exceeding 400 (Ohm × cm^2).

On day 21 after sowing permeability assays were performed from the apical to the basolateral compartment. For the permeability experiment, 1200 µL of Hank's Balanced Salt Solution pH = 7.4 (HBSS) were provided in the basolateral compartment and 500 µL of a 100 µM solution of VAS3947 in HBSS, 500 µL of 100 µM solution of Lucifer Yellow in HBSS (negative control), and 500 µL of a 100 µM solution of Fluorescein sodium in HBSS (positive control), respectively, were added to the apical side (n=3). After 30 min, 60 min, and 120 minutes of incubation at 37 °C, 7% CO_2, and orbital shaking at 150 rpm, 100 µL of the samples were removed from the basolateral side and the volume loss was compensated by adding fresh HBSS.

Additionally, 100 µL of the sample solution were taken from the apical side directly after adding the samples and after 120 minutes for the calculation of mass balance and P_{app}. The calculation of P_{app} was conducted according to the following formula:

$$P_{app} = \left(\frac{dQ}{dt}\right)\left(\frac{1}{A \times c_0}\right)$$

with P_{app} being the apparent permeability coefficient

$\left(\frac{dQ}{dt}\right)$ being the steady-state flux in µmol/sec,

A being the insert/filter surface area in cm^2, and

c_0 being the starting concentration in the apical (donor) chamber in µM.

The concentration of VAS3947 was analysed by HPLC using the same method as described for the stability testing (see p. 106).
Lucifer Yellow (negative control) and Fluorescein Sodium (positive control) were analysed using fluorescence detection. The following parameters were set for Lucifer Yellow (negative control): Excitation wavelength: 470 nm, excitation slit: 2.5 nm, emission wavelength: 535 nm, emission slit: 2.5 nm, and read time: 0.4 s.

The following parameters were set for Fluorescein sodium (positive control): Excitation wavelength: 490 nm, excitation slit: 2.5 nm, emission wavelength: 514 nm, emission slit: 15 nm, and read time: 0.4 s.

Cytotoxicity

Cytotoxicity assays were conducted in human liver cells (Hep-G2) and human embryonic kidney cells (HEK-293) according to ATCC protocols[16,17]. In brief, cells were seeded on 96-well plates at a cell density of 3.2 x 10^4 cells/mL for HEK-293 and 1.0 x 10^5 cells/mL for Hep-G2 (using 125 µL per well).
For Hep-G2 cells, a stock solution of VAS3947 was prepared in dimethylsulfoxide and serially diluted with growth medium (MEM) containing 10% heat inactivated fetal bovine serum, 0.1 mM of amino acid L-glutamine, 100 U/mL penicillin G, and 100 µg/mL streptomycin. The solutions of VAS 3947 were prepared in the following concentrations: 2.5 µM, 5 µM, 7.5 µM, 10 µM, 25 µM, 50 µM, 75 µM, 100 µM, and 200 µM. The residual content of dimethylsulfoxide was 0.5%.

For HEK-293 cells, a dilution series was prepared from the same stock solution in growth medium (DMEM) containing 10% heat inactivated fetal bovine serum, 100 U/mL penicillin G and 100 µg/mL streptomycin. The solutions of VAS 3947 were prepared in the following concentrations: 1 µM, 2.5 µM, 5 µM, 7.5 µM, 10 µM, 25 µM, 50 µM, 75 µM, and 100 µM. The residual content of DMSO was 0.5%.

VAS3947 solutions were incubated on cell layers for 24 h at 37 °C and 5% CO_2 (n=4). After that, water soluble tetrazolium solution (WST-1) was added to each well. The absorption of a product at 450 nm originating from an enzymatic reaction of living cells with tetrazolium chloride was measured using a SPECTRAmax 250 automated microtiter plate reader. The positive controls (Hep-G2/HEK-293 cells and respective medium including WST-1) and negative controls (respective medium and WST-1) were processed likewise. Finally, the percentage of surviving cells was calculated with the positive control normalized to 100% and the negative control normalized to 0% survival.

Nuclear Magnetic Resonance Measurements

^{1}H NMR spectra were recorded with a flip angle of 30°, spectral width of 20 ppm, transmitter offset of 6.15 ppm, acquisition time of 3.99 s followed by a relaxation delay of 1.00 s. 128 scans were collected to 64.000 data points, resulting in a digital resolution of 0.25 Hz. Processing parameters were set to an exponential line broadening window function of 0.3 Hz, an automatic baseline correction, and manual phasing.

^{13}C NMR spectra were recorded with a flip angle of 30°, spectral width of 240 ppm, transmitter offset of 100 ppm, acquisition time of 1.36 s followed by a relaxation delay of 2.00 s. 4096 scans were collected in 64.000 data points resulting in a digital resolution of 0.73 Hz. Processing parameters were set to an exponential line broadening window function of 1.0 Hz, an automatic baseline correction, and manual phasing.

Unless stated otherwise, 20 mg of every sample were dissolved in 700 µL of $CDCl_3$ or DMSO-d_6 and transferred into a standard 5 mm NMR tube. The solvent signal served as the field frequency lock. The temperature was adjusted to 300 K.

Results

Since preclinical studies are planned for the VAS compounds, they were assessed with regard to chemical and metabolic stability in addition to permeability and toxicity studies.

Photostability

A photostability testing of VAS3947 was performed according to Singh et al.[12] and the ICH guideline Q1B[13]. A mixture of acetonitrile and water (60/40% v/v) was used as solvent and two groups of samples were exposed to light illumination of 1.2 and 6 million lux h, respectively. The results summarized in **Figure 2** indicate a significant degradation of VAS3947 upon light exposition. Whereas the content of the samples stored in darkness decreased to 97% and 92% (being the control), light exposition of 1.2 million lux h led to a decrease of the content to 47% of the original amount and applying illumination of 6 million lux h to an almost complete decomposition.

To identify the degradation products, a forced degradation experiment in methanol using 6 million lux h was conducted. Approximately 5 mg of a mixture containing three different degradation products was obtained and the analytes were separated by means of column chromatography. The comparison of the ^{1}H NMR spectra of VAS3947 and its degradation products revealed the loss of two protons at δ = 7.96 ppm (H-11) and 7.44 to 7.38 (H-12) (**Figure 3**). Additionally, a new signal at δ = 4.26 ppm occurred which can be attributed to a methyl group. All other signals were identical to the parent compound VAS3947 indicating that the triazolopyrimidine skeleton was untouched and a methylation had taken place, most probably because of the usage of methanol.

The NMR spectrum of the degradation products (**Figure 3**) represents a mixture of all three degradation compounds. The degradation product with m/z = 242 g/mol hints to the methoxylated compound **a** (**Figure 4**). The degradation product with m/z = 260 g/mol, which also shows a methyl signal, might be in agreement with compound **c**. Again the methylation was caused by the solvent methanol. The degradation product with m/z = 243 g/mol did not exhibit any methyl signal and can be assigned to compound **b**.

It can be concluded that all degradation products were formed after hydrolysis of the chemically labile thiohemiaminal moiety and reaction with methanol.

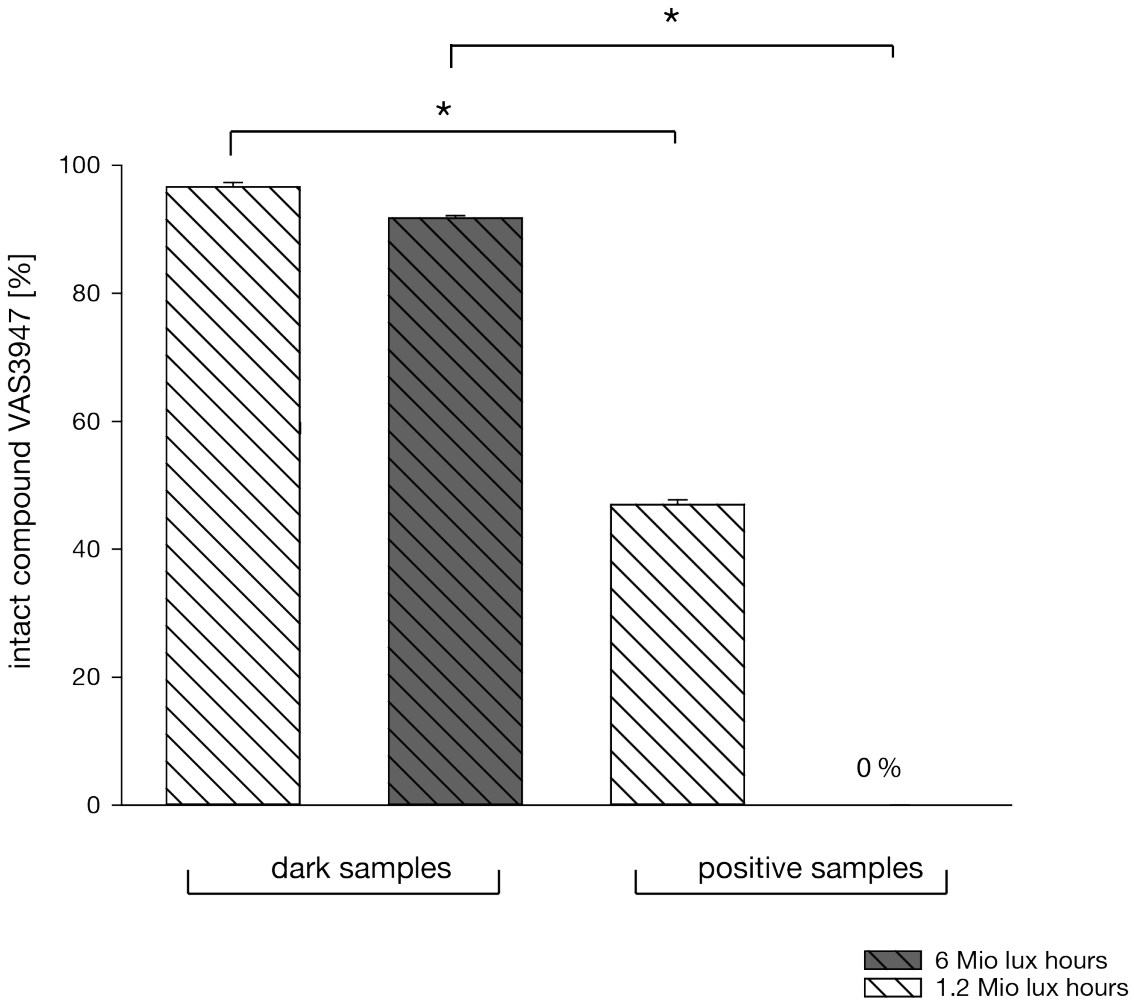

Figure 2 Photostability of VAS3947: Control samples wrapped in aluminium foil versus positive samples exposed to light illumination. The samples were exposed to 1.2 million lux h and 6 million lux h, respectively.

Microsomal Assay

The assessment of microsomal stability was performed for the prediction of Phase-I metabolism. First, the stability of VAS3947 was tested against NADPH+H^+ dissolved in a phosphate buffer serving as negative control. Within this experiment the content of VAS3947 decreased to 90%, indicating chemical instability (**Figure 5A**).

Second, VAS3947 was incubated with mice liver microsomes and NADPH+H^+ using the same buffer (**Figure 5A**). After 15 minutes a rapid decrease of the content was observed followed by a slower degradation of VAS3947. After 240 minutes the amount of intact compound VAS3947 reached a final value of 32%, indicating a substantial metabolic liability of compound VAS3947.

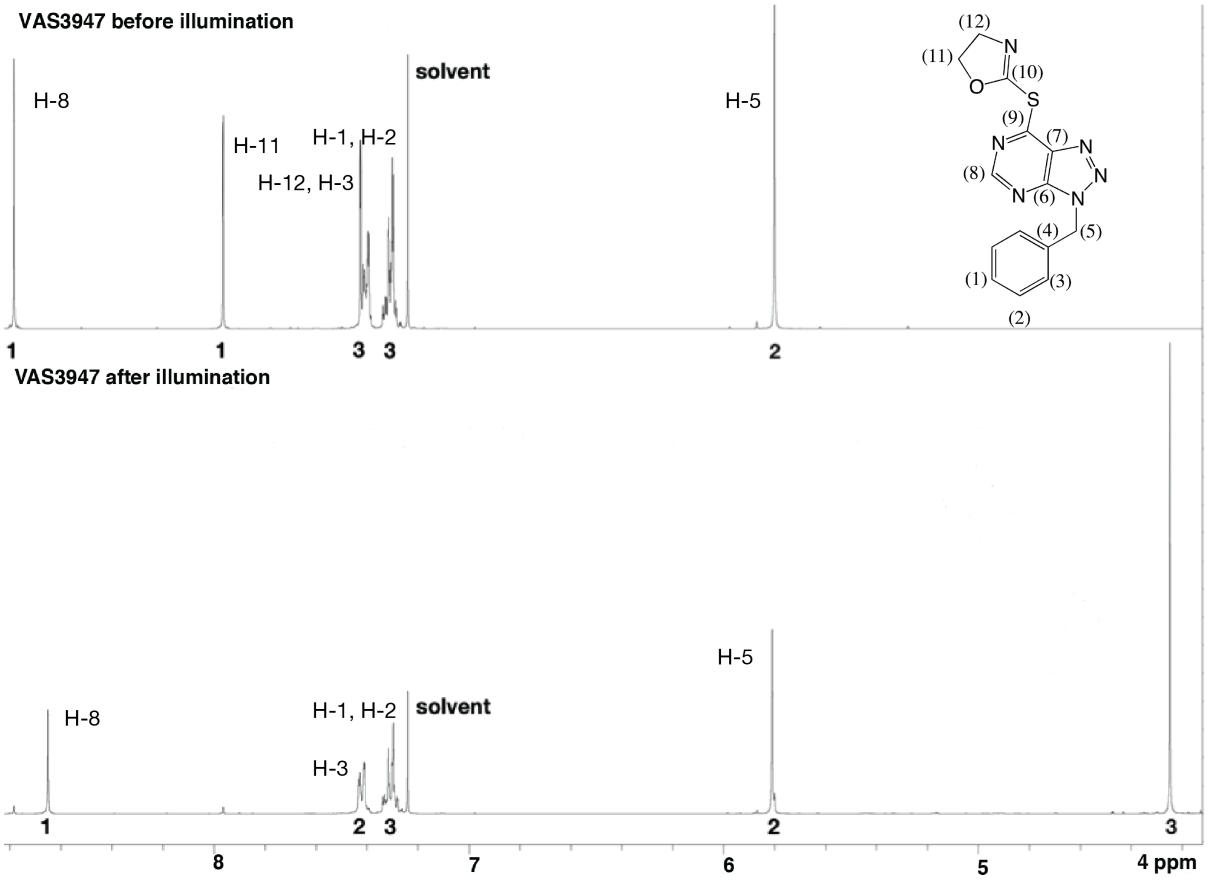

Figure 3 Comparison of the ^{1}H NMR spectra ($CDCl_3$) of VAS3947 before and after degradation by providing overall illumination of 6 million lux h.

Plasma Stability

VAS3947 was incubated in K2-EDTA plasma at 37 °C in order to study the stability against plasma. Control samples were incubated using water instead of plasma. After 30 minutes of incubation in plasma the API was completely degraded whereas the control samples showed no indication of degradation.

In order to find out whether this effect was induced by an interaction of VAS3947 with EDTA, the assay was repeated in heparinized plasma. Similar results were found; after 30 minutes the API was completely degraded.

Additionally, the experiment was repeated with heat inactivated human K2-EDTA plasma. Again a complete degradation of the substance was observed although no enzyme activity is expected due to the application of heat inactivated plasma.

In order to confirm that no enzyme activity is necessary for the degradation, VAS3947 was then tested in human plasma containing 0.5% sodium fluoride, acting as an enzyme inhibiting agent. The fact that a complete degradation was also found, supports the hypothesis that an enzyme mediated process is very unlikely.

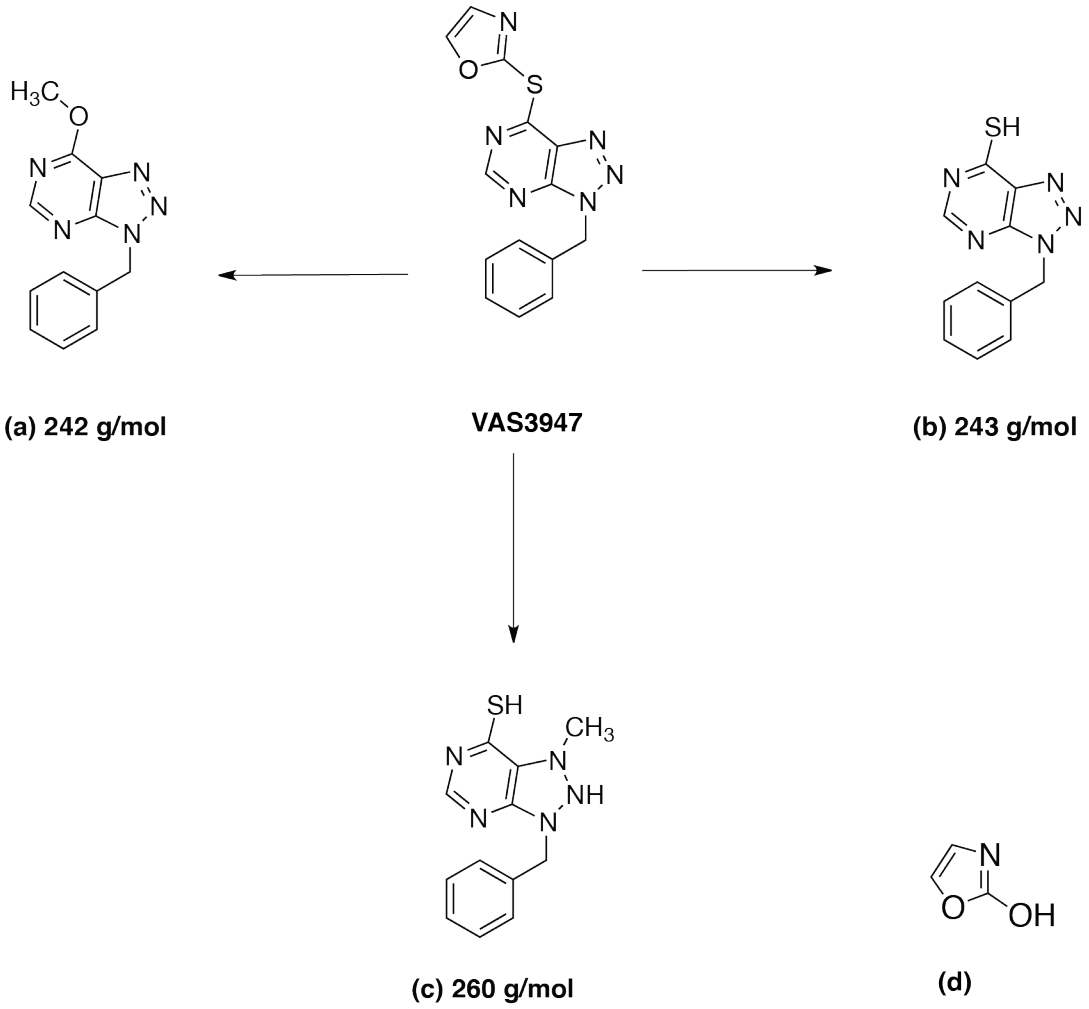

Figure 4 The structures of VAS3947 and the identified degradation products (**a-c**) after providing overall illumination of 6 million lux h. Structure (**d**) represents the hydroxylated isoaxazole moiety after separation from the N-benzyl compound.

Caco-2 Cell Assay

The permeability of VAS3947 across physiological membranes was examined by means of Caco-2 cell assays. Lucifer Yellow served as negative control and Fluorescein sodium was used as positive control[15]. The results are summarized in **Figure 5B**. The following parameters were calculated:

The monolayer tightness (by measuring the transepithelial resistance (TER) value), the mass ratio (which the is sum of the substance in the apical and the basolateral compartment after performing the permeability assay), and the apparent permeability coefficient (P_{app}) representing the permeability through the Caco-2 monolayer.

TER values were not allowed to decrease below 400 Ohm × cm^2 during the experiment. Monolayers showing TER values below 400 Ohm × cm^2 before performing the experiment were discarded.

For Lucifer Yellow (negative control), TER results were assessed as 528 Ohm × cm^2 before beginning the experiment and 664 Ohm × cm^2 after termination of the permeability experiment. The mass ratio was found to be 99.4% of the specified content after 120 minutes and P_{app} was calculated as 0.26×10^{-6} cm/s. For Fluorescein sodium (positive control), TER results were found to be 456 Ohm × cm^2 before and 596 Ohm × cm^2 after the experiment. The mass ratio was 99.2% of the specified content and P_{app} was 1.11×10^{-6} cm/s.

These results of the control prove an accurate procedure of the experiment and the existence of an intact cell monolayer. For VAS3947, the transepithelial resistance decreased considerably from 429 Ohm × cm^2 to 125 Ohm × cm^2 after 120 minutes of incubation. In addition, a low mass ratio of 25% of specified content was calculated after 120 minutes, indicating that VAS3947 leads to the destruction of cell monolayers and gets absorbed into the cells as well as to other equipment. Having no intact cell monolayer in place the calculated P_{app} result of 6.4×10^{-6} cm/s can be neglected.

Cytotoxicity

A cytotoxicity assessment of VAS3947 was performed in kidney cells (HEK-293) and hepatocytes (Hep-G2) and resulted in an IC_{50} of 7.29 µM (**Figure 5C**) and 12.56 µM (**Figure 5D**), respectively, indicating a substantial toxicity.

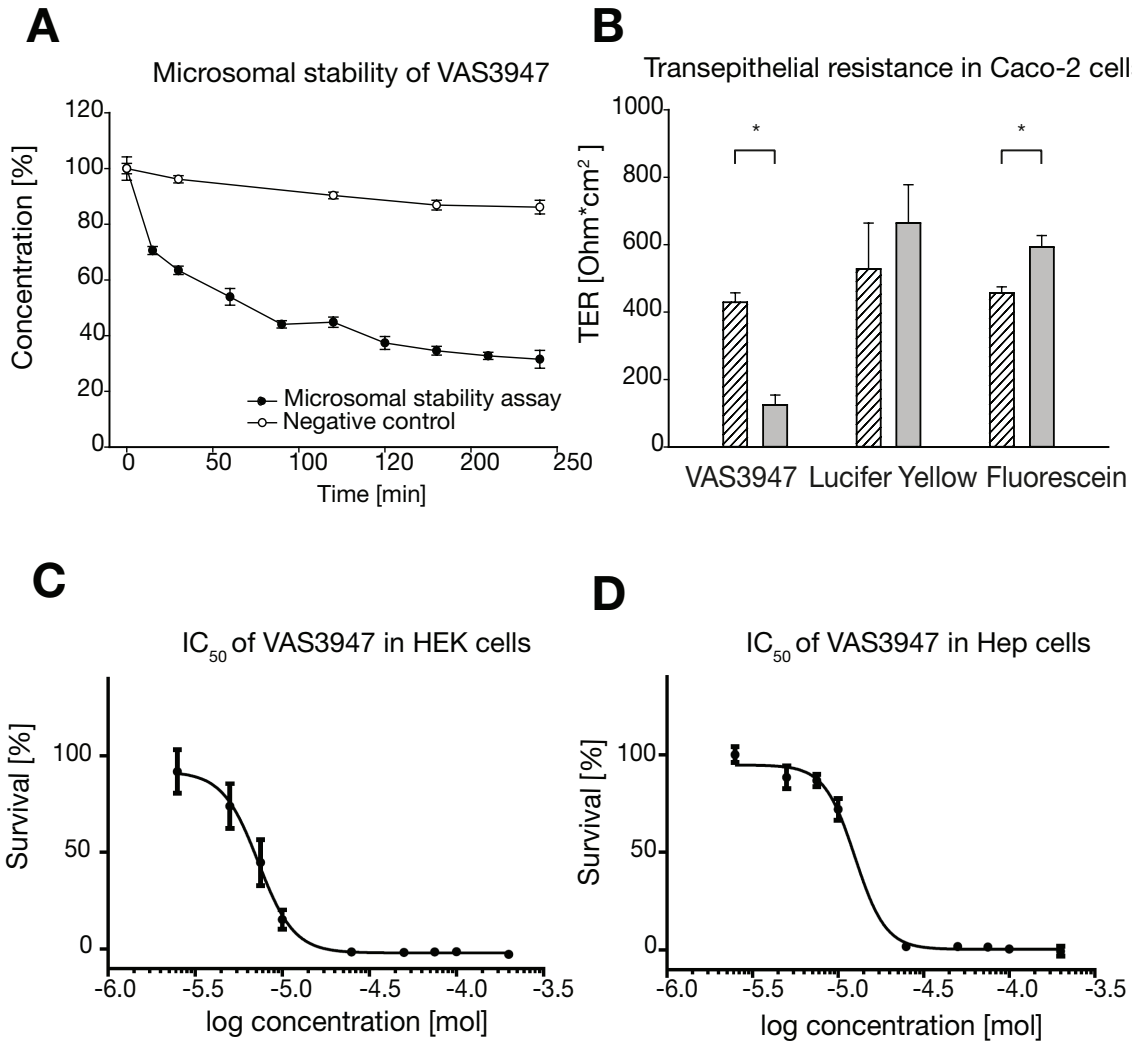

Figure 5 (**A**) The microsomal stability of VAS3947 in phosphate buffer / NADPH+H^+ (negative control) and in the respective medium including liver microsomes from mice (microsomal stability assay). **B**) The transepithelial resistance (TER) of Caco-2 cell layers before the addition of the test compounds (shaded bars) and incubated with VAS3947, Lucifer Yellow (negative control) and Fluorescein sodium (positive control) for 120 minutes (grey bars). **C**) IC_{50} of VAS3947 in HEK-293 cells, **D**) IC_{50} of VAS3947 in Hep-G2 cells.

Discussion

Although cardiovascular diseases are a major cause of death in the majority of the developed countries[1], an effective therapy preventing the formation of cardiovascular diseases is still missing. Previously, the novel small molecule drug candidates developed by Vasopharm[6,7] were described as specific inhibitors of the NADPH oxidases. They suppress the formation of ROS which is involved in the formation of cardiovascular diseases[2,8].

At a first glance, the development of these novel NOX inhibitors seems to be a reasonable approach to inhibit NADPH oxidases and ROS, respectively, in the formation of endothelial dysfunctions.

Instability of a drug candidate is always an issue. Thus, the VAS-compound having the highest aqueous solubility, namely VAS3947, was tested for its stability against light and was found to be highly labile (**Figure 2**). Moreover, even in the dark, a degradation was observed.

When exposed to the same physiological conditions as in human plasma, VAS3947 was completely degraded within 30 minutes. Experiments executed with heat inactivated plasma and enzyme inhibiting reagent fluoride also showed degradation, indicating that an enzyme mediated process is unlikely to be the reason for the instability in plasma. The results obtained in a buffered medium consisting of NADPH + H^+ hint to the same conclusions (**Figure 5A**).

The stability testing and the isolation of degradation products indicate that the chemical structure of VAS3947 causes its tendency to decompose (**Figure 2**, **3**). The isoxazolyl moiety of the molecule next to the thioether can be regarded as a thioacetale or thioaminale. Acetales and aminales are chemical structures which are principally prone to hydrolysis. Thus, the degradation reaction is likely to occur at the isoxazolyl part of the molecule. An intermediate hemiaminal is obtained from the hydrolysis which converts into the hydroxylated isoxazolyl moiety (**d**) and the N-benzylated compounds **a** to **c** (**Figure 4**). The main degradation product is compound **b** characterized by a thiol group in position 9 (**Figure 4**) which can also be found in compound **c**. The NMR and the mass spectra of compound **c** indicate an additional methylation of one triazol nitrogen (**Figure 4**) which might be caused by a radical reaction with methanol occurring upon illumination. In compound **b** the

thiol attached to position 9 of the triazolopyrimidine is substituted by a methoxy group originating from methanol which was used for dissolution of the drug.

Even though some of the reactions might need light and others might take advantage of the methanol, it becomes quite clear that the isoxazolyl ring which is linked to the triazolopyrimdine via a thioether is a highly labile moiety. Thus, it is not possible to decide whether the degradation upon incubation with mice liver microsomes is due to simple chemical reactions or enzyme driven reactions.

In the Caco-2 assays VAS3947 was found to have cell membrane disrupting properties resulting in a disintegration of the membranes. Furthermore, the cytotoxicity testing of VAS3947 conducted in HEK-293 and HEP-G2 cells resulted in IC_{50} values of 7.29 µM and 12.56 µM, respectively, which are in the same range as the efficacy data having IC_{50} values of 2 µM in HL-60 cells and 10.6 µM in a cell-free system measured by ten Freyhaus et al.[6] However, due to the high reactivity of the VAS drug it cannot be decided whether the membrane disintegration and the cytotoxicity is caused by the drug compound itself or its degradation products or some intermediates of the degradation process. It is not even possible to attribute the efficacy to VAS3947.

Conclusion

To the best of our knowledge stability studies of VAS3947 were conducted for the first time even though the compound was used in in numerous assays. VAS3947 was found to have a limited chemical stability against buffers and light, in the presence of metabolic enzymes, and in human plasma, all due to the hemiaminal structural element. Furthermore, it harmed Caco-2 cell membranes and cytotoxicity data were found to be in the same concentration range as efficacy data published for different cell lines before. This fact is a major issue and hinders further drug development process of the triazolopyrimidine substance class. Since the results cannot be attributed to the drug compound itself rather than the degradation products, VAS compounds are not appropriate candidates for the investigation of ROS involvement in the formation of cardiovascular diseases. Moreover, the stability limitations prevent further clinical development.

Acknowledgements

This study was funded by the Bayerische Forschungsstiftung – BFS – within the project 'Springs and Parachutes – New Formulations for Poorly Water Soluble Drugs'. We thank Vasopharm GmbH for financial support as well as for the input of scientific knowledge. We gratefully acknowledge ACC GmbH (Analytical Clinical Concepts GmbH, Leidersbach) for financial and instrumental support.

References

[1] Sans S., Kesteloot H., Kromhout D., The burden of cardiovascular diseases mortality in Europe. *Eur. Heart J.* **1997,** 18 (8): 1231–1248

[2] Rodiño-Janeiro B. K., Paradela-Dobarro B., Castineiras-Landeira M. I., Raposeiras-Roubin S., Gonzalez-Juanatey J. R., Álvarez E., Current status of NADPH oxidase research in cardiovascular pharmacology. *Vasc. Health Risk Manag.* **2013,** 9: 401–428

[3] Cai H., Harrison D. G., Endothelial dysfunction in cardiovascular diseases: The role of oxidant stress. *Circulation Research.* **2000,** 87 (10): 840–844

[4] Heumüller S., Wind S., Barbosa-Sicard E., Schmidt H. H., Busse R., Schröder K., Brandes R. P., Apocynin is not an inhibitor of vascular NADPH oxidases but an antioxidant. *Hypertension.* **2008,** 51 (2): 211–217

[5] Lassegue B., Clempus R. E., Vascular NAD (P) H oxidases: specific features, expression, and regulation. *Am. J. Physiol. Regul. Inte. Comp. Physiol.* **2003,** 285(2): R277–R297

[6] ten Freyhaus H., Huntgeburth M., Wingler K., Schnitker J., Baumer A. T., Vantler M., Bekhite M. M., Wartenberg M., Sauer H., Rosenkranz S., Novel Nox inhibitor VAS2870 attenuates PDGF-dependent smooth muscle cell chemotaxis, but not proliferation. *Cardiovasc. Res.* **2006,** 71 (2): 331–341

[7] Tegtmeier W. A., Schinzel R., Wingler K., Scheurer P., Schmidt H., Compounds containing a N-heteroaryl moiety linked to fused ring moieties for the inhibition of NAD(P)H oxidases and platelet activation *patent EP1598354.* **2005.**

[8] Wind S., Beuerlein K., Eucker T., Müller H., Scheurer P., Armitage M., Ho H., Schmidt H., Wingler K. Comparative pharmacology of chemically distinct NADPH oxidase inhibitors. *Br. J. Pharmacol.* **2010,** 161 (4): 885–898

[9] Stielow C., Catar R. A., Muller G., Wingler K., Scheurer P., Schmidt H. H., Morawietz H., Novel Nox inhibitor of oxLDL-induced reactive oxygen species formation in human endothelial cells. *Biochem. Biophys. Res Comun.* **2006,** 344 (1): 200–205

[10] Lange S., Heger J., Euler G., Wartenberg M., Piper H. M., Sauer H., Platelet-derived growth factor BB stimulates vasculogenesis of embryonic stem cell-derived endothelial cells by calcium-mediated generation of reactive oxygen species. *Cardiovasc. Res.* **2009,** 81 (1): 159–168

[11] Niethammer P., Grabher C., Look A. T., Mitchison T. J., A tissue-scale gradient of hydrogen peroxide mediates rapid wound detection in zebrafish. *Nature.* **2009,** 459 (7249): 996–999

[12] Singh S., Bakshi M., Guidance on Conduct of Stress Tests to Determine Inherent Stability of Drugs. *Pharm. Tech. On-Line.* **2000.**

[13] International Council on Harmonisation, Stability Testing: Photostability Testing Of New Drug Substances And Products Q1B, **1996.** http://www.ich.org/products/guidelines/quality/quality-single/article/stability-testing-photostability-testing-of-new-drug-substances-and-products.htmL. (access date: 23.06.2016)

[14] Montefiori Laboratory Duke University. Protocol for Heat-Inactivation of Serum and Plasma Samples. **2011.**

[15] Hubatsch I., Ragnarsson E. G., Artursson P., Determination of drug permeability and prediction of drug absorption in Caco-2 monolayers. *Nat. Protoc.* **2007,** 2 (9): 2111–2119

[16] ATCC (American Type Culture Collection). Hep G2 [Hep-G2] (ATTC® HB8065™).

[17] ATCC (American Type Culture Collection). 293 [HEK-293] (ATTC® CRL1573™).

4 Final Discussion

4 FINAL DISCUSSION

Low aqueous solubility is a common issue of most of the new APIs entering market access today. Looking at the portfolio of marketed drugs in comparison to developmental drugs, it becomes evident that there is a strong trend towards compounds which are poorly soluble in water[1]. The hit identification strategies of drug development in use today coming along with high throughput screening techniques led to a systematical increase in molecular weight and lipophilicity and a decrease of water solubility of lead compounds during the last years[2-4]. Whereas more than 40% of drug failures could be traced by poor biopharmaceutical properties in the late 1980's, today it becomes evident that the percentage of these lead compounds has increased dramatically[5,6]. Especially for small molecule drug candidates a customized formulation strategy has to be developed to reach acceptable concentration levels in the gastrointestinal fluids for the time window of the absorption process, finally resulting in therapeutic plasma concentrations.
For every API different parameters have to be considered influencing the formulation strategy: the route of administration, the property of the API to be in solid state or liquid at room temperature, the property to be crystalline or amorphous, water sorption, wettability, melting point, and the p*Ka* value play an important role.
In this study two different APIs were selected as examples of such poorly water-soluble drugs and were subjected to a specific formulation development aligning their special physicochemical characteristics.

The first drug candidate to be investigated for solubility improvement was imatinib. This tyrosine-kinase inhibitor is marketed by Novartis AG as crystalline imatinib mesylate salt (Gleevec®) and is intended for the treatment of the chronic myelogeous leukemia (CML)[7-9]. Imatinib as a crystalline free base has a very low aqueous solubility of 0.2 mM. However, the compound lends itself for salt formation because of its character as a strong base having a p*Ka* value of 8.36. Therefore, the transformation of imatinib into an ionic liquid was performed which proved to be a reliable concept for improving drug release and bioavailability before[10-12]. Presenting the API as an ionic liquid using different acetylated amino acids as counterions actually illustrated some major advantages: On the one hand lowering lattice forces by transforming the API into an amorphous solid state led to an increase of the

dissolution rate. The supersaturation time was prolonged and no recrystallization was observed as compared to the crystalline mesylate salt. On the other hand the usage of alkyl sulfonates like the mesylate anion as counterions, which were criticised for the last years because of their genotoxic risks, could be resigned[13]. By selecting counterions which proved to be safe substances because of their character as amino acids, the total potential toxicity was reduced.

In this study the formation of a stable ion pair preventing recrystallization was proved by NMR spectroscopy, and the long term stability was demonstrated by performing a stress testing under forcing conditions.

However, the increased dissolution rate as a consequence of the amorphisation process comes along with in increased property of water vapour sorption which is a disadvantage in handling and shouldn't be neglected. Therefore, special demands on the packaging material are necessary. Additionally, further experiments have to be performed: The implementation of the Caco-2 monolayer model is necessary to estimate the transport of the ionized formulation across physiological membranes[14]. Animal trials have to be performed to estimate if there is actually an increased bioavailability to observe when presenting imatinib as an IL.

Generally, it can be declared that the IL concept offers a great potential for formulation scientists to tune the physicochemical properties of a given poorly water-soluble API to therapeutic needs. The IL concept gains from the ionized amorphous state. Due to ionization, a higher interaction with the aqueous dissolution medium takes place which causes the increase in solubility. ILs may be solids or liquids at room temperature depending on the glass transition temperature, but always be amorphous. This can be achieved by choosing bulky counterions having a soft electron density, being asymmetric, and possessing flexible alkyl chains[15]. The amorphous state causes that there is no risk of polymorphism which is a major disadvantage of crystalline substances.

The huge variability justifies the advantage of the concept: More hydrophilic counterions led to the increase of the solubility and the dissolution rate, more lipophilic counterions led to the increase of the absorption across physiological membranes. For acidic APIs an augmented drug release coming along with a pronounced supersaturation is needed for the time window of absorption.

In contrast, basic APIs are ionized in gastrointestinal fluids after oral administration and their solubility is favoured by the low pH value. Beside an acceptable dissolution rate especially the stabilization against precipitation has to be favoured by means of a stable ion pair.

The other small molecule drug candidate which was addressed for the development of different formulation strategies was the triazolopyrimidine derivative VAS3947, developed by Vasopharm GmbH[16-17]. This compound is intended for the treatment of endothelial dysfunctions causing diseases such as hypercholesterolemia, atherosclerosis, hypertension, diabetes, and heart failure. The API acts as a specific inhibitor of the NADPH oxidase[18] being the predominant source of ROS in the vascular cell[17,19]. It has been known for decades that ROS are involved in the formation of cardiovascular diseases beyond doubt[20] and that an accelerated inactivation of nitric monoxide by ROS constitutes the endothelial dysfunction[21].
VAS3947 is an extremely poorly water-soluble, neutral compound without any remarkable p*Ka* value hindering the salt formation strategy.
Therefore, a solid dispersion of VAS3947 and Eudragit® L100 was prepared by means of spray drying from a methanolic solution. The solid dispersion approach gains from the enormous increase of the product surface. By reduction of the particle size to its absolute minimum the product offers much more surface for the interaction with the gastrointestinal fluids. Thus, an increased bioavailability up to several orders of magnitude is possible. Additionally, the spray drying process leads to an amorphous product which gains from lowering lattice forces. Preparation of a spray dried solid dispersion is a reliable, gentle manufacturing process resulting in a product of good flowability ready for encapsulation or compression into tablets.
However, the spray dried formulation of VAS3947 showed a ‘spring’ resulting in a three times increased solubility as compared to the starting material. But afterwards some recrystallization occurred and the concentration of VAS3947 in solution after 24 h exceeded the equilibrium solubility of the pure API just to a minor degree. The overall solubility remained in the low µM range being far away from reaching therapeutic concentration levels.

Therefore, a second formulation strategy was applied for VAS3947: The complexation with different cyclodextrin molecules resulted in enormous ‘spring and

parachute' effects. Hence, the formulation using methyl-β-cyclodextrin resulted in a 760-fold increased aqueous solubility of VAS3947 as compared to the starting material. NMR spectroscopic studies proved the incorporation of the API into the cyclodextrin cavity. These kind of host-guest interaction forms water-soluble dynamic and reversible inclusion complexes and makes cyclodextrins to be ideal candidates for the formulation of poorly water-soluble compounds[22]. Cyclodextrin containing formulations primarily are intended for oral administration. It is assumed that the cyclodextrin molecule holds the guest molecule in solution until striking the intestinal wall. Only the small molecule API is absorbed across the physiological membrane. The cyclodextrin molecule is excluded because of its size and will be resigned by faeces. Nonetheless, several derivatives of cyclodextrins are allowed for intravenous application.

Beside a first screening for solubility improvement a formulation of VAS3947 intended for the intravenous route of administration was prepared using hydroxy-propyl-β-cyclodextrin as excipient. The formulation led to remain the labile compound VAS3947 at a stable concentration of 1 mg/mL for 24 h. As compared to an aqueous solubility of nearly 15 µg/mL of the starting material a massive increase in solubility was achieved. Additionally, the compound was completely prevented from recrystallization and degradation. Therefore, the enormous potential of cyclodextrins as pharmaceutical solubilizers was demonstrated.

Finally, four microemulsion formulations using different liquid excipients were prepared for increasing the aqueous solubility of VAS3947. Microemulsions are defined as isotropically clear liquid solutions composed of water, oil, and an amphiphile[23]. The microemulsion formulations took advantage of their thermodynamical stability over a sufficient time period and of providing an acceptable solubilizing capacity for VAS3947. Having an up to 18-fold increased solubility as compared to the starting material, the microemulsions exceeded the solid dispersion formulation by far. Because of an increased long term stability microemulsions are mostly administered orally as preconcentrates incorporated into gelatine capsules. Upon contact with the aqueous gastrointestinal fluids, microemulsions form fine dispersions in the low nanomolar range favouring dissolution, re-dissolution, and equilibrium solubility due to a high wettability and a great surface area of the particles.

Taken together, the incorporation into cyclodextrins is the most effective of the three formulation concepts applied to this neutral compound. The effects of ‘spring and parachute’ improving the dissolution as well as the extent and the time of supersaturation exceed the effects of the other formulations. Additionally, the formulation prevented the drug from precipitation and degradation for a sufficient time period of 24 h. The cyclodextrin inclusion complex is a stable product of a defined chemical stoichiometry which not only gains from amorphization like the unstable solid dispersion does. Hence, there is no risk of recrystallization. Instead of the solid dispersion it can easily be prepared having the chance to scale up the manufacturing process. Additionally, it is a solid dry product unlike the microemulsion which has enormous advantages in handling and packaging as well as administration.

Otherwise, the ionic liquid concept demonstrated to offer great possibilities to adjust the bioavailability of a given drug and to beat crystalline salts in some cases, but the concept is exclusively suitable for acidic or basic compounds.

The formulation development in this studies was focused on oral administration. But some of the concepts may easily be extended to other routes of administration. Especially for the cyclodextrins there are a lot of applications described to be used as pharmaceutical solubilizers in eye-drop solutions, intravenous solutions, and ointments[24].

Nonetheless, another very important factor during the drug development process mustn’t be neglected: Beside having a potent new chemical entity showing high efficacy data and low toxicity, showing excellent permeability, and being presented in an adequate formulation resulting in high bioavailability, inherent stability of the API is absolutely necessary for further drug development. The compounds of the VAS-library are such drug candidates having a limited stability because of presence of a hemiaminal moiety in the chemical structure which is typically prone to hydrolysis. Investigations performed in this study reveal a limited chemical stability of VAS3947 against light illumination, in the presence of metabolic enzymes, and in human plasma. For this reason, the stability limitations prevent further clinical development and make the compound fail. The most powerful formulation becomes redundant when the API is prone to degradation.

References

[1] Lipp R., The Innovator pipeline: bioavailability challenges and advanced oral drug delivery opportunities. *Am. Pharm. Rev.* **2013,**16(3) 10–12

[2] Brewster M. E., Loftsson T. Cyclodextrins as pharmaceutical solubilizers. *Adv. Drug Deliv. Rev.* **2007,** 59(7): 645–666

[3] Lipinski C. A., Avoiding investment in doomed drugs. *Curr. Drug Discov.* **2001,** 1: 17–19

[4] Lipinski C. A., Lombardo F., Dominy B. W., Feeney P. J., Experimental and computational approaches to estimate solubility and permeability in drug discovery and development settings. *Adv. Drug Deliv. Rev.* **2012,** 64: 4–17

[5] Kola I., Landis J., Can the pharmaceutical industry reduce attrition rates? *Nat. Rev. Drug Disc.* **2004,** 3(8): 711–716

[6] Prentis R., Lis Y., Walker S., Pharmaceutical innovation by the seven UK-owned pharmaceutical companies (1964-1985). *Brit. J. Clin. Pharm.* **1988,** 25(3): 387–396

[7] Deininger M., Buchdunger E., Druker B. J., The development of imatinib as a therapeutic agent for chronic myeloid leukemia. *Blood.* **2005,** 105(7): 2640–2653

[8] O'Brien S. G., Guilhot F., Larson R. A., Gathmann I., Baccarani M., Cervantes F., Cornelissen J. J., Fischer T., Hochhaus A., Hughes T., Imatinib compared with interferon and low-dose cytarabine for newly diagnosed chronic-phase chronic myeloid leukemia. *New Eng. J. Med.* **2003,** 348(11): 994–1004

[9] Savage D. G., Antman K. H., Imatinib mesylate—a new oral targeted therapy. *New Eng. J. Med.* **2002,** 346(9): 683–693

[10] Balk A., Wiest J., Widmer T., Galli B., Holzgrabe U., Meinel L., Transformation of acidic poorly water-soluble drugs into ionic liquids. *Eur. J. Pharm. Biopharm.* **2015,** 94: 73–82.

[11] Marrucho I. M., Branco L. C., Rebelo L. P., Ionic liquids in pharmaceutical applications. *Ann. Rev. Chem. Biomol. Eng.* **2014,** 5: 527–546.

[12] Shamshina J. L., Barber P. S., Rogers R. D., Ionic liquids in drug delivery. *Exp. Opin. Drug Deliv.* **2013,** 10(10): 1367–1381.

[13] Kim S., Salt Formation of Pharmaceutical Compounds and Associated Genotoxic Risks. Pharmaceutical Industry Practices on Genotoxic Impurities. *Lee, Heewon.* **2014,** 1: 385–426.

[14] Hubatsch I., Ragnarsson E. G., Artursson P., Determination of drug permeability and prediction of drug absorption in Caco-2 monolayers. *Nat. Prot.* **2007,** 2(9): 2111–2119

[15] Balk A., Holzgrabe U., Meinel L., 'Pro et contra' ionic liquid drugs - Challenges and opportunities for pharmaceutical translation. *Eur. J. Pharm. Biopharm.* **2015,** 94: 291–304.

[16] Tegtmeier W., Schinzel R., Wingler K., Scheurer P., Schmidt H., Compounds containing a N-heteroaryl moiety linked to fused ring moieties for the inhibition of NAD(P)H oxidases and platelet activation, *patent EP1598354*. **2005.**

[17] ten Freyhaus H., Huntgeburth M., Wingler K., Schnitker J., Baumer A. T., Vantler M., Bekhite M. M., Wartenberg M., Sauer H., Rosenkranz S., Novel Nox inhibitor VAS2870 attenuates PDGF-dependent smooth muscle cell chemotaxis, but not proliferation. *Cardiovasc. Res.* **2006,** 71(2): 331–341.

[18] Wind S., Beuerlein K., Eucker T., Müller H., Scheurer P., Armitage M., Ho H., Schmidt H., Wingler K., Comparative pharmacology of chemically distinct NADPH oxidase inhibitors. *Br. J. Pharm.* **2010,** 161(4): 885–898

[19] Lassegue B., Clempus R. E., Vascular NAD (P) H oxidases: specific features, expression, and regulation. *Amer. J. Phys. Reg. Int. Comp. Phys.* **2003,** 285(2): R277–R297

[20] Rodiño-Janeiro B. K., Paradela-Dobarro B., Castineiras-Landeira M. I., Raposeiras-Roubin S., Gonzalez-Juanatey J. R., Álvarez E., Current status of NADPH oxidase research in cardiovascular pharmacology. *Vasc. Health. Risk. Manag.* **2013,** 9: 401–428

[21] Cai H., Harrison D. G., Endothelial dysfunction in cardiovascular diseases: the role of oxidant stress. *Circ. Res.* **2000,** 87(10): 840–844

[22] Williams R. O., Watts A. B., Miller D. A., Formulating Poorly Water-soluble Drugs. *Springer,* **2012.**

[23] Danielsson I., Lindman B., The definition of microemulsion. *Coll. Surf.* **1981,** 3(4): 391–392

[24] Loftsson T., Duchêne D., Cyclodextrins and their pharmaceutical applications. *Int. J. Pharm.* **2007,** 329(1): 1–11

5 Summary / Zusammenfassung

5 SUMMARY

Successful formulation development of novel, particularly organic APIs of low molecular weight as candidates for ground-breaking pharmaceutical products is a major challenge for the pharmaceutical industry because of the poor aqueous solubility of most of these compounds.
The hit identification strategies of drug development in use today apply high throughput screening techniques for the investigation of thousands of substances. This approach led to a systematical increase in molecular weight and lipophilicity and a decrease of water solubility of lead compounds reaching market access.

The high lipophilicity causes an excellent permeability of the compounds which favours the absorption process from the small intestine, but it causes a decrease of water-solubility. It becomes evident that an adequate aqueous solubility is necessary for absorption of the API from the gastrointestinal fluids into the systemic circulation and hence for efficacy of the pharmaceutical product. Only an dissolved API is getting absorbed and becomes efficacious. The precipitated proportion is resigned directly. Therefore, the development of an individual formulation aligning the physicochemical characteristics is necessary for every API to produce supersaturated solutions in the small intestine and to reach an adequate bioavailability after absorption into the systemic circulation.

In this thesis a specific formulation development was investigated for two exemplary poorly water-soluble APIs to replace the empirical approach often used today. The basic tyrosine-kinase inhibitor imatinib and six different acetylated amino acids were transferred into ILs. As compared to the free base and the mesylate salt, which is marketed by Novartis AG as Gleevec®, the dissolution rate as well as the supersaturation time was increased significantly. By changing the mesylate anion with its potential genotoxic risks, the total toxicity of the drug product could be decreased. The amorphous ILs proved adequate stability under forcing conditions and there was no recrystallization of the free base observed. The amorphous character of the ILs caused an increased amount of water vapour sorption which can be compensated by special packaging materials. Taken together, the presentation of imatinib as an IL is intended for oral administration as a tablet and

can cause a reduction of dose because of the increased solubility. Therefore, the occurrence of side effects can be reduced as compared to Gleevec®. If there is actually an increased bioavailability to observe, has to be proved by the execution of animal trials.

The novel NOX inhibitor VAS3947 is intended for the treatment of endothelial dysfunctions causing diseases like heart failure and stroke. The compounds poor aqueous solubility hindered further clinical development so far and make the drug candidate to remain in a very early stage of the drug development process. Therefore, different formulation concepts were evaluated in this study:
An amorphous solid dispersion prepared from VAS3947 and Eudragit® L100 by means of spray drying was able to increase the dissolution rate and solubility of the compound significantly, but with the accomplished kinetic solubility being in the low µM range it is not possible to reach therapeutic plasma concentrations.

In contrast, the incorporation into cyclodextrins resulted in an 760-fold increased solubility. Different cyclodextrins were evaluated. Especially the lipophilic derivatives of the β-cyclodextrin showed to be the most adequate excipients. The incorporation of the API into the cyclodextrin cavity was proved by means of NMR spectroscopy. Additionally, a formulation of VAS3947 and hydroxypropyl-β-cyclodextrin was prepared. This formulation is intended for the intravenous application during animal trials, which have to be conducted to get to know the pharmacokinetics of VAS3947. This formulation reached a concentration of 1 mg/mL spending striking protection of VAS3947 against degradation.

Presentation of VAS3947 as a microemulsion system led also to increase the aqueous solubility of the compound, but not in the same extent as the cyclodextrin formulation. Beside the formulation development a physicochemical characterization was performed to get to know important parameters such as log *P* and p*Ka* values of VAS3947. An HPLC method was developed and validated to analyse the extent of solubility improvement.

A major issue of the compound VAS3947 and all related triazolopyrimidine derivatives, developed by Vasopharm GmbH, is the insufficient chemical stability because of presence of a hemiaminal moiety in the chemical structure. Stability investigations and an extensive biopharmaceutical characterization confirm the hindering of further clinical development by insufficient drug stability and high cytotoxicity. Poor aqueous solubility is an additional disadvantage which can be handled by a concerted formulation development.

5.1 ZUSAMMENFASSUNG

Die erfolgreiche Formulierung von neuen, insbesondere organischen Wirkstoffen geringen Molekulargewichtes als Entwicklungskandidaten für innovative Arzneimittel stellt eine erhebliche Herausforderung für die pharmazeutische Industrie dar, weil ein Großteil dieser Substanzen ausgesprochen schlecht wasserlöslich ist.

Die moderne Wirkstoffentwicklung basiert meistens auf der Zielstruktur und erfolgt unter Anwendung von Hochdurchsatzmethoden, bei denen Tausende an verschiedenen Substanzen getestet werden. Dieses Vorgehen hat in den letzten Jahrzehnten dazu geführt, dass die molare Masse und die Lipohilie derjenigen Entwicklungskandidaten, die eine Zulassung als Arzneimittel erreicht haben, kontinuierlich zugenommen haben. Durch die hohe Lipophilie weisen diese Wirkstoffe eine ausgezeichnete Permeabilität auf, die für den Absorptionsprozess aus dem Magen-Darm-Trakt notwendig ist. Jedoch geht damit gleichzeitig eine Abnahme der Wasserlöslichkeit einher. Es ist offensichtlich, dass eine ausreichendende hohe Wasserlöslichkeit die Grundvoraussetzung für die Absorption des Wirkstoffes aus dem Gastrointestinaltrakt in den systemischen Kreislauf und damit für die Wirksamkeit des Arzneimittels darstellt. Nur in Lösung befindlicher Wirkstoff kann absorbiert werden und seine Wirkung erzielen. Der ungelöste Anteil wird unverändert wieder ausgeschieden.

Aus diesem Grunde ist die Entwicklung einer individuellen, an die physiko-chemischen Eigenschaften angepassten Formulierung für jeden Wirkstoff unbedingt erforderlich, um im Magen-Darm-Trakt übersättigte Lösungen zu generieren und dadurch eine ausreichende Bioverfügbarkeit zu erzielen.

In dieser Arbeit wurden exemplarisch zwei schlecht lösliche Wirkstoffe ausgesucht und einer gezielten Formulierungsentwicklung unterzogen, um die bisher oft angewandte rein empirische Vorgehensweise abzulösen.
Aus dem basischen Tyrosinkinase-Inhibitor Imatinib und unterschiedlichen acetylierten Aminosäuren wurden 6 verschiedene ionische Flüssigkeiten hergestellt. Im Vergleich mit der freien Base und dem Mesilat-Salz, welches die Firma Novartis AG unter dem Namen Gleevec® im Handel hat, wurden sowohl die Auflösungsrate als auch die zeitliche Dauer der Übersättigung signifikant vergrößert. Durch den Austausch des potentiell genotoxischen Mesilat-Anions gegen die acetylierten Aminosäuren konnte zusätzlich das Toxizitätsrisiko gesenkt werden. Die amorphen Formulierungen der ionische Flüssigkeiten waren unter Stressbedingungen ausreichend stabil und zeigten kein erhöhtes Risiko für eine Rekristallisation der freien Base. Die durch den amorphen Charakter gesteigerte Hygroskopizität lässt sich durch den Einsatz entsprechender Packmittel kompensieren. Generell eignet sich die Formulierung von Imatinib als ionische Flüssigkeit für die orale Applikation als Tablette und kann durch die Verbesserung der Wasserlöslichkeit zu einer Dosisreduktion beitragen, sodass weniger Nebenwirkungen auftreten als bei dem im Handel befindlichen Mesilat-Salz. Ob tatsächlich eine Verbesserung der Bioverfügbarkeit eintritt, muss noch durch Experimente im Tiermodell bestätigt werden.

Der neuartige NOX-Inhibitor VAS3947 ist zur Behandlung von arteriosklerotischen Veränderungen im Gefäßendothel und damit allen verbunden Folgeerkrankungen wie zum Beispiel Herzinfarkt oder Schlaganfall von der Vasopharm GmbH entwickelt worden. Die extrem schlechte Wasserlöslichkeit hat bisher die klinische Forschung verhindert und der Wirkstoff befindet sich nach wie vor in einer sehr frühen Phase der Entwicklung. Aus diesem Grund wurden im Zuge dieser Arbeit verschiedene Formulierungskonzepte erforscht:

Eine erste sprühgetrocknete, amorphe Formulierung mit dem Polymer Eudragit® L100 konnte zwar die Auflösungsrate und die Löslichkeit signifikant verbessern, allerdings kam es schnell zur Rekristallisation des Wirkstoffes und mit der erzielten kinetischen Löslichkeit im niedrigen µM Bereich ließen sich keine therapeutischen Plasmaspiegel erreichen.

Durch die Herstellung einer Cyclodextrineinschlussverbindung von VAS3947 hingegen konnte die Löslichkeit um den Faktor 760 gesteigert werden. Verschiedene Cyclodextrine wurden getestet. Dabei erwiesen sich insbesondere die lipophilen Derivate des β-Cyclodextrins als geeignet. Die Einlagerung des Wirkstoffes in das Innere der Kavität wurde mittels NMR-Spektroskopie bestätigt. Zusätzlich wurde erstmals eine Formulierung von VAS3947 mit Hydroxypropyl-β-Cyclodextrin zur intravenösen Anwendung im Tiermodell für die Durchführung von geplanten Pharmakokinetikstudien hergestellt. Diese erzielte über 24 Stunden eine Löslichkeit von 1 mg/mL und schütze den Wirkstoff effektiv vor Zersetzung.

Durch die Formulierung von VAS3947 als halbfeste Mikroemulsion konnte die Wasserlöslichkeit ebenfalls gesteigert werden, allerdings längst nicht in dem Maße wie durch die Cyclodextrine.

Neben der Formulierungsentwicklung wurde eine physiko-chemische Charakterisierung des Wirkstoffes durchgeführt, um wichtige Parameter wie zum Beispiel die log *P*- und *pKs*-Werte einschätzen zu können. Des Weiteren wurde eine HPLC-Methode entwickelt und validiert, um die erzielte Löslichkeit quantifizieren zu können.

Ein großes Problem dieses Wirkstoffes und damit aller Derivate vom Triazolopyrimidine-Typ, welche die Vasopharm GmbH in der Entwicklung hat, ist die mangelnde chemische Stabilität aufgrund einer Halbaminal-Partialstruktur im Molekül. Durchgeführte Stabilitätsuntersuchungen sowie eine umfangreiche biopharmazeutische Charakterisierung bestätigten letztendlich, dass eine weitere Entwicklung dieser Wirkstoffe aufgrund ihrer ungenügenden Stabilität und ihrer hohen Zytotoxizität nicht möglich ist. Die niedrige Wasserlöslichkeit stellt ein zusätzliches Problem dar, das sich durch eine gezielte Formulierungsentwicklung lösen lässt.

6 Appendix

6 APPENDIX

6.1 Documentation of Authorship

M1	**Terveer N, Schollmayer C, Steiger C, Holzgrabe U, Meinel L** Ionic Liquid Concept for Improving the Solubility Profile of the Tyrosine-Kinase Inhibitor Imatinib Manuscript in preparation (2016)

Author	**1**	**2**	**3**	**4**	**5**
Study design / concept development	X			X	X
Preparation of imatinib free base	X				
Preparation of ILs	X				
Preparation of potassium salts of counterions	X				
Investigation of NMR studies	X	X			
X-ray powder diffractometry	X				
Investigation of DSC studies			X		
Determination of water vapour sorption	X				
Determination of dissolution rate and solubility	X				
Determination of p*Ka* values	X				
Stress testing	X				
Data analysis and interpretation	X	X			
Manuscript planning	X			X	X
Manuscript writing	X				
Correction of manuscript		X		X	X
Supervision of Nils Terveer				X	X

M2	**Hecht N, Terveer N, Schollmayer C, Holzgrabe U, Meinel L** Overcoming Solubility Challenges of Triazolopyrimidine NOX-Inhibitors Manuscript in preparation (2016)

Author	**1**	**2**	**3**	**4**	**5**
Study design / concept development	X	X		X	X
Differential scanning calorimetry	X				
log *P* assessment		X			
Solubility assessment of the API	X				
Preparation of spray dried formulations	X				
X-ray powder diffractometry	X				
Spray dried formulation studies	X				
Determination of pH, particle size	X				
Microemulsion formulation studies	X				
Cyclodextrin formulation studies		X			
^{1}H NMR investigation of CICS		X			
ROESY measurements		X	X		
Cyclodextrin formulation for i.v. application		X			
Data analysis and interpretation	X	X	X		
Manuscript planning	X	X		X	X
Manuscript writing	X	X			
Correction of manuscript				X	X
Supervision of Nils Terveer				X	X

This chapter or its content or parts of its content will also be published in the dissertation of Nina Hecht.

M3	**Terveer N, Hecht N, Gutmann M, Saedtler M, Meinel L, Holzgrabe U** Triazolopyrimidines as NOX-Inhibitors: Limited Drug Stability of VAS3947 Hindering Investigation of ROS Formation by NADPH Oxidases and Preventing Further Clinical Development Manuscript in preparation (2016)

Author	**1**	**2**	**3**	**4**	**5**	**6**
Study design / concept development	X	X			X	X
Stability testing	X					
Production and isolation of degradation products	X					
Microsomal assay		X				
Plasma stability assessment		X				
Caco-2 cell assay			X	X		
Cytotoxicity cell assay			X	X		
Chromatographic studies	X	X				
NMR studies	X					
Data analysis and interpretation	X	X				
Manuscript planning	X	X			X	X
Manuscript writing	X	X				
Correction of manuscript					X	X
Supervision of Nils Terveer					X	X

This chapter or its content or parts of its content will also be published in the dissertation of Nina Hecht.

6.2 List of Abbreviations

API	Active Pharmaceutical Ingredient
BCS	Biopharmaceutical Classification System
Caco-2	Caucasian Colon Adenocarcinoma Cells
CICS	Complexation Induced Chemical Shifts
DAD	Diode Array Detector
D_2O	Deuterium Oxide
EDTA	Ethylendiaminetetraacetic Acid
ESI	Electro Spray Ionization
DSC	Differential Scanning Calorimetry
DMEM	Dulbecco´s Modified Eagle Medium
FaSSIF	Fasted State Simulated Intestinal Fluid
FBS	Fetal Bovine Serum
HBSS	Hank’s Balanced Salt Solution
HEP-G2	Hepatoblastoma G2 Cell Line
HEK-293	Human Embryonic Kidney 293 Cell Line
HPLC	High Performance Liquid Chromatography
HPMC	Hydroxypropyl Methylcellulose
IL	Ionic Liquid
K	Kelvin
LOD	Limit of Detection
LOQ	Limit of Quantification
MEM	Minimum Essential Medium
NADPH	Nicotineamid Adenine Dinucleotide Phosphate
NEAA	Non-Essential Amino Acids Solution

NCE	New Chemical Entity
NMR	Nuclear Magnetic Resonance
NO	Nitrogen Monoxide
oxLDL	Oxidized Low-Density Lipoprotein
PDGF	Platelet-derived growth factor
PBS	Phosphate Buffered Saline
ROS	Reactive Oxygen Species
UV	Ultra Violet
VAS	Vasopharm GmbH
XRPD	X-ray Powder Diffractometry